JOÃO MIGUEL ALMEIDA SANTOS

Cited2 in cardiac development: an inside and outside job

UAlg
UNIVERSIDADE DO ALGARVE
DEPARTAMENTO DE CIÊNCIAS BIOMÉDICAS E MEDICINA

2019

JOÃO MIGUEL ALMEIDA SANTOS

Cited2 in cardiac development: an inside and outside job

PhD in Mechanisms of Disease and Regenerative Medicine

Work developed under supervision of:

Prof. Doctor José Eduardo Bragança

Prof. Doctor Matthias Futschik

UNIVERSIDADE DO ALGARVE

DEPARTAMENTO DE CIÊNCIAS BIOMÉDICAS E MEDICINA

January 2019

Cited2 in Cardiac Development: an inside and outside job

Declaração de autoria de trabalho

Declaro ser o autor deste trabalho, que é original e inédito. Autores e trabalhos consultados estão devidamente citados no texto e constam da listagem de referências incluída.

_____

(João Miguel Almeida Santos)

“ The problem with the world is that intelligent people are full of doubts, while the stupid ones are full of confidence”

Charles Bukowski

ACKNOWLEDGMENTS

First and foremost, I would like to start by thanking my family for all their support. For always giving me the necessary tools and the liberty to pursue my studies.

To my girlfriend Carina, for always being there whenever I needed and for encouraging me to go into this PhD programme. If not for her, this experience would not have happened.

To my supervisor, José Bragança, for accepting this challenge together with me and supporting, mentoring and teaching me across these 4 years.

To all the colleagues from ProRegeM PhD programme, especially the 2nd edition "ProRegeMers", for all the fun moments and memories which I will never forget.

To all the Stem Cells lab members that positively contributed to this work, most notably Leonardo Silva and João Lopes.

To the different members of CBMR that positively contributed to my every-day life.

To Matthias Futschik and Rui Machado, for their support with microarray analysis.

To Agapios Sachinidis for having me in his lab and support with microarrays.

To Gil Martins, Paulo Gavaia and Leonor Cancela for helping me with the in vivo experiments or, as I like to call it, "the zebrafish experience".

To all the bachelors, medical students, and volunteers that I had the opportunity of supervising which helped me develop important soft skills.

To Rui Martinho and his group, for the very interesting lab meetings that helped me with very simple yet complex aspects of science that made me grow as scientist.

And lastly, but not least, to all the readers who had the opportunity to read this thesis.

Thank you all.
Sincerely,

João Santos

.

This work was supported by the Portuguese Foundation for Science (FCT) through the doctoral grant PD/BD/105896/2014 from the ProRegeM PhD Programme (PD/00117/2012).

ABSTRACT

Despite the remarkable knowledge acquired in the formation of the heart during embryonic development and the molecular mechanisms involved in heart function and physiology, there is no efficient way to prevent adult heart disease and congenital heart disease (CHD). The transcriptional modulator Cited2 is required for normal embryogenesis of mice and humans, particularly for heart development. Indeed, mouse lacking *Cited2* alleles die *in utero* displaying many cardiovascular defects, and mutations in human CITED2 have long been associated with CHD. However, the exact role and the molecular mechanisms involving Cited2 during these processes are largely unknown.

Using mouse Embryonic Stem Cells (ESC) as a model system, we have established that the depletion of *Cited2* at the onset of differentiation resulted in a decline of ESC ability to generate cardiac cells. These cardiogenic defects in *Cited2*-depleted cells were rescued by treatment with a recombinant CITED2 protein.

To further investigate the mechanisms caused by the loss of *Cited2* in pluripotency and differentiation, we compared the gene expression profiles of control cells and *Cited2*-depleted cells upon differentiation. We determined that loss of *Cited2* expression delays the expression of early mesoderm transcription factors and cardiopoietic factors.

We found that the secretome of *Cited2* overexpressing ESC is enough to restore the emergence of beating colonies in *Cited2* depleted cells, upon differentiation. We identified WNT5a and WNT11 as two of the proteins enriched in the Conditioned Medium and crucial for rescuing cardiomyocyte differentiation defects caused by *Cited2* depletion.

Our results point that *Cited2* is a co-transcriptional activator of *Wnt5a* and *Wnt11* and that both proteins can restore cardiogenesis in *Cited2*-depleted cells. Additionally, using zebrafish as a model system, we demonstrated that WNT5a and WNT11 also rescued the development defects caused by *Cited2* depletion *in vivo*.

Collectively, our results show that WNT5a and WNT11 rescue cardiogenic defects caused by *Cited2* depletion both *in vitro*, as well as *in vivo*.

Keywords: CITED2, WNT5a, WNT11, Cardiovascular Defects, Embryonic Stem Cells.

RESUMO

Apesar do notável conhecimento adquirido sobre o desenvolvimento cardíaco, as doenças cardiovasculares e as doenças congénitas cardíacas (CHD), continuam a ser a principal causa de morte no mundo tanto nos adultos como em recém-nascidos. Estima-se que cerca de 1% da população mundial seja portadora de uma forma de CHD e, espera-se que este número aumente substancialmente nas próximas décadas. Um ponto crucial do desenvolvimento cardíaco é a expressão primorosamente controlada de fatores de transcrição e vias de sinalização cardíacas. Pequenos desvios na estrita expressão de fatores de transcrição e das vias de sinalização cardíacas, podem resultar num mau desenvolvimento do coração e no aparecimento de CHD, ou em casos mais extremos à morte do embrião ainda no útero. Dentro dos fatores de transcrição importantes para a formação do coração destacam-se inicialmente os genes importantes para a regulação da pluripotência OCT4, SOX2 e NANOG. Após a gastrulação, as células da mesoderme começam inicialmente a expressar BRACHYURY, MIXL1 e EOMES, e mais tarde o gene da mesoderme cardiaca MESP1. Por último, os progenitores cardíacos começam a expressar os fatores de transcrição cardíacos GATA4, NKX2.5, HAND2, TBX5, MEF2C e ISL1. As principais vias de sinalização cardíacas são a ACTIVIN/NODAL e as BMP, ambas pertencentes à via TGFβ, a via canónica e não canónica da WNT e por último, a via FGF.

Um ótimo modelo, *in vitro,* para se estudar os mecanismos moleculares, responsáveis pela formação do coração, são as células estaminais embrionárias (ESC). Algumas das características que tornam as ESC um bom modelo para estudar o desenvolvimento cardíaco são, o fato de se dividirem indefinidamente e de se diferenciarem em todas as células do adulto, após o correto estímulo, incluindo cardiomiócitos com a capacidade de produzirem focos de contração.

O fator de transcrição Cited2*,* é importante para o desenvolvimento cardíaco, uma vez que a remoção de ambos os alelos de *Cited2* no ratinho é letal ainda no útero, enquanto que mutações pontuais na proteína CITED2 foram previamente associadas com o aparecimento de CHD. No entanto, a função de CITED2 no desenvolvimento cardíaco e no aparecimento das CHD é ainda bastante desconhecida. Como tal, o objetivo deste trabalho foi estudar o papel de *Cited2* durante o processo de diferenciação cardíaco de ESC.

Para estudar o efeito de depleção de Cited2, durante a diferenciação cardíaca, utilizamos no laboratório uma linha de ESC com "*Knock-out"* condicional de Cited2*,* que

quando suplementado com 4-hydroxytamoxifen, no meio de cultura, resulta na excisão e depleção de Cited2. Começamos por ver que *Cited2* é expresso ao longo do processo de diferenciação cardíaca, sendo a sua expressão mínima no dia 2 de diferenciação. De seguida, vimos que a depleção de *Cited2,* no início da diferenciação, reduz a capacidade das ESC de se diferenciarem em cardiomiócitos. Para demonstrar que os defeitos cardíacos eram causados pela falta de *Cited2,* tratámos as ESC com uma proteína recombinante CITED2. Os resultados obtidos indicam que esta proteína reverte os defeitos cardíacos quando adicionado no segundo dia de diferenciação.

Para perceber melhor os mecanismos subjacentes à perda de função de CITED2, comparámos o perfil genético de células controlo (com Cited2) e células sem Cited2 no início da diferenciação. Neste sentido, realizámos uma análise de "microarrays", e observámos que as células sem *Cited2* têm vários genes, importantes para a diferenciação em endoderme e mesoderme desregulados. Comprovámos que a depleção de *Cited2* atrasa a expressão de fatores de transcrição da mesoderme (*Brachyury, Mixl1*) e da mesoderme cardíaca (*Mesp1* e *Eomes*). Observámos também, que a depleção de *Cited2* inibe a expressão de várias vias de sinalização cardíacas, o que nos fez colocar a hipótese de que a deficiência cardíaca, causada pela falta de *Cited2*, resultaria da desregulação da expressão de proteínas extracelulares.

Para o estudo de proteínas extracelulares considerámos o uso de Meio Condicionado (CM), ou seja, recorremos ao meio de cultura que contém, entre vários componentes, proteínas secretadas pelas células (secretoma). Portanto, através do secretoma de ESC, que sobre expressam *Cited2,* observámos que este é suficiente para recuperar os defeitos cardíacos causados pela falta de *Cited2*. Vimos também que o CM é crítico para a correta expressão do fator de transcrição *Brachyury*. Ao imunoprecipitarmos o CM contra WNT5a e WNT11, seguido de um Western Blot, identificámos que as proteínas WNT5a e WNT11 se encontravam enriquecidas no CM proveniente das células que sobre expressavam *Cited2*. Vimos também que estas duas proteínas eram críticas no CM, uma vez que quando as depletavámos, víamos que o CM perdia a sua capacidade de recuperar os defeitos cardiovasculares das células sem *Cited2*.

A WNT5a e a WNT11 são duas proteínas pertencentes à via não canónica da WNT e que cooperam para promover o desenvolvimento cardíaco, mais propriamente, para promover a formação do campo secundário cardíaco. Os nossos resultados, *in vitro*, apontam para que Cited2 seja um co-ativador transcricional do *Wnt5a* e do *Wnt11*. Mostrámos, que existe uma sinergia entre a WNT5a e WNT11 para corrigir os defeitos cardíacos causados

pela falta de *Cited2 in vitro*, não só em termos de diferenciação celular e surgimento de focos de contração, mas também para a correta expressão de fatores de transcrição da mesoderme e da mesoderme cardiaca.

Adicionalmente, para estudar a perda de função de *Cited2 in vivo,* estabelecemos um sistema de "Knockdown" de *Cited2* no peixe zebra *(Danio renio*). *Cited2*, é um gene conservado entre os vertebrados e, portanto, tal como acontece nos mamíferos, *Cited2* é necessário para o correto desenvolvimento do peixe zebra. Através das experiências realizadas, vimos que a falta de *Cited2* atrasa o desenvolvimento dos embriões às 24 horas pós fertilização (hpf), reduz o número de batimentos médio por minuto às 48 hpf e, causa letalidade e o surgimento de defeitos cardíacos em embriões de peixe zebra às 72hpf. Demonstrámos que estes defeitos eram específicos de *Cited2,* uma vez que conseguimos recuperar a maioria dos defeitos causados pela falta de *Cited2,* quando usámos a proteína recombinante CITED2. Por último, como acontece *in vitro*, a combinação da WNT5a e da WNT11 é capaz de compensar a falta de *Cited2,* também, *in vivo.*

Em suma, os nossos resultados indicam que a WNT5a e a WNT11 corrigem, *in vitro* e *in vivo*, os defeitos cardíacos causados pela perda de *Cited2,* sendo o nosso objetivo, no futuro, desenvolver uma nova opção terapêutica para reduzir o número de pacientes com CHD.

Palavras-chave: CITED2, WNT5a, WNT11, Defeitos Cardíacos, Células estaminais embrionárias.

TABLE OF CONTENTS

LIST OF FIGURES

LIST OF TABLES

ABBREVIATIONS

Δneo	Neomycin Resistant Gene
4HT	4-Hydroxytamoxifen
Ao	Aorta
APC	Adenomatosis polyposis coli
AS	Aortic Stenosis
ASD	Atrial Septal Defects
AV	Atrioventricular
BMP	Bone Morphogenic Protein
bp	Base Pairs
bpm	Beating per Minute
BSA	Bovine Serum Albumin
Cer1	Cerberus
cDNA	Complementary DNA
CH1	Cysteine-Histidine rich domain 1
CHD	Congenital Heart Disease
CITED2	CBP/p300 Interacting Transactivator with ED tail rich family member 2
CM	Conditioned Medium
CNCC	Cardiac Neural Crest Cell
CoA	Coarctation of Aorta
CPC	Cardiac Progenitor Cells
CR	Conserved Regions
CRE-ERT	Cre fused to a domain of the Estrogen Receptor
DEGS	Differentially Expressed Genes
DKK1	Dickkopf related protein 1
DMEM	Dulbecco's Modified Eagle Medium
DNA	Deoxyribonucleic Acid
DPF	Days Post-Fertilization

DVL	Dishevelled
EB	Embryoid Body
eGFP	Enhanced Green Fluorescent Protein
ESC	Embryonic Stem Cells
EtOH	Ethanol
FBS	Fetal Bovine Serum
FC2	Flag-tagged *CITED2*
FGF	Fibroblast Growth Factor
FHF	First Heart Field
FLK	Fetal Liver Kinase
FZD	Frizzled
GATA4	GATA binding protein 4
GMEM	Glasgow Minimum Essential Medium
GSK	Glycogen Synthase Kinase
hESC	human Embryonic Stem Cells
Hh	Hedgehog
HIF	Hypoxia-Inducible Factor
Hprt	Hypoxanthine guanine phosphoribosyltransferase
HRP	Horseradish Peroxidase
HSC	Hematopoietic Stem Cells
ICC	Immunocytochemistry
ICM	Inner Cell Mass
IT	Inflow Tract
IP	Immunoprecipitation
iPSC	induced Pluripotent Stem Cell
ISL1	Islet 1
JNK	c-Jun N-terminal Kinases
KD	Knockdown
KO	Knock-Out

LA	Left Auricula
lacZ	β-Galactosidase
LEF	Leukemia Enhancer factor
LIF	Leukemia Inhibitory Factor
LogFC	Logarithm Fold Change
LRP	Lipoprotein Receptor Related Protein
LV	Left Ventricle
MAPK	Mitogen-Activated Protein Kinase
MEF	Mouse Embryonic Fibroblasts
MEM	Minimum Essential Medium
NEAA	Non-Essential Amino Acids
MHC	Myosin Heavy Chain II
mEpiSC	Mouse Epiblast Stem Cells
mESC	mouse Embryonic Stem Cells
MO	Morpholino
n/s	non-significant
NKX2.5	Nk2-related homeobox 5
ORI	Origin of Replication
OT	Outflow Tract
PBS	Phosphate Buffered Saline
PBS-T	PBS with 0.1% Tween 20
PCA	Principal Component analysis
PCP	Planar Cell Polarity
PDA	Patent Ductus Arteriosus
pROSA	ROSA Promoter
P/S	Penicillin-Streptomycin
PMSF	Phenylmethylsulfonyl Fluoride
PS	Primitive Streak
PSC	Pluripotent Stem Cell

PSt	Pulmonary Stenosis
PT	Pulmonary Trunk
qPCR	Quantitative Polymerase Chain Reaction
RA	Right Auricula
RNA	Ribonucleic Acid
ROCK	Rho-associated Protein Kinase
RT	Room Temperature
rtTA	Reverse Tetracycline Transactivators
RV	Right Ventricle
SHF	Second Heart Field
SpM	Splanchnic Mesoderm
SRJ	Serine-Rich Junction
T	Brachyury
TAD	Transactivation Domain
TBX	T-box
TCF	T-cell factor
TE	Trophectoderm
TGA	Transposition of the Great Arteries
TGF	Transforming Growth Factor
TOF	Tetralogy of Fallot
TRE	Tetracycline Response Elements
VSD	Ventricular Septal Defect
WB	Western Blot

CHAPTER I

GENERAL INTRODUCTION

"It's a world full of children that die far, far before their time, in the arms of their parents as they sob and they mourn and they curse the giant that is congenital heart disease."

by Lexi Behrndt

1.1 The Heart

The heart is a midline structure located in the superior and posterior region of the mediastinum. The heart is the first organ to form and ensures the pumping of nutrients and waste removal as soon as the body reaches a point where passive diffusion is no longer enough to ensure the survival of the embryo (1).

1.1.1 Congenital Heart Disease

Cardiovascular diseases are the leading cause of death and morbidity in developed countries (2, 3). Cardiac complications are a complex pathology, in which multi-genetic and environmental factors often interplay, thus making them difficult to predict and prevent.

Congenital heart disease (CHD), refers to structural and functional anomalies of the heart that occur prior to birth. Early heart defects are a common cause of mortality and it is expected that nearly 1% of newborns manifest some form of CHD (4). Worryingly, these numbers do not take into consideration the embryos or fetus which are lost before birth. In fact, it is estimated that nearly 30% of the miscarriages, in developed countries, are due to heart defects (5). In the last decades, novel surgical procedures and advances in diagnoses have drastically decreased the number of deaths due to CHD (6). Nonetheless, many children and adults with heart defects need lifelong medical surveillance and, this raises new issues such as the increased risk for the offspring of patients with a CHD to contract a CHD.

1.1.2 Mutations in Congenital Heart Disease

CHD are caused by a combination of genetic and environmental factors. Environmental factors are usually associated with maternal exposure to environmental teratogens or metabolic disorders (7, 8). The genetic causes of CHD are diverse, but chromosomal aneuploidy remains the largest genetic cause of CHD. For example, nearly half of the individuals with Trisomy 21 or Turner Syndrome, manifest some form of CHD (9, 10).

More recently, it was found that cardiac defects are not necessarily due to big global changes in the genomic content but rather from an altered expression dosage of specific genes (11). A good example is the deletion found in the chromosome 22q11 syndrome, also known as the DiGeorge syndrome. Although more than 30 genes are involved in the DiGeorge syndrome, studies have shown that the cardiac defects were caused by the loss of T-box (TBX)1 gene. Tbx1 is important for proper cardiac development, and its haploinsufficiency matches the defects observed in patients and animals suffering from DiGeorge syndrome (12, 13).

Table 1.1 Most common types of CHD worldwide (14).

Types	Description	Prevalence
Coarctation of Aorta (CoA)	Narrowing of the aorta, resulting in a reduced flow of blood throughout the body	5%
Atrial Septal Defects (ASD)	Anomaly in the wall between the left and right atriums.	13%
Tetralogy of Fallot (TOF)	Combined effects of PSt, VSD, RV hypertrophy and overriding aorta (aorta receives blood from both RV and LV)	5%
Patent Ductus Arteriosus (PDA)	Failure in closure of the ductus arteriosus. Ductus arteriosus is a blood vessel that connects the pulmonary artery to the aorta which closes at birth.	10%
Pulmonary Stenosis (PSt)	Narrowing between the RV and the pulmonary artery which results in a reduced flow of blood to the pulmonary artery.	8%
Aortic Stenosis (AS)	Narrowing of the aortic valve, resulting in a reduced flow of blood throughout the body	4%
Ventricular Septal Defects (VSD)	The anomaly in the wall between the left and right ventricle.	34%

Thus, CHD is usually associated with genes which function is essential for cardiac development. As such, non-syndromic CHD patients are quite likely to have mutations either in a transcription factor or a signalling pathway involved in cardiogenesis. The best characterized cardiac defects and their worldwide prevalence are presented in Table 1.1, and the most common and critical mutations in transcription factors or signalling molecules associated with these defects are presented in Figure 1.1.

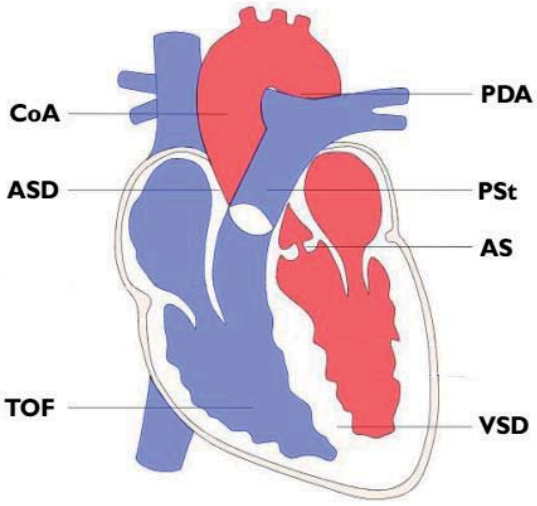

Gene	Phenotype
Cited2	ASD and VSD
Fog2	TOF
Gata4	ASD, PSt, VSD and TOF
Gata6	ASD, TOF, PSt, PDA and VSD
Hand2	TOF, VSD
Nkx2.5	ASD, VSD, TOF and COA
Tbx1	TOF
Tbx5	ASD and VSD
Tbx20	ASD and VSD
Zic3	PSt, ASD and VSD

Gene	Phenotype
ACVR2B	PSt
CFC1	TOF, ASD and VSD
FOXH1	TOF
GDF1	TOF
JAG1	TOF
LEFTY2	COA
NODAL	TOF
NOTCH1	AS and COA
SMAD6	AS and COA
VEGF	COA

Figure 1.1 Common gene mutations in CHD patients and their phenotype. Blue Box Transcription Factors. Orange Box Signalling Pathways. Abbreviations: CoA, Coarctation of Aorta; ASD, Atrial Septal Defects; TOF, Tetralogy of Fallot; PDA, Patent Ductus Arteriosus; PSt, Pulmonary Stenosis; AS, Aortic Stenosis; VSD, Ventricular Septal Defects. Adapted from (11).

1.1.3 The Mammalian Development

Mammalian embryogenesis begins with the totipotent unicellular zygote, which can form both fetal and extraembryonic lineages. While the fetal cells are responsible for originating most of the cells that constitute the adult body, extraembryonic tissue nourishes the fetus and provide patterning signals that direct embryogenesis (15). The zygote continues to divide and eventually forms a structure of cells called blastocyst. The blastocyst is a spherical structure delimited by cells forming an outer structure, termed the trophectoderm (TE), and cells gathering inside of this structure termed the inner cell mass (ICM). The ICM is composed by bipotent progenitor cells that can give rise to the epiblast and the primitive endoderm.

As the blastocyst expands and implants into the uterine wall, it undergoes dramatic morphological changes. At this point, the uncommitted epiblast cells undergo lineage specification during gastrulation. Gastrulation is the developmental process through which the three fetal germ layers, definitive endoderm, mesoderm, and definitive ectoderm are formed. (Figure 1.2) (16).

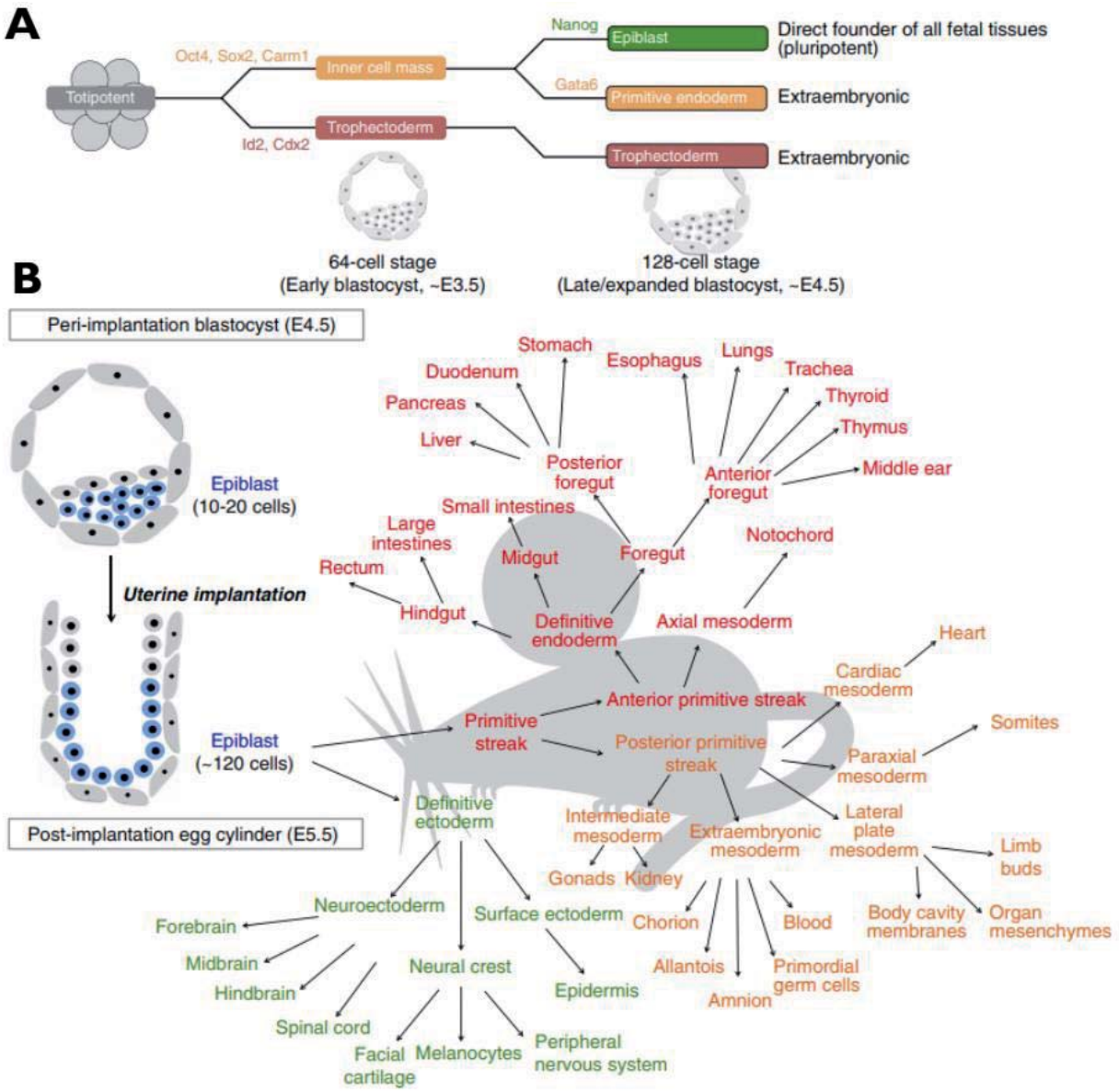

Figure 1.2 Early steps of development. A) Totipotent cells go through successive cell divisions until the development of the blastocyst. Epiblast cells are isolated from the ICM of the blastocyst. B) Post uterine implantation epiblast cells differentiate into the three germ layers: ectoderm, mesoderm, and endoderm. These three germ layers are responsible for the development of most of the tissues that comprise the adult body. Image adapted from (17).

Cells derived from the definitive endoderm, hereafter simply referred as endoderm, originate many of the internal parts of the body, including the gastrointestinal tract, the liver, the pancreas, and other glands. On the other hand, the definitive ectoderm, hereafter referred simply as ectoderm, gives rise to the epidermis, the outermost skin layer, mammary glands, and the central and peripheral nervous system.

The third and last germ layer is the mesoderm, which is divided into three major areas: the paraxial, intermediate and lateral plate. The paraxial mesoderm is the area closest to the primitive streak (PS) and gives rise to the somites and the muscles. The intermediate mesoderm gives rise to the urogenital system. On either side of the intermediate mesoderm resides the lateral plate mesoderm. The lateral plate mesoderm splits into somatic and splanchnic layers. The somatic mesoderm forms the connective tissue of the body wall while, the splanchnic mesoderm (SpM) forms the visceral layer, blood vessels and, most of the cells of the heart.

1.1.4 The development of the human heart

At around 18 days post-fertilization (dpf) in humans, two tubes called endothelial tubes will fuse to form the primitive heart tube. At 20dpf the linear heart tube is composed of an inner cell layer called the endocardium and an outer cell layer called the myocardium where the first beating cells emerge. At 23dpf the cardiac tube starts bending and the cardiac looping occurs so that the mature outflow tract (OT) and inflow tract (IT) are aligned anteriorly. At this stage, the heart is composed of a primitive right ventricle (RV), a primitive left ventricle (LV) and a single primordium atrium. As the primitive heart tube elongates, it begins to fold eventually forming an S shape. The heart becomes complete at the end of the fifth week of development (Figure 1.3) (1, 18, 19). Apart from proepicardium cells, derived also from the SpM, and cardiac neural crest cells (CNCC), derived from the ectoderm, all structural cells present in the main heart derive from a common cardiac progenitor cells (CPC). The CPC can originate three different types of cells: cardiomyocytes, endothelial cells and smooth muscle cells (20). The heart is formed of three layers: the endocardium, the myocardium and the epicardium. The innermost layer is the endocardium where endothelial cells, some smooth muscle cells, and CNCCs can be found. The myocardium is mostly composed of cardiomyocytes, while the outermost layer, the epicardium, is composed of proepicardium cells (21). Proepicardium cells are multipotent cells that contribute to the development of the epicardium, but can also differentiate into fibroblasts, cardiomyocytes and coronary vessels (22). On the other hand, CNCC, of ectoderm origin, contributes to the development of the aorta and pulmonary trunk (21).

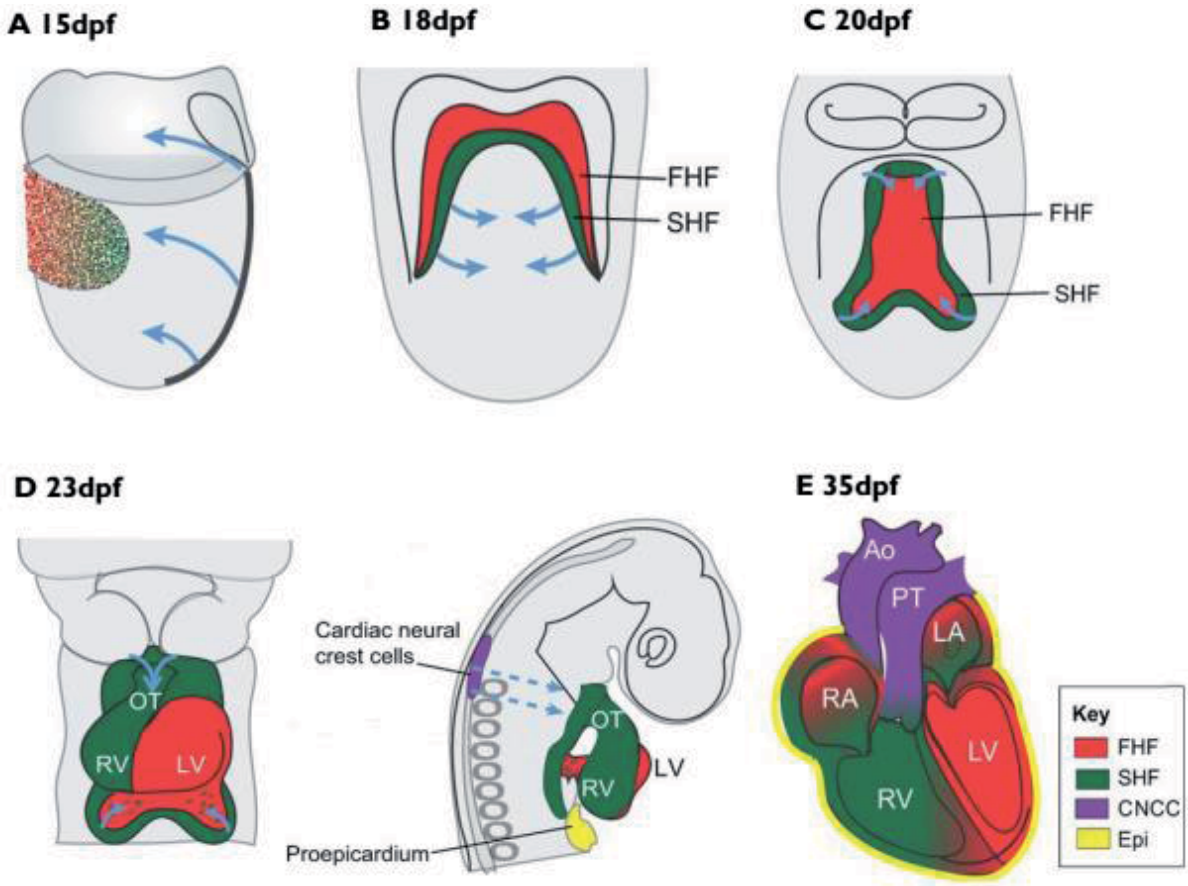

Figure 1.3 Embryology of the human heart. A) After gastrulation two pools of CPC will give to the heart: the FHF (red) and the SHF (green). B) Migration of the FHF progenitors to form the primitive heart tube while the SHF progenitors are proliferating. C) Migration of the SHF progenitors. D) Bending and looping of the heart. The different chambers of the heart start to be evident. The contribution of the cells of the proepicardium and cardiac neural crest cells to the development of the heart. E) The heart becomes complete at 35 dpf. Abbreviations: FHF, First Heart Field; SHF, Second Heart Field; RV, Right Ventricle; LV, Left Ventricle; OT, Outflow Tract; AO, Aorta; PT, Pulmonary Trunk; RA, Right Auricula; LA, Left Auricula; CNCC, Cardiac Neural Crest Cells; Epi, Epicardium, Adapted from (23).

1.1.5 First Heart and Second Heart Field

The embryonic heart was initially thought to derive from a unique population. This idea was first challenged in 1977 when a research group found that the OT region did not derive from the initial cells that comprise the heart tube (24). However, it was only in 2001 that three distinct groups, using different cell lineage tracking methods, confirmed the existence of two main and distinct groups of CPC: the progenitors derived from the first heart field (FHF) and the progenitors derived from the second heart field (SHF). (25-27).

The FHF refers to the initial CPC that differentiate to form the initial heart tube. The SHF refers to the second wave of CPC that do not differentiate until the linear tube starts looping. As soon as the FHF progenitors migrate, the SHF progenitors are maintained in a proliferative state without differentiating. This process is tightly regulated by a specific set of transcription factors and signalling molecules. The cells derived from the FHF will later contribute to the development of the LV and the atria. On the other hand, the SHF originates the RV, OT and will also contribute to the development of the atria (Figure 1.3).

Interestingly, the segregation between FHF and SHF progenitors has been reported to occur very early during gastrulation. Indeed, clonal analysis of cardiovascular progenitors in a temporally controlled manner during gastrulation showed two temporally distinct pools of progenitors which are already committed either to FHF or SHF (28).

The first gene identified to play a critical role in the SHF was the gene encoding the transcription factor *ISLET1* (*ISL1*) (29). Lineage tracing analysis using an *Isl1*-CRE driver system in mice showed, that Isl1+ cells contributed to the development of the OT, RV, and Atria (30). Lack of ISL1 results in structures, derived from the SHF, failing to form while structures from the FHF were not affected (29). Subsequent studies have provided evidence that low levels of ISL1 expression are also present in the FHF (31). Even so, ISL1 remains a key regulator and marker of the SHF cells.

Cells of the SHF are initially highly proliferative to ensure an expansion of CPC. This balance between proliferation and differentiation is maintained by signalling pathways. Fibroblast Growth Factor (FGF), canonical Wnt and Hedgehog (Hh) signalling pathways have been shown to promote the proliferation of CPC. Meanwhile Bone Morphogenic Proteins (BMP), non-canonical Wnt and Notch have an opposite effect and force the differentiation and maturation of the cells (32, 33) (Figure 1.4).

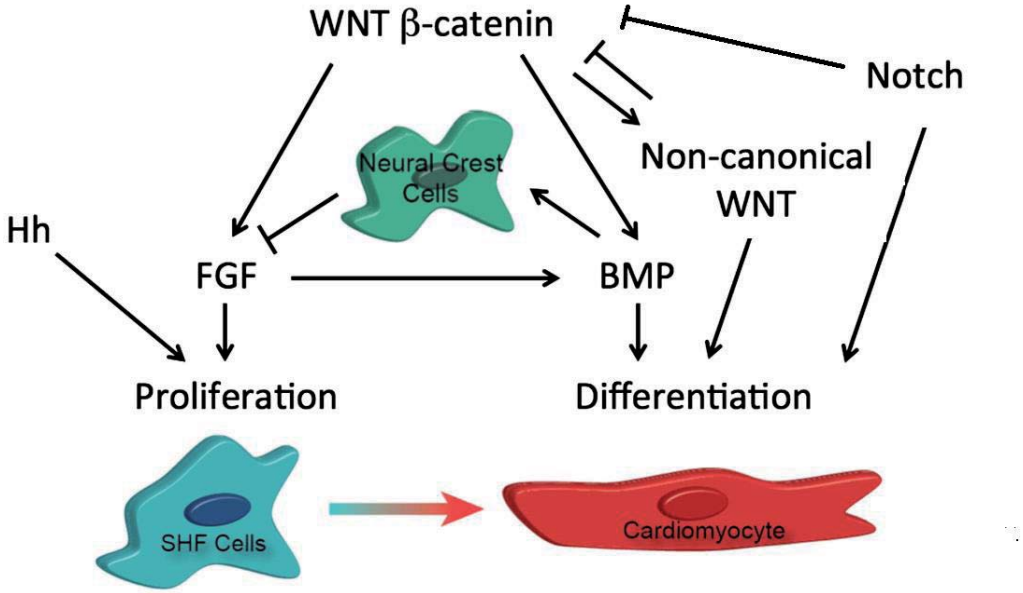

Figure 1.4 Pathways involved in SHF proliferation and differentiation. Hedgehog (Hh), Fibroblast growth factor (FGF) and Wnt β-catenin lead to SHF proliferation while Notch, BMP, and Non-canonical Wnt lead to SHF differentiation. Adapted from (34).

1.2 Molecular Mechanism in Cardiogenesis

The mammalian development is a tightly regulated spatiotemporal process. The molecular mechanisms involved in cardiogenesis are very well conserved across mammals both *in vitro* and *in vivo*. In this chapter, we expose both the main transcription factors as well as the signalling pathways involved in cardiogenesis.

1.2.1 Transcription Factors

A transcription factor is a protein that controls the transcription of genes by binding to a specific deoxyribonucleic acid (DNA) sequence. The transcription factors may act as activators or repressors by enabling or disabling the ability of the ribonucleic acid (RNA) polymerase to bind to a specific gene. Here, we focus our attention on the most important transcription factors at specific time points for the establishment and maintenance of pluripotency, mesoderm specification and cardiac differentiation (Figure 1.5).

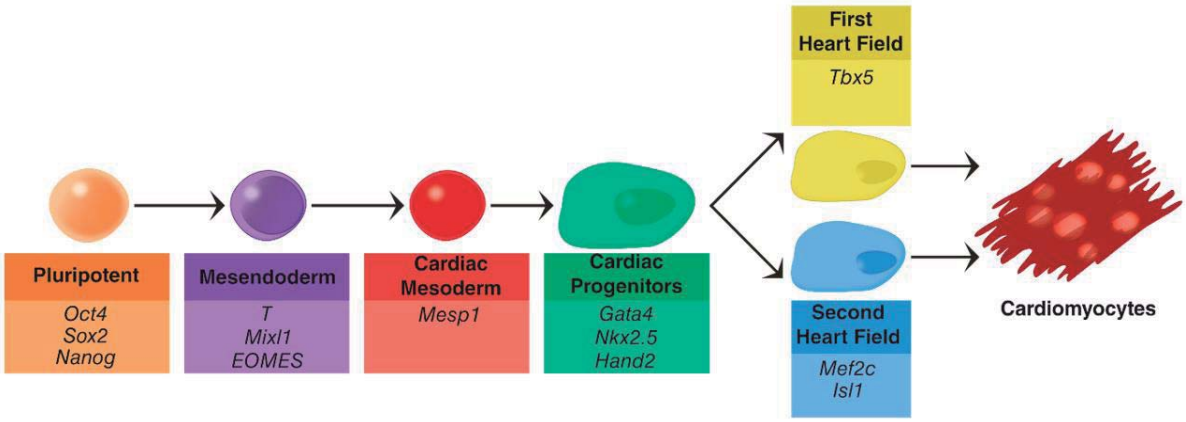

Figure 1.5 Key transcription factors involved in cardiac development. Pluripotent cells are characterized by the expression of *Oct4, Sox2,* and *Nanog*. Upon gastrulation, early mesoderm cells express *T, Mixl1, and Eomes* and late mesodermal cells, that become cardiac commitment, start to express *Mesp1*. CPC express *Gata4, Nkx2.5,* and *Hand2*. CPC of the FHF start to express more *Tbx5,* whereas progenitors of the SHF start to express *Mef2c* and *Isl1*. Both progenitors can differentiate into cardiomyocytes.

1.2.1.1 Pluripotency

Oct4, Sox2, and Nanog are the master regulators in the pluripotency. These three genes regulate each other's expression in a positive feedback loop. These genes are expressed in the pluripotent section of the mouse embryo, prior to implantation and gastrulation. Cells expressing these three transcription factors, generally maintain the ability to differentiate into three germ layers.

Oct4 was the first key transcription factor identified in pluripotency (35). OCT4 is encoded by the gene *POU5f1* a member of the POU family. OCT4 expression is activated prior to the 8-cell stage and remains highly expressed in the ICM of the blastocyst. After gastrulation OCT4 expression becomes restricted in the primitive ectoderm and the mesodermal precursors that will give rise to the primordial germ cells (36). The Knock-out (KO) of *Oct4* in mice results in defective epiblast development and early embryonic lethality (37, 38). The depletion of OCT4 in embryonic stem cells (ESC) results in spontaneous differentiation and impaired ability to differentiate into mesoderm cell fates (39). Ectopic expression of OCT4 results in primitive endoderm and mesoderm differentiation (40).

Sox2 is another transcription factor crucial for the maintenance of pluripotency. SOX2 is highly expressed in the ICM of the blastocyst and post gastrulation is found expressed in the early ectodermal lineages (41). Like Oct4, the KO of *Sox2* in mice results in defective epiblast development and early embryonic lethality (42). Loss of SOX2 considerably compromises the pluripotent state of both mouse and human ESC as shown by the changes in cell morphology, loss of pluripotent marker expression and their spontaneous differentiation into PS (43-45). On the other hand, overexpression of SOX2 in ESC leads to a predisposition of these cells to differentiate into neuroectodermal cell fate and inhibition of PS differentiation (45, 46).

Nanog is the most recently identified core pluripotent gene. NANOG is expressed in the morulae, then in the ICM until gastrulation (47). Comparable to the other previously mentioned genes, the KO of *Nanog* is early embryonic lethal with elevated ICM apoptosis (48). The depletion of NANOG in mouse ESC (mESC) results in premature mesoderm and ectoderm differentiation (49, 50). Moreover, while *Nanog* null mESC can be maintained, these cells ability to self-renewal is severely affected (51). Overexpression of NANOG results in enhancement of human ESC (hESC) commitment to PS differentiation and inhibition of

ectoderm differentiation (45). Surprisingly, only overexpression of NANOG has been associated with pluripotency maintenance and self-renewal (47, 52, 53).

1.2.1.2 Mesoderm

Upon gastrulation, pluripotent stem cells (PSC) start to lose their potency. PSC either become ectoderm or, mesendoderm. Indeed, mesendoderm is a term used to define cells that can still differentiate into both mesoderm or endoderm. All cells from mesendoderm and early mesoderm co-express two transcription factors: Brachyury and Mixl1.

Early mesoderm commitment is mostly controlled by BRACHYURY, also known as T, expression. KO of *Brachyury* is lethal, with embryos dying at very early stages due to multiple defects in the mesoderm-derived tissues including, complete lack of limb development. BRACHYURY expression is first found in the ICM. However, its peak of expression becomes more prominent during the PS. While both mesoderm and endoderm cells express BRACHYURY, endoderm cells express low levels of BRACHYURY while mesoderm cells express high levels of BRACHYURY (54). BRACHYURY expression is silenced in pre-cardiac mesoderm (55).

The earliest known committed cardiac precursors express the transcription factor Eomesodermin (Eomes) (56). The transient expression of EOMES promotes cardiovascular fate during ESC differentiation. Moreover, EOMES is important for activating *MESP1* a key regulator of cardiovascular cell fate (57). Mesp1 was first identified as a marker of early cardiac mesoderm in 1999 (58). A β-Galactosidase (lacZ) under the control of the *Mesp1* promoter showed that all MESP1 expressing cells contribute to the heart (58). However, the *Mesp1* lineage is not specific to the heart and also contributes to the mesenchyme and the limbs (59). Loss of MESP1 results in cardiac defects attributed to defects in cell migration and embryonic lethality by E10.5 (58). On the other hand, its gain of function strongly increases cardiac differentiation both *in vitro* and *in vivo* (60, 61). More recently, Mesp1 was found to be required for cells to exit the pluripotent state and promote, migration and cardiovascular specification (62). Furthermore, temporally inducible *Mesp1* lineage tracing shows that at E6.5, *Mesp1*+ cells will form the LV, whereas *Mesp1*+ cells at E7.25 will form the RV, OT, and atria. This

suggests that Mesp1 progenitors consist of two distinct pools of progenitors restricted to either FHF or the SHF (28, 62).

1.2.1.3 Cardiac Mesoderm

Cardiac development is a fine-tuned process controlled by key transcription factors. The core transcription factors include Nkx2.5, Gata4, Mef2c, Tbx5, Isl1, and Hand2. These factors regulate each other's expression and affect common downstream targets (Figure 1.6).

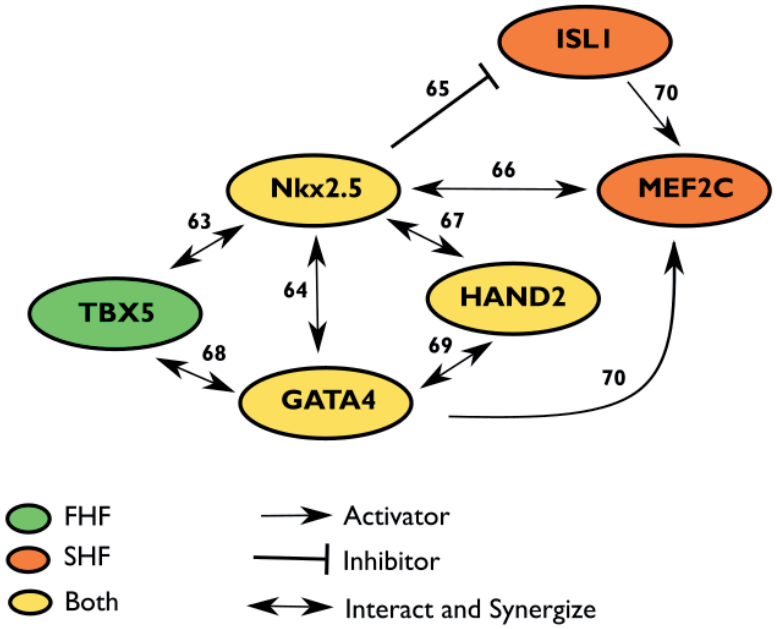

Figure 1.6. Cardiac Transcription factors interactions. Numbers indicate published paper where interaction has been identified.

The discovery of *Nk2-related homeobox 5* (*Nkx2.5)* in the fly was the founding event in the molecular study of heart development (71). The subsequent analysis of *NKX2.5* led to the identification of the first mutated gene in a CHD patient (72). Mutations of NKX2.5 remains the most commonly identified in CHD patients, accounting to approximately 4% of the patients suffering from CHD (73). Its expression is first detected in CPC and its expression remains high in cardiac tissue throughout adulthood (73). *Nkx2.5* is essential for heart development and mice lacking its expression show abnormal morphogenesis of the heart and abnormal LV resulting in embryonic lethality at E9.5 (74).

The zinc finger transcription factor GATA binding protein 4 (Gata4*)* is expressed in cells of the cardiac lineage through adulthood and plays an important role in cardiac development. The *Gata4* KO in mice results in embryonic lethality by E10.5 with abnormal ventral folding, failure of midline fusion of the heart, and extensive endoderm defects (75). Furthermore, GATA4 is known to regulate the transcription of multiple genes encoding contractile elements like the Myosin Heavy Chain (MHC) and α-ACTININ (76). Interestingly, overexpression of GATA4 in ESCs directs cells towards endoderm rather than cardiac mesoderm. However, endoderm cells that overexpress *GATA4,* produce paracrine factors that stimulate adjacent cells to differentiate into cardiac mesoderm (77). Moreover, forced expression of GATA4 in mesoderm cells forced the expression of cardiomyocyte-specific markers (78).

Myocyte enhancer factor 2 (Mef2) is a family of transcription factors that play an important role in cardiac differentiation. The family of MEF2 is composed of 4 genes *MEF2A, MEF2B, MEF2C* and *MEF2D*, all expressed in cardiac development with partly redundant function. One of the well-described MEF2 genes in cardiac cell fate is Mef2c. *Mef2c* null mice die at E9.5 with the heart tube failing to undergo cardiac looping and apparent lack of RV is observed (79, 80).

Tbx5 has been associated with cardiovascular development ever since, *TBX5* mutations have been associated with Holt-Aram syndrome (81, 82). TBX5 is expressed during the development of the heart and the limbs (83, 84). In mice, TBX5 is expressed around E8.0 throughout the cardiac crescent. At E8.5 it starts to become expressed in the cells that will give rise to the atria and, at E9.0 it becomes expressed in the LV (83). Mice embryos that lack *Tbx5* die *in utero* around E10.5 with abnormal heart tube, hypoplastic LV and complete absence of forelimbs (85, 86).

Isl1 has been highly associated with the SHF. Using an *Isl1*-CRE system that permits the labeling of *Isl1*-derived cells showed, that these cells mostly contribute to the cells of the RV, OT, and atria (29). Indeed, the KO of *Isl1* in mice embryos results in their death at midgestation with an absence of OT and RV and reduced atria (29). Transcription of *Isl1* is shut off as soon as the CPC enter the forming embryonic heart, suggesting that Isl1 is required for the proliferation, expansion, and migration of CPCs but not for differentiation (87). Isl1 was initially hypothesized to be a specific marker of the SHF. However, in some studies, ISL1 was shown to be expressed in CPC common to FHF and SHF (88).

Finally, Hand2 is essential for the development of the heart, brachial arches and limb buds (89). During heart development, HAND2 is expressed in the RV, OT and the epicardium (90). The KO of *Hand2* results in embryonic lethality, partly due to defects in the aortic arch arteries and RV (89). Hand2 is essential for CNCC in the OT where loss of *Hand2* reduces the number of CNCC, affecting the survival of the SHF progenitors and proepicardial cells differentiation (91-93). In humans, mutations in *HAND2* are mostly associated with CHD with VSD (94).

1.2.2 Signalling Pathways

Signalling between cells coordinates the complex event of cardiac development that culminates in the development of the heart. Specific factors are released from cells that, at a given time point of development, direct and control differentiation, proliferation or migration of multiple neighbouring cells. Since every signalling pathway may affect cardiogenesis, I will give an overview of the pathways having a well-established role and that has been determined to be crucial for heart development (Figure 1.7).

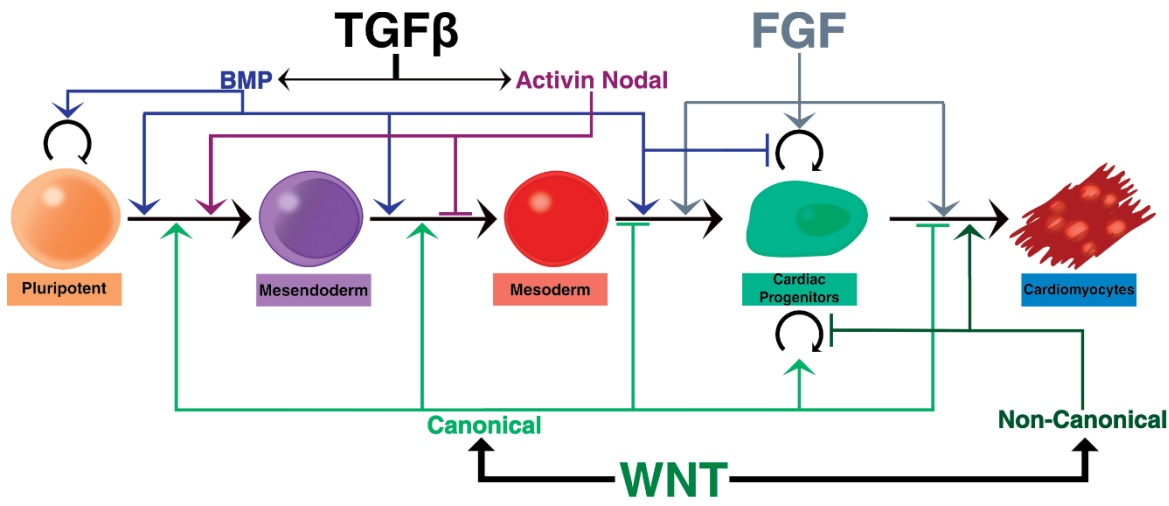

Figure 1.7 Key Signalling Pathways involved in cardiac development. ACTIVIN/NODAL (Pink line) and BMP (Blue line) from the TGFβ pathway, Canonical (Light Green line) and Non-Canonical (Dark Green Line) WNT pathway and FGF (Grey Line) pathway activate or repress cardiac development depending on the time of activation.

1.2.2.1 TGFβ Signalling Pathway

The Transforming Growth Factor β (TGFβ) signalling pathway is involved in many cellular processes in both the adult organism and developing embryo including cell growth, cell differentiation, apoptosis, and cellular homeostasis. The TGFβ superfamily ligands bind to the TGFβ receptor type II, which recruits and phosphorylates TGFβ receptor type I. This results in the activation and accumulation of SMAD2/3 in the nucleus where they associate with other co-transcription factors and regulate the expression of target genes. The TGFβ superfamily ligands includes both Bmp and Activin/Nodal (Figure 1.8b) (95).

Bmp were originally discovered because of their ability to induce the development of bone and cartilage in rabbits (96). The canonical Bmp signalling is Smad dependent. In the canonical pathway, BMP initiate the signal transduction cascade by binding to the type I/II serine/threonine kinase receptors and forming a heterotetrameric complex. The constitutively active type II receptor then transphosphorylases the type I receptor which results in the phosphorylation of SMAD1/5/8. Phosphorylated SMAD1/5/8 associates with Smad4 and the complex translocates into the nucleus to regulate gene expression (Figure 1.8f).

Several Bmp are essential during embryogenesis, most noticeable for mesoderm and cardiac development both *in vitro* and *in vivo (97, 98)*. Indeed, *Bmp2* homozygous mutants are embryonic lethal with abnormal development of the heart (99). The BMP2 expression is detected in mesoderm, CPC and myocardium (100). On the other hand, *Bmp4* deficient mice do not differentiate into mesoderm, indicating that BMP4 might be important during gastrulation (101). Moreover, BMP4 forces PSC to differentiate into mesoderm by increasing the expression of BRACHYURY and CDX2, while inhibiting endoderm differentiation (102). However, BMP expression beyond cardiac mesoderm forces cells to differentiate into epicardial lineages instead of cardiomyocytes (103).

Activin/Nodal exert their biological effects by binding to the heterodimeric complexes activin-like kinases (ALK) receptors. This results in the phosphorylation and activation of SMAD2 and SMAD3. Phosphorylated SMAD2 and SMAD3 associates with SMAD4 and translocates to the nucleus, where it regulates gene expression through its association with transcription factors (Figure 1.8g) (104).

Activin/Nodal are necessary at the early epiblast stage during implantation. Activin/Nodal signalling has been shown to maintain pluripotency of both human and mouse ESC (105, 106). Loss of *Activin/Nodal* signalling in PSC results in loss of pluripotency markers and premature ectoderm differentiation (107). Moreover, Activin/Nodal signalling is important in germ layer specification and early ESC commitment (105). Absence, of ACTIVIN/NODAL, drives cells to differentiate into ectoderm, while its expression induces mesendoderm. Upon the mesendoderm, high levels of ACTIVIN/NODAL promote endoderm, while low levels of ACTIVIN/NODAL promote mesoderm (108, 109).

1.2.2.2 Wnt Signalling Pathway

Wnt proteins play a critical role in cell fate decisions, cell proliferation, and cellular migration. The Wnt signalling begins with the secretion of the Wnt proteins outside of the cell. Wnt proteins can be divided into two groups: the canonical and non-canonical Wnts (Figure 1.8A).

The Canonical Wnt Signalling Pathway refers to a pathway where β-CATENIN acts as a signal transducer (33, 110-112). In the absence of Wnt proteins, β-CATENIN is phosphorylated by a destruction complex composed of glycogen synthase kinase (GSK)-3, adenomatosis polyposis coli (APC) and AXIN and subsequently ubiquitylated and targeted for degradation by the proteosome. In the presence of WNT, the Frizzled (FZD) and co-receptor lipoprotein receptor-related protein (LRP)5/6 are activated. This results in the recruitment of the Dishevelled (DVL) proteins, which prevents the degradation of β-CATENIN, resulting in its accumulation in the nucleus. β-CATENIN is then free to act as a transcriptional co-activator of the transcription factors T-cell factor (TCF) and Leukemia enhancer factor (LEF) (Figure 1.8d). On the other hand, Non-Canonical Wnts, do not rely on β-catenin as a signal transducer. These Wnts activate different co-receptors, the best described are Ror1/Ror2, Ryk and PTK. Two Non-Canonical Wnt Pathways have been suggested, the Wnt/Ca^{2+} Pathway and the Planar Cell Polarity (PCP) pathway. In the case of the Ca^{2+} pathway, Wnt activation results in an increase of intracellular calcium levels, and activation of CAMKII, PKC and NFAT transcription factors in the nucleus. On the other hand, in the PCP pathway Wnt proteins activate small GTPASES RHOA and RAC1 which leads to the activation of c-Jun N-

terminal kinases (JNK) and Rho-associated protein kinase (ROCK) in the nucleus (Figure 1.8e)(113).

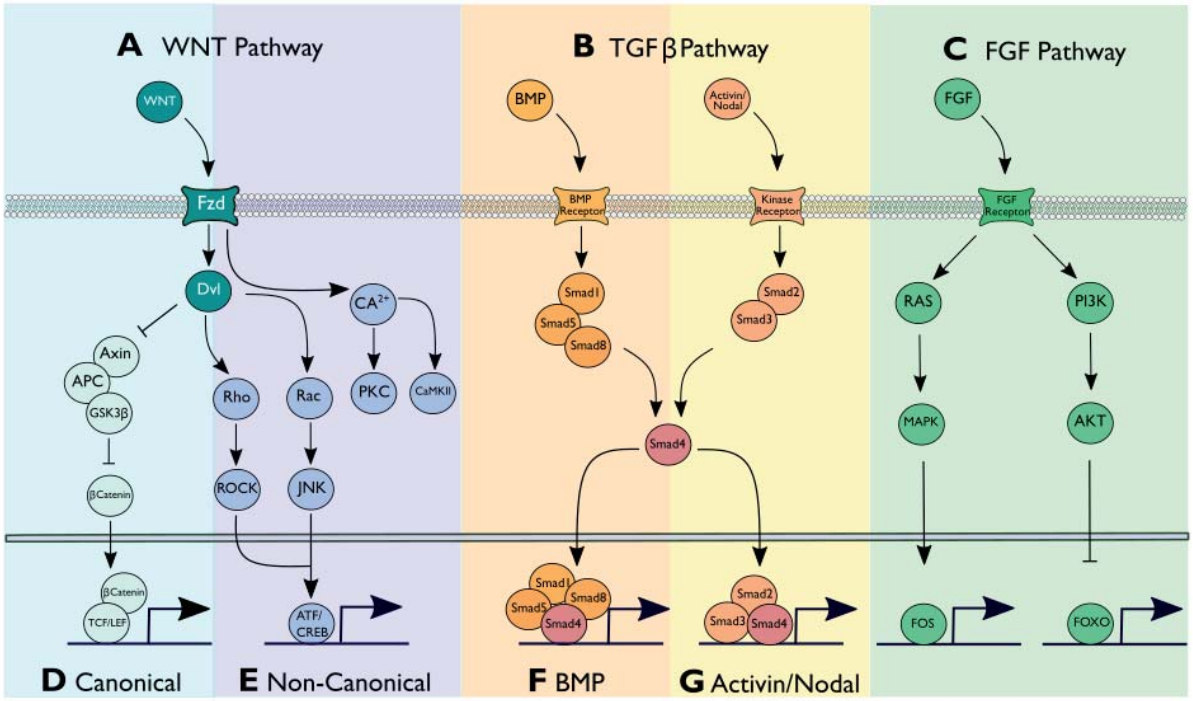

Figure 1.8 WNT, TGFβ, and FGF Signalling Pathways. A Diagram presenting the most important pathways involved in cardiogenesis. A) WNT Signalling Pathway; B) TGFβ Signalling Pathway; C) FGF Signalling Pathway. D) Canonical if WNT activity is β-catenin dependent; E) Non-Canonical If WNT activity is β-catenin independent; F) BMP dependent; G) ACTIVIN/NODAL dependent.

1.2.2.3 Fibroblast Growth Factor

The FGF family comprises 22 proteins of approximately 150 to 300 amino acids. Most FGF play roles as paracrine or endocrine signals in development, health and, disease in major organs including the heart. FGF signalling starts with the binding of the FGF to FGF receptors. The activated receptor is coupled to intracellular signalling pathways which include the RAS-MAPK and the PI3K-AKT pathways resulting in the transcriptional activity of FOS and FOXO (114) (Figure 1.8c). In terms of cardiac development, several paracrine FGF play an important role in cardiac development (115). For example, FGF8 is expressed in early embryonic stages and its KO is lethal with several mesodermal problems including improper cardiac looping and migration of CNCC (116). As for *Fgf10*, its KO is also lethal with abnormal ventricle morphology associated with an impairment of proliferation of cardiomyocytes (117).

1.2.3 From pluripotent to cardiac cell fate

Oct4, Sox2, and Nanog are essential in early cell fate commitment. KO of any of the previously mentioned genes compromises the epiblast resulting in early embryonic lethality. Until recently, it was thought, that pluripotency was maintained, and differentiation blocked, by the expression of OCT4, SOX2, and NANOG. However, if any of these genes block differentiation, their overexpression should further induce cells self-renewal. Surprisingly, overexpression of OCT4 in mESC induces mesoderm differentiation rather than more self-renewal (40). Similar findings were also observed in the other two genes. Induced expression of SOX2 leads to neuroectoderm lineage differentiation (118) whereas NANOG expression in hESC results in an increased PS differentiation (119). These core pluripotent factors seem critical to prime cells to go to a specific cell fate. For instance, SOX2 induces ectoderm differentiation repressing endoderm and mesoderm. In contrast, *NANOG* induces endoderm by inhibiting mesoderm and ectoderm. Lastly, OCT4 induces mesoderm by inhibiting ectoderm and endoderm (Figure 1.9) (17, 45, 120, 121).

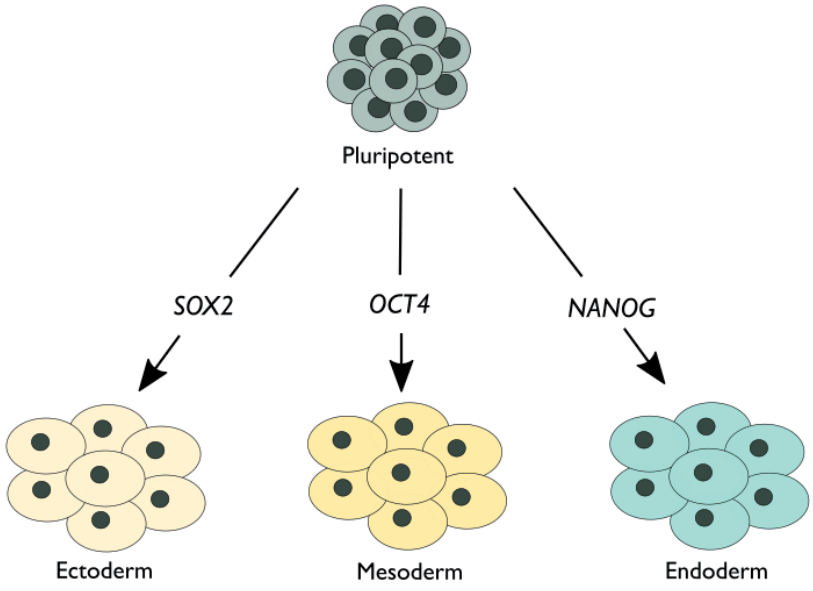

Figure 1.9 Distinct lineage specification roles of key pluripotent genes. Model of cell fate regulation by increased expression of NANOG, OCT4 or SOX2 in pluripotent cells.

The balance between OCT4, SOX2 and NANOG expression is mostly achieved by changes in ACTIVIN/NODAL expression. Although ACTIVIN/NODAL is uniformly

expressed through the epiblast, its expression becomes spatially asymmetric upon epiblast implantation. ACTIVIN/NODAL expression is amplified in the posterior epiblast (PS) and its expression becomes repressed in the anterior region of the epiblast (ectoderm) (122). High levels of ACTIVIN/NODAL result in the upregulation of OCT4 and NANOG while downregulating SOX2. Consequently, high levels of OCT4 and NANOG specifies the PS by directly inducing expression of EOMES *(45, 50)*. These results contribute to an initial bifurcation in which PSC become ectoderm lineage when the expression of ACTIVIN/NODAL is low, or mesendoderm lineage when high levels of ACTIVIN/NODAL are present. Mesendoderm are cells that express both OCT4 and NANOG that can still go to either mesoderm or endoderm cell fate (123). Mesendoderm cells share the expression of genes from both mesoderm and endoderm such as BRACHYURY and MIXL1.

The bifurcation between mesoderm and endoderm fate specification occurs when the anterior and posterior regions of the PS start to become evident. The most anterior part of the PS will give rise to the definitive endoderm, while the posterior area is responsible for originating the mesoderm. Once more, ACTIVIN/NODAL are key regulators in cell commitment. High concentrations of ACTIVIN/NODAL direct definitive endoderm differentiation whereas, low concentrations of ACTIVIN/NODAL specifies mesoderm differentiation. Mesoderm-derived cells start to express high levels of BRACHYURY. The expression of BRACHYURY indicates commitment to mesoderm (Figure 1.10A) (124).

As the PS elongates, a paraxial and a lateral mesoderm is formed. The commitment to either paraxial mesoderm or lateral mesoderm is in part controlled by BMP and Canonical WNT expression (Figure 1.10B). Both BMP and Canonical WNT direct a PS-like differentiation in ESC (125-128). Post gastrulation, BMP activation induces lateral mesoderm whereas WNT activation induces paraxial mesoderm. Indeed, Wnt and β-catenin are required and induce paraxial mesoderm development in mice (129). Moreover, studies on chick and frog showed that induced activation of WNT signalling in the anterior mesoderm inhibits the expression of core cardiac markers (130, 131). On the other hand, BMP expression is detected when cardiac mesoderm starts to form. Both BMP2 and BMP receptor 1A are expressed in the cardiac crescent and their deletion, in the cardiac mesoderm, results in embryos lacking cardiac crescent and cardiomyocytes (132). Furthermore, expression of BMP4 in the paraxial mesoderm prevents the development of somites, converting the cells instead into lateral plate mesoderm (133).

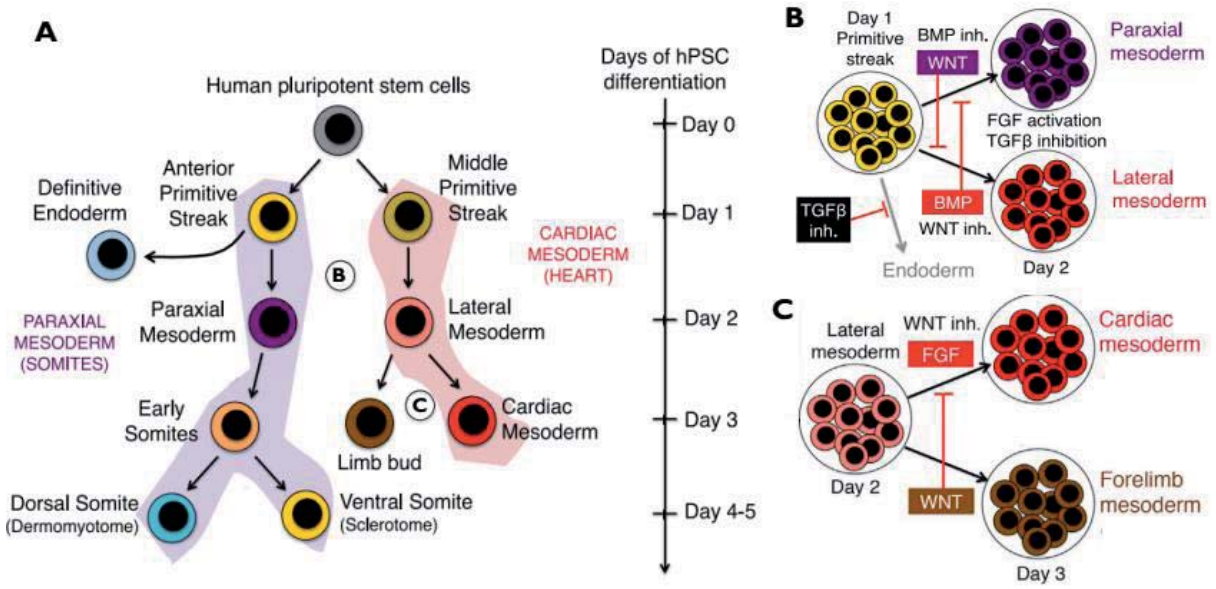

Figure 1.10 Mapping of cardiac mesoderm development. A) Schematic representation of mesoderm cell fate decisions. B) Bifurcation between lateral and paraxial mesoderm. C) Bifurcation between Cardiac mesoderm and Forelimb mesoderm. Image adapted from (134).

Lateral plate mesoderm can be subdivided into an anterior and a posterior region. The anterior region forms the CPC and the posterior region will result in the development of the limbs. The cell fate decision between anterior and posterior is controlled by the expression of FGF and WNT signalling (Figure 1.10C). The WNT expression in the lateral mesoderm induces limb-specific markers, while suppressing cardiac markers such as Nkx2.5. Reciprocally, WNT inhibition suppresses posterior lateral mesoderm, instead inducing cardiac mesoderm. *Dickkopf* related protein 1 (DKK1), a potent Wnt inhibitor, induces heart-specific gene expression in posterior lateral plate mesoderm (131, 135). Furthermore, most of the robust protocols to generate cardiomyocytes from ESC, are based on the inhibition of WNT signalling, after mesoderm induction (136, 137). On the other hand, FGF is responsible for the development of the anterior region of lateral plate mesoderm. FGF is expressed in cardiac precursors and later in the heart and required for the expression of NKX2.5 and GATA4 *(138)*. Moreover, deletion of FGF8 and FGF10 using a *Mesp1*-CRE mouse system showed several cardiac defects (139).

Overall, the cardiac developmental program starts as soon as pluripotent cells start to lose the expression of pluripotent markers until the acquisition of cardiac transcription markers and specification into CPC. Therefore, transcription factors have widely been used as markers for specific lineages. For example, cells that express high levels *Brachyury* are

indicative of early mesoderm and cells that express NKX2.*5* are already cardiac committed. On the other hand, signalling pathways can work as paracrine factors influencing surrounding cells to become committed to different cell fates. Stem cell biologists have as such, taken advantage of this, to direct cell fate decision *in vitro* (140).

1.3 Animal Models to study Cardiovascular Development

In recent years, great progress has been made in determining many of the factors that regulate cardiovascular development. This has been possible through both *in vivo* and *in vitro* model systems. The mouse is a very interesting model not only because it has a cardiovascular system like the human but also because it provides the advantages of a highly tractable organism for genetic studies. The ability to introduce or remove DNA sequences of interest in the germline genome has rendered the mouse a powerful and indispensable experimental model in fundamental and medical research (141, 142). Furthermore, conditional gene activation or inactivation through, for example, Cre recombinase and loxP system, permit precise temporal and spatial assessment of gene function (143). Even so, like any other mammal system, mice embryos are hard to access and/or observe as they develop inside their mother which is inconvenient for studying cardiac development and CHD.

The chick model is also widely used to study cardiac morphogenesis. The embryos are large and develop externally to the mother. The avian heart is also four-chambered but, the major advantage of chick embryos is their accessibility for surgical manipulation and functional interference approaches, through both gain and loss of function. Furthermore, chick embryos can be cultured for time-lapse imaging, which enables tracking of fluorescently labelled cells and detailed analysis of tissue morphogenesis (144).

Other vertebrate models include the frog and the fish. *Xenopus laevis,* the clawed frog, offers very similar advantages to the chick model (145). Zebrafish have two muscular cardiac chambers and is highly sought as model for questions concerning the development and looping of the heart tube, atrial and ventricular patterning, and myocardial differentiation. The zebrafish is also widely used as a powerful genetic and drug screening system. Finally, zebrafish is a very interesting model to study cardiac regeneration due their regeneration capability (146).

The fruit fly, *Drosophila melanogaster,* has emerged as a useful model for cardiac development and diseases. The fly is a unique and valuable system as it is the only invertebrate genetic model with a working heart developmentally homologous to the vertebrate heart. Thus, the fly model combines the advantages of invertebrate such as large populations, easy genetic manipulation and short lifespan with physiological measurement techniques that allow

meaningful comparisons with data from vertebrate model systems. As such, the fly has been mostly contributing to the understanding of complicated interactions between environmental factors and genetics in the long-term regulation of cardiac development (147, 148).

Although *in vivo* models are critically important, their intrinsic complexity can bring several disadvantages. While their application can be limited, *in vitro* models can offer unique advantages. The major advantages of *in vitro* model systems are the precise control of experimental conditions and access to a large pool of sample. This results in an ability to efficiently conduct studies regarding signalling pathways, cell-specific mechanisms studies, and high-throughput drug screening.

Neonatal mouse cardiomyocytes are easily isolated and can be maintained in proliferation, *in vitro,* for a few passages (149, 150). They are mainly sought for drug screening and response to stimulus because these cellular responses closely represent the changes found in cardiomyocytes *in vivo* (150). To overcome the limited cultured ability of primary cardiomyocytes, efforts have been made to develop cardiac cell lines (151). Nowadays, immortalized cell lines exist that retain phenotypical and contractible characteristics of cardiomyocytes (152, 153).

1.4 Stem Cells

Stem cells remain the most used *in vitro* model system to study cardiovascular development. Stem cells have the innate ability of self-renewal and ability to differentiate. Self-renewal refers to their ability through (a)symmetric cell division to generate daughter cells that can maintain their stemness under the appropriate stimulus. Differentiation is the ability of these cells to give rise to new specialized cells (154). Stem cells can be divided in two main groups: PSC and adult stem cell (ASC). PSC can give rise to all the cell types that make up the body, and therefor termed pluripotent, while ASC include cells with a differentiation capacity that ranges from a subgroup of cells and therefore considered multipotent, to one unique cell type, referred as unipotent.

1.4.1 Pluripotent Stem Cells

The usage of the term PSC started when the first mESC were first isolated from the ICM of the blastocyst back in 1981 (155, 156). The definitive proof of the pluripotency of these cells was confirmed by the ability to generate adult mice entirely derived from these cells (154). The first hESC were successfully isolated in 1998 from preimplantation blastocysts donated from fertility facilities (157). The fact that hESC lines were isolated from "excess" embryos has quickly generated ethical and political issues, halting their obtention (158).

However, this problem was solved in 2006 when the group led by Yamanaka was able to generate pluripotent cells from differentiated cells, *in vitro*, by exogenous expression of four transcriptions factors important for the pluripotency establishment and maintenance (159). These reprogrammed cells have then been called induced pluripotent stem cells (iPSC).

Mouse PSC can be isolated from the epiblast of the blastocyst. In the mice, two temporally distinct PSC can be isolated. PSC isolated from the blastocyst that has yet to implant in the uterus (E4.5), are called mESC, while PSC isolated from post-implanted blastocyst (E5.5) are called mouse epiblast stem cells (mEpiSC). (106, 160). Both cell types can give rise to the three germ layers *in vitro*, but only mESC can aggregate to the ICM-cells and contribute to originate all cells of the embryo *in vivo*. Furthermore, the core pluripotent

factors Oct4, Sox2, and Nanog, which are the hallmark of pluripotency, are expressed in both cell types.

However, the fact that mEpiSC are isolated post-implantation, means that they are closer to gastrulation. As such, they are molecularly and functionally different from mESC. This led to the consensus that mEpiSC are more "primed" for differentiation, while mESC remain more dormant or more "naïve" (161). Indeed, since mEpiSC are more prone for differentiation they express epiblast markers such as Nodal or Fgf5 (162, 163).

1.4.1.2 Mechanisms Behind Pluripotency

The use of serum in combination with a feeder layer, made of mitotically inactivated mouse embryonic fibroblasts (MEF), was the key to successfully maintain mESC in culture. In 1988, leukemia inhibitory factor (LIF) was identified as the protein secreted from MEF responsible for mESC self-renewal (106). Later in 2008, it was shown that pluripotency can be maintained in the absence of serum and growth factors by two chemical inhibitors, PD0325901, which inhibits mitogen-activated protein kinase (MAPK) and CHIR99021 which inhibits GSK-3 (164).

Surprisingly, the extrinsic stimuli necessary to maintain undifferentiated mESC and mEpiSC are different. Indeed, TGFβ and FGF are responsible for maintaining mEpiSC undifferentiated. However, treating mESC with TGFβ and FGF results in the loss of their "naïve" state, priming them to differentiate and enter in a mEpiSC-like state. Interestingly, while hESC are also isolated from preimplantation blastocyst, they need the exact same extrinsic factors as mEpiSC to remain undifferentiated. Furthermore, hESC are molecularly and functionally closer to mEpiSC, than mESC, which have led scientists to believe that they are also in a primed state (165, 166). LIF signalling also fails to maintain self-renewal of hESC (167). Moreover, while hESC require both TGFβ and FGF for their self-renewal, these factors drive mESC into differentiation (160). In contrast, while BMP and WNT activity induces mESC pluripotency, their activity in hESC results in their differentiation (106, 168) (Figure 1.11).

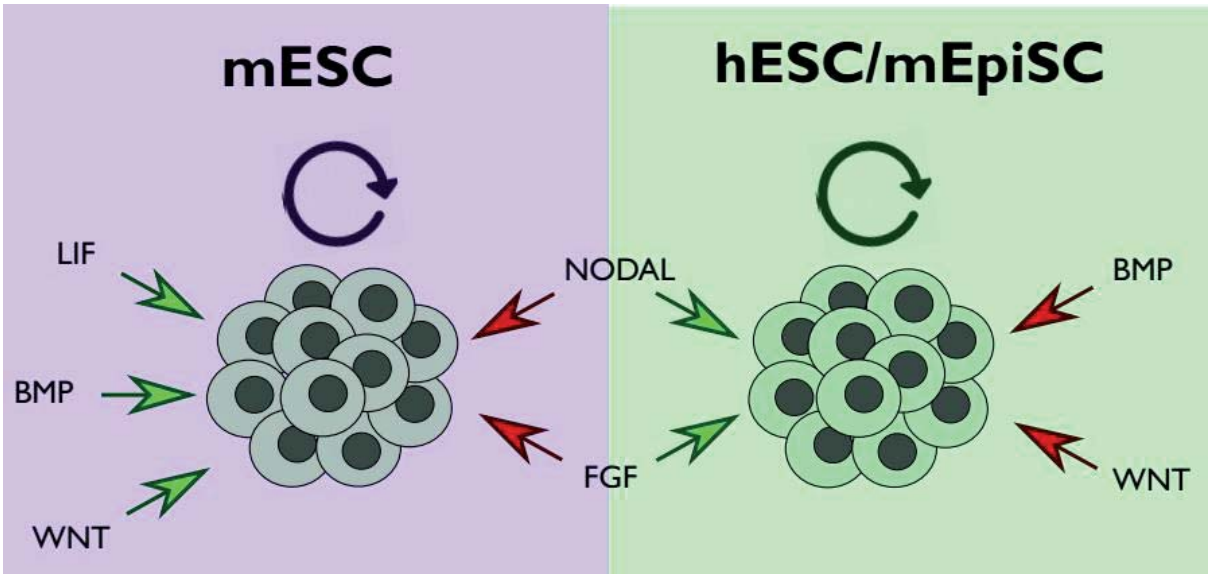

Figure 1.11 Regulation of pluripotency. Left panel – Mechanism behind self-renewal of mESC. Right panel – Mechanism behind self-renewal of hESC and mEpiSC. Green arrow – promotes self-renewal. Red arrow – induces differentiation.

1.4.1.3 Cardiac Differentiation

The two major approaches to differentiate PSC into cardiomyocytes are through Embryoid Bodies (EB) differentiation or Directed differentiation.

The first method established to induce ESC differentiation and to promote the emergence of cells with spontaneous contractile capacity, specific to cardiomyocytes, was through the formation of EB. This method consists on the dissociation of ESC into single cells and their subsequent aggregation through the formation of hanging drops. This method consists in creating droplets in the lid of a Petri dish, which is then inverted, causing the ESC to generate under gravity spheroid bodies which undergo differentiation. Unlike normal embryonic development, EB are highly variable in structure and composition, but a fraction of the EB exhibit spontaneously contracting regions. Alternatively, EB can be generated by suspension cultures in which ESC are cultivated in a non-coated Petri dish and allowed to generate three-dimensional aggregates (169). The amount of serum and cell number used, seem to influence EB ability to differentiate into cardiomyocytes. However, the data is conflicting and controversial (170-172).

The use of directed differentiation is particularly useful to address specific issues regarding lineage commitment, in a more defined differentiation condition. Most of the methods involve the addition of recombinant growth factors or small molecules compounds. The directed differentiation typically consists on activating the same steps by compounds that mimic the process of embryonic development, as previously mentioned. This method can increase results robustness and yield of the desired cells. For cardiomyocytes, many different differentiation protocols have been optimized, and most of them have a cardiomyocyte yield superior to 90% (Figure 1.12).

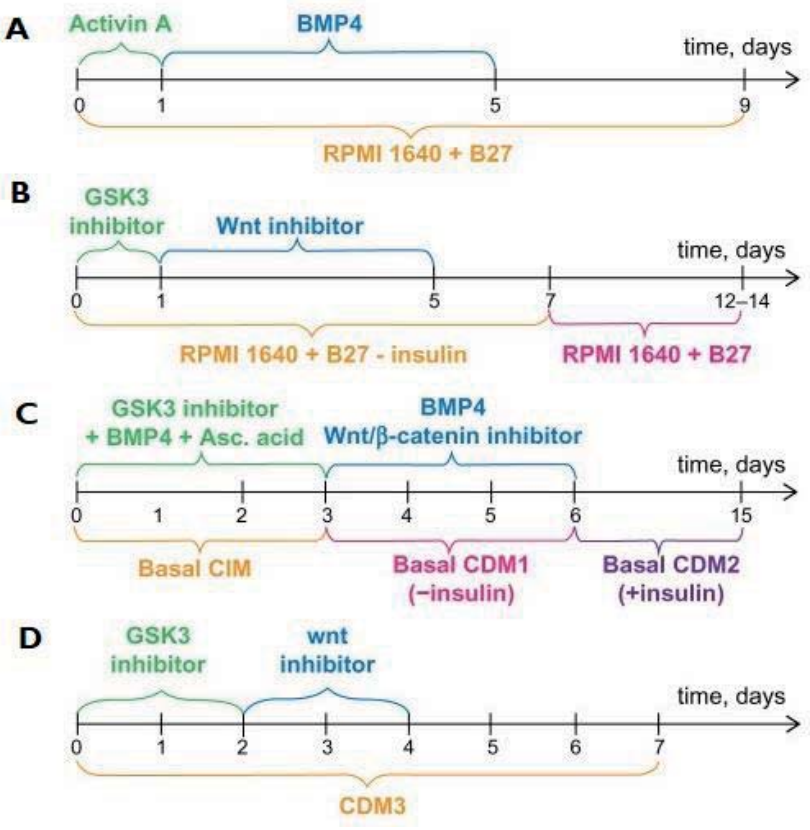

Figure 1.12 Monolayer cardiac differentiation protocols. A) LaFlamme et al, 2007 (173); B) Lian et al, 2012 (136, 137); C) Coa et al. 2013 (174) D) Burridge et al. 2014 (175). Image adapted from (176).

1.4.2 Stem Cells as a therapeutic approach for Cardiovascular Disease

Stem cell research offers great promise for understanding basic mechanisms of human development and differentiation, as well as appealing for treatment of several cardiovascular problems including myocardial infarction. Nevertheless, the ethical dilemma involving the destruction of a human embryo was, and remains, a major factor that has slowed down the development of hESC-based clinical therapies (177). It is also important to highlight that besides ethical concerns, safety issues regarding hESC based therapy are a major concern. Based on their characteristics of unlimited self-renewal and high proliferation rate, hESC-based transplantations are often associated with tumorigenicity, immunogenicity and genomic instability (178, 179).

One possible alternative to hESC are ASC. Compared to hESC they are safer, can circumvent many of the ethical issues and, in some cases, it is possible to use patient´s own cells. Different sources of ASC have been reported to differentiate into cardiomyocyte including the bone marrow, skeletal muscle, adipose tissue, peripheral blood and the heart (180-182). The major problem is that ASC are rare in mature tissues, and the most accessible have low efficiency in generating cardiomyocytes (180-182).

CPC are another interesting option which has gained strength in the last few years. CPC have the interesting feature that can self-renew for multiple passages, but their differentiation potential is restricted to cardiovascular cells only. Results with CPC have been very promising. After injury, CPC spontaneously differentiated into cardiomyocytes, endothelial cells and smooth muscle cells in infarcted mouse hearts and improved heart function after cardiac injury (183, 184). However, acquiring and maintaining large amounts of CPC has been challenging because the culture requirements of CPC are not optimized, and their molecular identity is poorly understood. Recently, the necessary conditions needed to maintain inducible expandable CPC that can robustly self-renew for several passages while maintaining their original morphology, gene expression pattern and potential to differentiate into cardiovascular lineages within the heart, have been reported (185, 186).

iPSC technology has provided new possibilities to model human diseases. Reprogramming somatic cells from patients into a pluripotent state followed by differentiation to disease-relevant cell types can generate an unlimited source of human tissue carrying the genetic variations that caused the development of the disease (187). Moreover, iPSC derived

issues can be used to understand the complex mechanisms underlying the various diseases (188) and for assessing cytotoxicity of small chemicals in drug development (188). One of the main challenges for the clinical application of hESC is the immune rejection which can be overcome with the usage of iPSC. The technology to generate autologous iPSC raised the possibility that cells can be transplanted into the patients with reduced concern of immune rejection (189) (Figure 1.13).

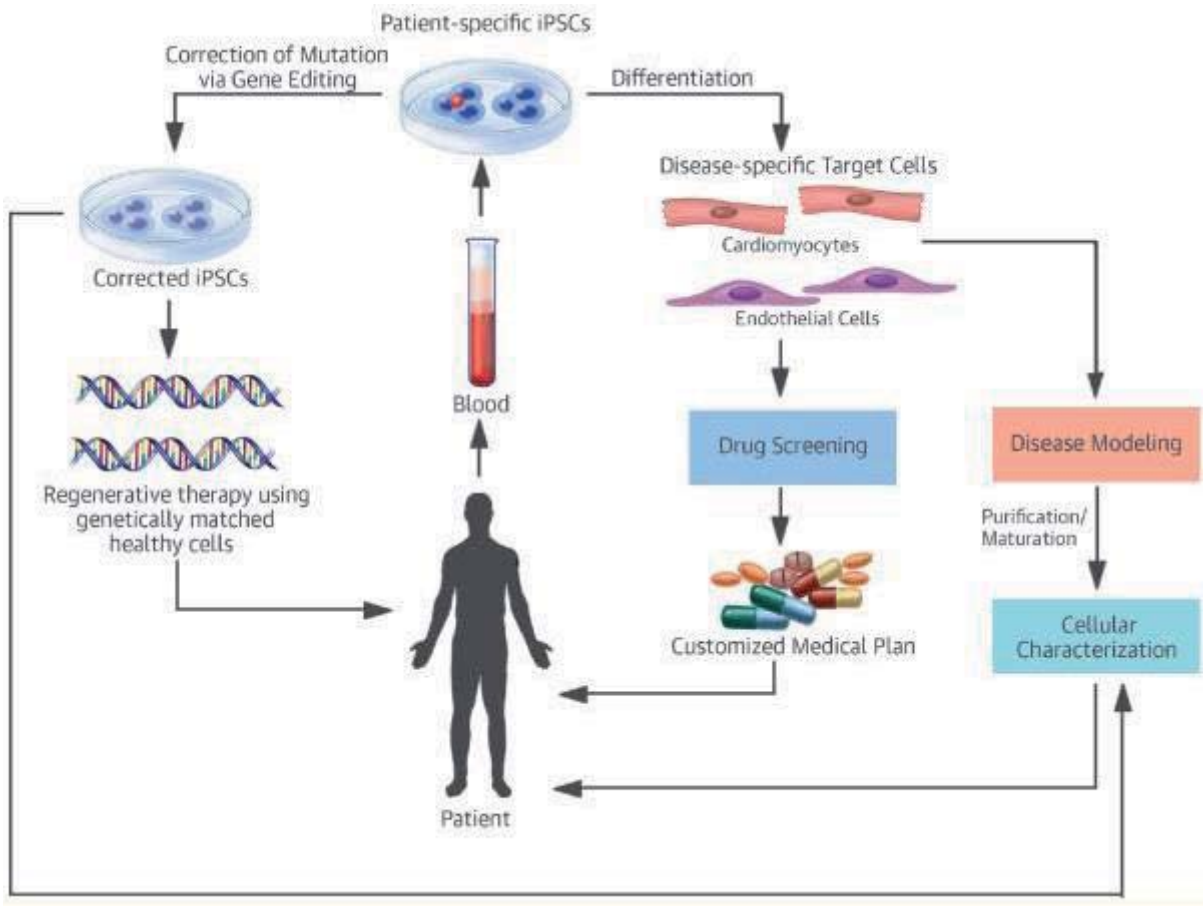

Figure 1.13 Application of iPSC for therapy. Somatic cells from patients harbouring a disease can be reprogrammed into iPSC. IPSC are differentiated into disease-specific tissue for cellular characterization or drug screening. iPSC genome can be corrected through gene editing and be used as a regenerative therapy. Image adapted from (190).

1.5 Cited2

The CBP/p300 interacting transactivator with ED tail rich family member 2 (Cited2) is a transcription factor which binds with high affinity to the transcriptional co-activator p300/CBP (191, 192). CITED2 does not bind to the DNA directly and acts as a co-activator or co-inhibitor of transcription factors that require an interaction with the Cysteine-Histidine rich domain 1 (CHI) of p300/CBP for their increased activity (193). Cited2 is found in all vertebrates but not in invertebrates such as *Drosophila melanogaster*. The CITED2 protein shares three conserved regions (CR) with the other Cited family members. However, to date, only the function of CR2, which encompasses a binding domain for CBP/p300, has clearly been identified as a transactivation domain (Figure 1.14).

Mouse *Cited2* KO embryos die *in utero* with multiple organs affected (194-196). In humans, CITED2 gene is located in the 6q23 region and mutations in CITED2 have been previously associated with CHD (197-201).

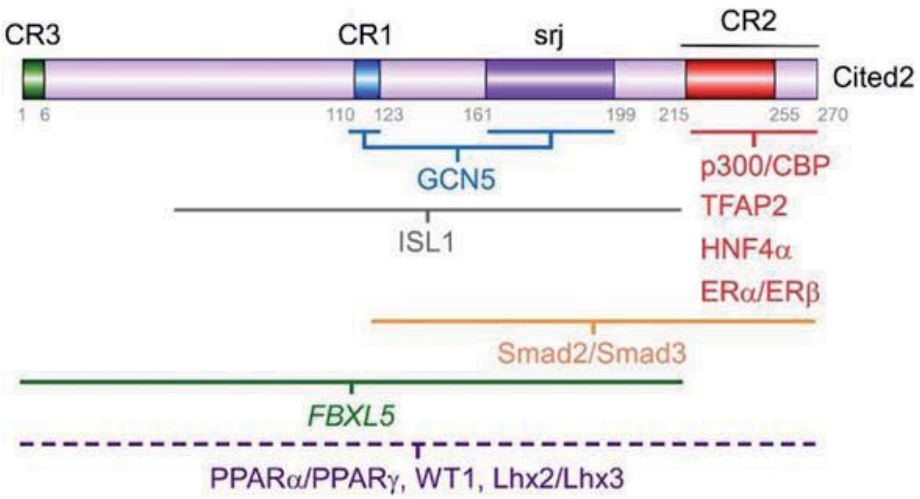

Figure 1.14 Schematic representation of CITED2 Protein. CITED2 protein is composed of 270 amino acids, three conserved regions (CR)1-3 and a serine-rich junction (srj). The region of interaction and the transcription factors, co-activators of transcription and F-box protein FBXL5 that interact with CITED2 are indicated. Image adapted from José Bragança, Joao Santos and Leonardo Silva, manuscript in preparation.

1.5.1 Cited2 Gene regulatory network

The best-described role of Cited2 is in regulating of hypoxia. Indeed, Cited2 was first described as a new p300-Cysteine-Histidine rich domain 1 (CH1) interacting protein that inhibits hypoxia-inducible factor (HIF)1α transactivation by blocking its interaction with p300-CH1 (191). In fact, part of the cardiac defects observed in *Cited2* null embryos are likely due to an enhanced activity of HIF1α (202). Indeed, the persistent hypoxia found in *Cited2* null hearts is rescued by HIF1α haploinsufficiency (203). In terms of molecular mechanisms, Cited2 transactivation domain (TAD/CR2) disrupts the complex between the CH1 domain of p300/CBP and HIF1α by binding to the CH1 with higher affinity than HIF1α. CITED2 activates a highly responsive negative feedback circuit that rapidly and efficiently attenuates hypoxic response, even at modest CITED2 concentrations (192, 204).

Besides HIF1α, CITED2 also negatively regulates the activity of other transcription factors, such as RXRα, NF-κB, STAT2, p53, and ETS-1, which have been shown to bind and compete, with CITED2, for the CH1 domain of CBP/p300 (205-211). On the other hand, CITED2 co-activates many other transcription factors that require a cooperation with CBP/p300 to be transcriptionally efficient such as, the TFAP2 members, LHX2/3, SMAD2/3, PPARα/β HNF4α, WT1, GCN5 and ISL1 (212-223) (Figure 1.15).

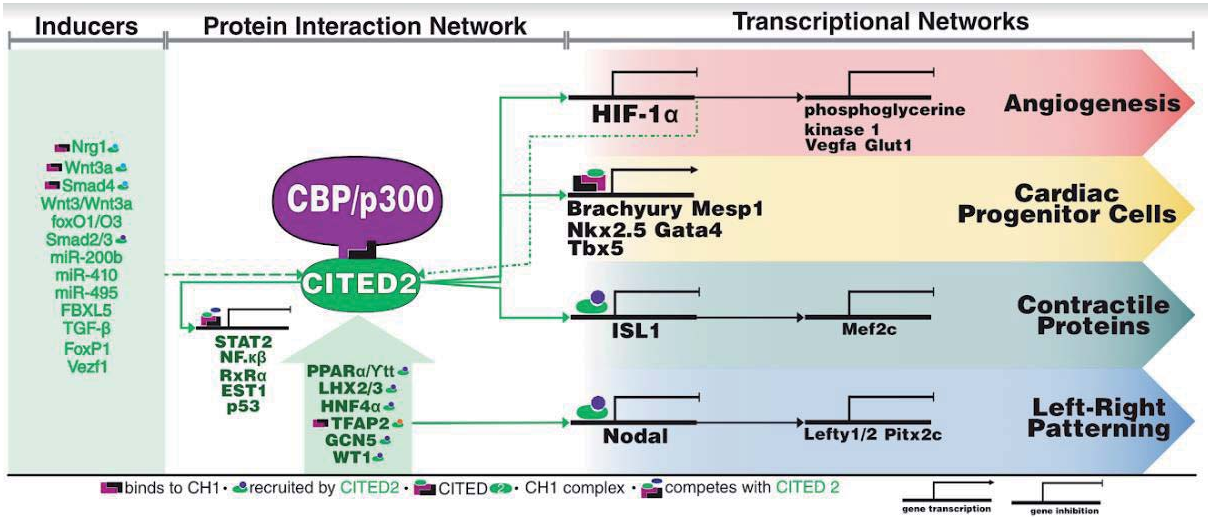

Figure 1.15 CITED2 gene regulatory network. Schematic representation of described inducers of *Cited2*, proteins that interact with CITED2 and the transcriptional activity of CITED2 in networks involved in cardiogenesis. Image adapted from José Bragança, Joao Santos and Leonardo Silva, manuscript in preparation.

1.5.2 Role of Cited2 in Stem Cells

Cited2 is involved in the maintenance of ESC pluripotency. Overexpression of CITED2 in mESC sustains their ability to self-renewal and proliferate even in the absence of LIF (224). Our group has also reported that Cited2 is a key player in pluripotency acting upstream of *Nanog*, *Klf4*, and *Tbx3* (224). Furthermore, acute loss of *Cited2* in mESC impairs NANOG expression causing mESC to spontaneously differentiate or die (224). Interestingly, a very small fraction of mESC were able to remain pluripotent without *Cited2*. However, *Cited2* null mESC have defective ability to differentiate into cardiac, hematopoietic and neuronal lineages (224, 225). This is likely to result from the delayed silencing of OCT4 and SOX2, disturbing ESCs ability to differentiate (225) (Figure 1.16).

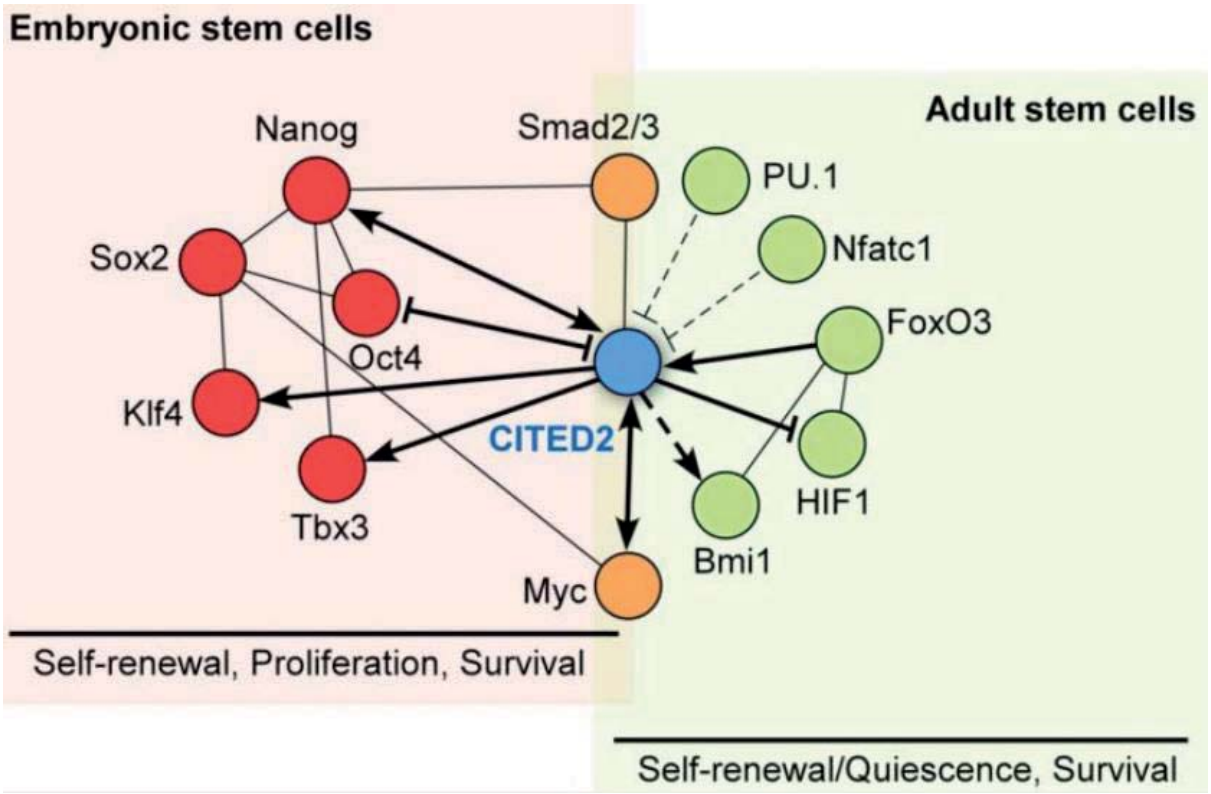

Figure 1.16 Stem cells gene regulatory network associating CITED2. Factors important for ESC (red background) and adult stem cells (green background) and their interaction with CITED2 (193).

Lastly, Cited2 plays a role in both fetal and ASC. Cited2 is required for the normal formation of the placenta and trophoblast stem cell differentiation (194, 226-229). In adult hematopoietic stem cells (HSC), loss of *Cited2* increases cell death by apoptosis and impairs

their residence in the bone marrow in a quiescent state, resulting in a reduction on the pool of undifferentiated HSC (230, 231). Conversely, overexpression of CITED2 in CD34+ cells of the blood decreases apoptosis and enhances their quiescence *in vitro* (232).

1.5.2 Role of Cited2 in cardiac development

During mouse embryogenesis, CITED2 is expressed in both early extraembryonic and embryonic structures. At E5.5, prior to gastrulation, CITE2 is expressed in the most anterior domain of the visceral endoderm. Upon gastrulation, its expression is detected in the anterior mesoderm adjacent to the visceral endoderm. At E7.5 CITED2 is expressed in the ventral node and in the cardiogenic mesoderm and its expression is maintained throughout the entire myocardium and the formation of the heart tube. Between E9.5 and E10.5, Cited2 expression is elevated in heart forming structures, including the aortic sac, ventricles, myocardium, OT, atria and IT. Finally, at E13.5 CITED2 expression was predominantly found in the OT, IT, septum premium, around the vena cava and endocardial cushions of the atrioventricular (AV) canal and the tip of the intraventricular septum (233, 234) (Figure 1.17).

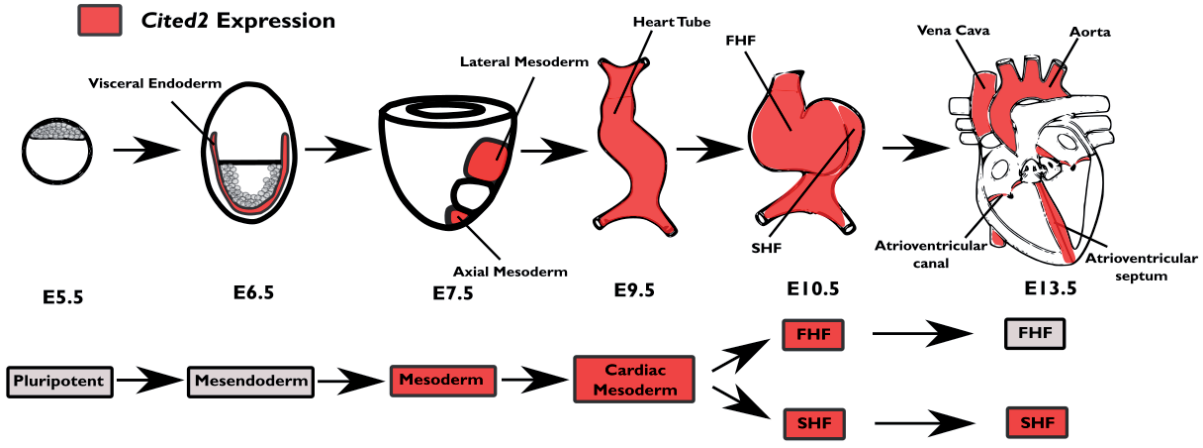

Figure 1.17 CITED2 expression throughout heart development. Schematic representation of *Cited2* expression during mice heart development according to the following articles (233, 234).

1.5.3 Congenital Heart Diseases

Heart abnormalities have been reported in patients carrying CITED2 mutations. Indeed, cardiac defects observed in *Cited2*-null embryos are phenotypically comparable to the heart problems of patients harbouring CITED2 mutations. Worldwide genetic screenings of cohort of patients have associated variants in *CITED2* sequences mostly to sporadic non-syndromic CHD.

The most frequent heart anomalies associated with Cited2 are: VSD, ASD, TOF and the transposition of the great arteries (TGA), a CHD where the aorta is connected to the RV, and the pulmonary artery is connected to the LV (Figure 1.18). Interestingly, most of the missense mutations clustered in the serine-rich junction (SRJ) domain. Remarkably, transgenic mice in which the SRJ domain of *Cited2* is removed are viable with normal hearts (199, 235).

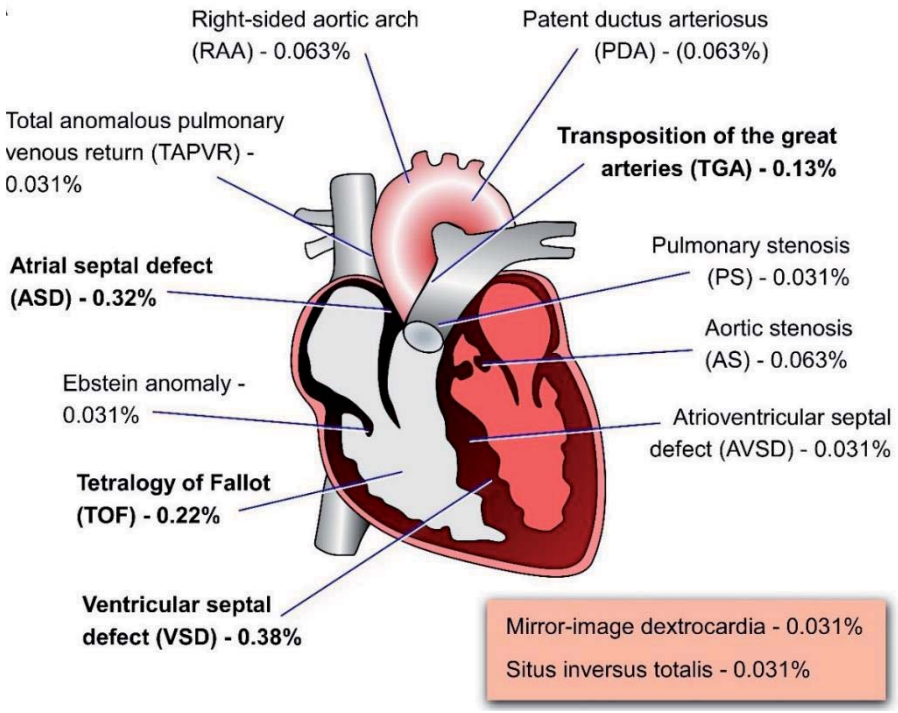

Figure 1.18 Prevalence of CITED2 mutations in CHD patients. Schematic representation of the adult human heart indicating the heart defects detected in patients of CHD carrying CITED2 mutations. The percentages represent the proportion of each of the heart abnormalities associated with CITED2 mutations in a cohort of patients with CHD. Image adapted from José Bragança, Joao Santos and Leonardo Silva, manuscript in preparation, the data compiled in the figure was published elsewhere (197-201).

Most of CITED2 variants identified in patients with CHD, only marginally affected the ability of CITED2 to repress HIF-1α and/or co-activate TFAP2C transcription factor *ex vivo* (235-241).

1.6 Objectives

Cardiomyopathies and CHD are the leading cause of death worldwide both in adults and newborns respectively. It is expected that nearly 1% of the population manifest some form of CHD. Many laboratories across the world have studied the mechanisms of normal heart development and the causes leading to CHD. While the number of transcription factors and signalling pathways contributing to cardiogenesis is largely known, the fine regulation of this process is still not fully understood.

Cited2 is important for heart development, and *Cited2* KO embryos die *in utero* with multiple heart defects. Certain CITED2 mutations in humans have strongly been associated with CHD. However, its function is largely unknown.

As such, the goal of this thesis is to better understand the function of CITED2 in cardiac development. Thus, the first objective consisted in understanding the impact of Cited2 in cardiac commitment through CITED2 gain or loss function approaches. Given that, the second objective consisted on identifying the transcriptomic profile of *Cited2* depletion through microarray analysis and candidate gene approach. The third objective was the identification of new candidate genes downstream of *Cited2* important for cardiogenesis. Last objective was to attempt the rescue cardiac defects caused by *Cited2* depletion through candidate genes both *in vitro*, as well as *in vivo*.

CHAPTER 2

Materials and Methods

2.1 Materials

2.1.1 Mouse embryonic stem cell lines

2.1.1.2 *Cited2*$^{fl/fl}$

Cited2$^{fl/fl}$ are a mESC that permit the spatiotemporal conditional KO of *Cited2*. *Cited2*$^{fl/fl}$ mESC derive from the blastocyst of mice *Cited2*$^{fl/fl}$ (242) and were successfully isolated and characterized *in vitro* (224). Excision of *Cited2* can be achieved by the activity of the Cre recombinase enzyme. Lastly, the excised region of the exon2 is replaced by a cassette of LacZ reporter that allows the verification of *Cited2* depletion and track cells where it occurred (Figure 2.1).

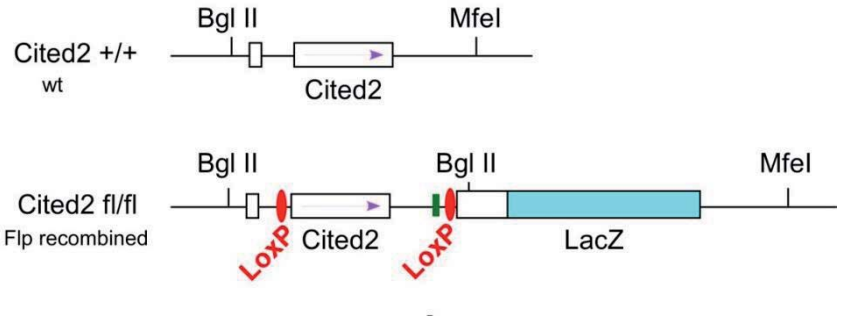

Figure 2.1 *Cited2* Conditional KO system. The exon2 of the Cited2 is flanked by two LoxP sites. Upon Cited2 excision, the exon is replaced by a LacZ cassette.

2.1.1.2 *Cited2*$^{fl/fl}$ [Cre]

Cited2$^{fl/fl}$ mESC were stably transfected with a plasmid expressing Cre fused to a domain of the Estrogen Receptor containing a ligand binding domain (Cre-ERt) (224). Excision of Cited2 can be triggered by supplementation of 4-Hydroxytamoxifen (4HT), a potent Estrogen antagonist, that causes Cre-ERt to enter the nucleus and excise the exon 2 of Cited2 encompassed by loxP sites.

2.1.1.3 *Cited2*$^{\Delta/\Delta}$

Cited2$^{fl/fl}$ mESC that lost both *Cited2* alleles, which have acquired compensation for CITED2 function and remained in culture with pluripotent-like features. *Cited2*$^{\Delta/\Delta}$, represent a minority of mESC that were able to adapt to the loss of *Cited2* and managed to survive. Even so, *Cited2*$^{\Delta/\Delta}$ ability to differentiate to cardiac lineage is severely compromised (224).

2.1.1.4 E14/T

E14/T is a mESC line derived from the blastocyst of a mouse strain 12910la that express polyomavirus large T antigen that can be transfected with plasmids carrying a polyomavirus origin of replication (ORI) at three orders of magnitude greater than DNA transfection efficiencies than other ESC. Provided selection, the transfected plasmid with the polyomavirus ORI is maintained episomal and propagates without the risk of chromosomal the integration (47). These cells were gently given by Austin Smith (University of Cambridge, UK).

2.1.1.5 A2loxCRE

A2loxCRE cells are a mESC line that can be targeted with a specific plasmid vector harbouring an inducible gene expression cassette to generate a derivative ESC line. A2loxCRE were derived from E14Tg2a ESC by targeting them with an Inducible Cassette Exchange (ICE) locus on the X chromosome (243) (Figure 2.2). To generate A2loxCRE, harbouring the inducible CITED2 expression, hereafter termed as A2UpC2, cells were treated with 0.5µg/mL doxycycline, one day before transfection, in order to induce the expression of Cre (244). On the following day, cells were transfected with P2lox harbouring Flag-tagged CITED2 (FC2) and, after 24h, selection medium containing 300µg/mL of geneticin (Invivogen G418) was added to the cells and selection was maintained for 10 days (Figure 2.2). Resistant colonies were then individually picked into 96-well plates and expanded. To confirm integration of the plasmid sequence, DNA was isolated from resistant clones and sent for sequencing (Stabvida).

CITED2 expression was induced by adding 2 μg/ml of doxycycline (Sigma) to the culture medium every two days. A2loxCre mESC were gently given by Prof. Michael Kyba (University of Minnesota, USA) (245).

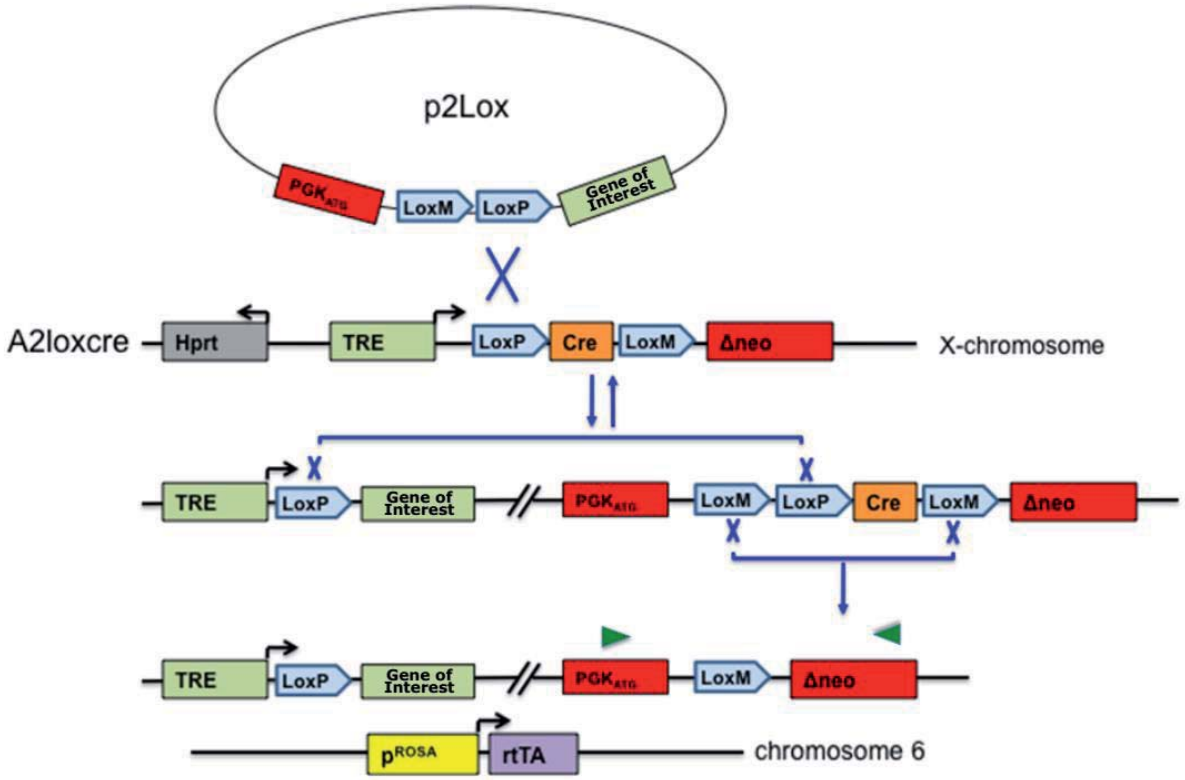

Figure 2.2. Schematic representation of the A2loxCre System. Site-specific recombination between the loxP sites in p2Lox plasmid and in A2loxcre ESC leading to the integration of our gene of interest into the X-chromosome of the cells along with the PGK-ATG that complements the mutated version of the neomycin resistance gene (Δneo). The recombination between the loxM sites excises Cre leading a stable integration. Reverse Tetracycline transactivators (rtTA); ROSA promoter (pROSA); tetracycline response elements (TRE); Hypoxanthine guanine phosphoribosyltransferase (Hprt) Image adapted from (245),

2.1.2 Plasmid Vectors

2.1.2.1 pPyCAGIP

The pPyCAGIP, hereafter referred as CAGIP, is an episomal expression vector that harbours a polyoma ORI with the F101 mutation allowing episomal replication in ESC. Complementary DNA (cDNA) may be cloned in place of the stuffer fragment linked to the

puromycin resistance gene. The CAGIP backbone was used to generate two different vectors used in this study. A vector harbouring an enhanced green fluorescent protein (eGFP), hereafter termed CAGIP-eGFP and, a vector harbouring the human full-length CITED2 (FC2) fused to a flag peptide at its N-terminal domain, hereafter termed CAGIP-FC2. The pPyCAGIP vector was gently given by Austin Smith (University of Cambridge, UK) (47).

2.1.2.2 P2lox

P2lox is a vector with a backbone size of 2660 base pair (bp) used to recombine with the ICE of the A2loxCre mESC. In the present work, we used a P2lox vector harbouring an eGFP, hereafter termed P2lox-eGFP, gently given by Prof. Michael Kiba (University of Minnesota, USA)(245). Furthermore, we generated a P2lox vector harbouring an FC2, hereafter known as P2lox-FC2.

2.1.2.3 Plasmid for Luciferase Assay

pGL3-Basic vector (Promega) is a promoter-less *luciferase* reporter, into which promoter fragments can be cloned to control the expression of the *luciferase* in mammalian cells. After transfection, the expression of the *luciferase* and its subsequent activity is proportional to the promoter transcriptional activity. In the present work, we used a Wnt11-luc vector harboring the luciferase activity under the promoter of *Wnt11*. This plasmid was a kind gift from Dr. Hiroyuki Mori (University of Michigan, USA) (246).

2.2. Methods

2.2.1 Embryonic Stem Cell culture

Except for A2loxCRE mESC, all ESC were cultured in Glasgow Minimum Essential Medium (GMEM) BHK-21 (Gibco®, 21710) supplemented with 10% Fetal Bovine Serum (FBS) (Sigma®, F7524), 1x L-Glutamine 200mM (Gibco®, 25030), 1% Penicillin-Streptomycin (P/S) (Gibco®, 15140), 1x Sodium Pyruvate 100mM (Gibco®, 11360), 1x Minimum Essential Medium Non-Essential Amino Acids (MEM-NEAA) (Gibco®, 11140) and 0.05mM 2-Mercaptoethanol (Gibco®, 31350).

A2loxCRE mESC, were cultured in Dulbecco's Modified Eagle Medium (DMEM) (Gibco®, 41966) supplemented with 15% FBS (Sigma®, F7524), 1x L-Glutamine 200mM (Gibco®, 25030), 1% P/S (Gibco®, 15140), 1x Sodium Pyruvate 100mM (Gibco®, 11360), 1x MEM-NEAA (Gibco®, 11140) and 0.05mM 2-Mercaptoethanol (Gibco®, 31350).

Cells were maintained on plates previously coated with 0.1% Gelatine (Sigma®, G1393) and kept at 37°C in a humidified incubator with 5% CO_2. To maintain the cells under pluripotency conditions 10^3 U/ml LIF (Merck Millipore, ESG1107) was added to the medium. The cell medium was changed every two days, and cells were split when 60%-70% confluent. Cells were dissociated in Trypsin EDTA (0.25%) (Gibco®, 25200) after washed with phosphate buffered saline (PBS), followed by centrifugation at 300g for 4 min.

2.2.2 Embryoid Bodies Formation and Cardiac Differentiation

To induce mESC differentiation, we used a hanging-drop method. The differentiation medium used was the same used to maintain mESC pluripotent but without LIF. $5x10^4$ cells, previously dissociated and separated by trypsinization, were resuspended in 1mL of differentiation medium. After that, approximately 50 droplets of 20µL were prepared in low adhesion plates and inverted to ensure the formation of EB with, approximately, 1000 cells/drop. After 2 days, the plates were inverted and supplemented with 5mL of differentiation medium. By day 5 of the differentiation, the EB were transferred to a previously 0.1% gelatine-coated plate allowing their adhesion to the plate. By day 7, the first beating foci

normally appear. From day 8 to day 10 of the differentiation, we assess the cardiac differentiation by counting the percentage of EB that have beating foci and the average beating foci per EB.

The differentiation medium used on Cited2$^{fl/fl}$[CRE] was supplemented at D0 with 4HT at a final concentration of 1μM (Sigma H7904) or treated with the same volume of Ethanol (EtOH) used as a vehicle. The differentiation medium used on A2uPC2 was supplemented at different time points with 1μg/mL of Doxycycline Hyclate (Sigma, D9891).

2.2.3 pPyCAGIP-based vectors transfection

All transfections were performed with Lipofectamine® 2000 (Invitrogen, 11668). In brief, 2.5x10^5 ESC were plated in 0.1% gelatine-coated 6-well plate. On the following day, 1μg of total DNA vectors were transfected per well according to the recommendation of the manufacturer. After 4 hours, the ESC medium was added to cultures. On the following day, selection antibiotic was supplemented to the medium.

2.2.3 RNA extraction and cDNA synthesis

Total RNA extraction and purification were performed according to the manufacturer's protocol of the RNeasy Mini Kit (Qiagen 74104). Total RNA concentration was measured with Nanodrop2000 (Thermo Scientific). To prepare cDNA from total RNA, 1μg of total RNA was used for reverse transcriptase according to the manufacturer's protocol, using the NZY First-Strand cDNA Synthesis Kit (Nzytech MB125).

2.2.5 Quantitative polymerase chain reaction

Quantitative polymerase chain reaction (qPCR) was performed using SsoFast Evagreen Supermix (BioRad), in a CFX96™ Real-Time PCR detection system (BioRad) and using the CFX Manager™ Software (BioRad). For all primers, we used an annealing temperature of 65°C

and we normalized gene expression levels to the levels of *Gapdh* expression. The list of primers used for qRT-PCR is presented in Table 2.1.

Table 2.1. List of primers used for qPCR

Gene	Forward Primer	Reverse	Reference
Bmp4	TTCCTGGTAACCGAATGCTGA	CCTGAATCTCGGCGACTTTTT	(247)
Brachyury	CTCTAATGTCCTCCCTTGTTGCC	TGCAGATTGTCTTTGGCTACTTTG	(49)
Cer1	CTCTGGGGAAGGCAGACCTAT	CCACAAACAGATCCGGCTT	(248)
Cited2 #1	CGCATCATCACCAGCAGCAG	CGCTCGTGGCATTCATGTTG	(249)
Cited2 #2	AAATCGCAAAGACGGAAGGACTGG	ATGCGGGCTCGGGAACTGC	(224)
Dkk1	CTGAAGATGAGGAGTGCGGCTC	GGCTGTGGTCAGAGGGCATC	(250)
Gapdh	TCCCACTCTTCCACCTTCGATGC	GGGTCTGGGATGGAAATTGTGAGG	(49)
Fgf5	CTGTATGGACCCACAGGGAGTAAC	ATTAAGCTCCTGGGTCGCAAG	(49)
Fgf8	CCAGCCCCAAACTACCCCGAGGAG	CGCGCAGACCCAGCCCAGGAT	(251)
Fgf10	CAGCGGGACCAAGAATGAAG	TGACGGCAACAACTCCGATTT	(252)
Isl1	CTTAAGCATGCCCTGTAGCTGG	CAGACAGGAGTCAAACACAATCCC	(49)
Mesp1	TGTACGCAGAAACAGCATCC	TTGTCCCCTCCACTCTTCAG	(253)
Nkx2.5	CCACTCTCTGCTACCCACCT	CCAGGTTCAGGATGTCTTTGA	(254)
Nodal	TGGCGTACATGTTGAGCCTCT	TGAAAGTCCAGTTCTGTCCGG	(255)
Tbx5	GGACCCAGTCCCTTGAATGG	TCCAGGCTGAGGAGTTCTAGGC	(49)
Wnt3	ACCTGGAGAAGGCTGGAAGT	CTTGTCCTTGAGGAAGTCGC	(252)
Wnt3a	TGGCTCCTCTCGGATACCTC	AAAGCTACTCCAGCGGAGGC	(256)
Wnt5a	CAAATAGGCAGCCGAGAGAC	TCTAGCGTCCACGAACTCCT	(249)
Wnt11	GCTCCATCCGCACCTGTT	CGCTCCACCACTCTGTCC	(252)

2.2.6 Microarray

Total RNA was isolated using TRIzol and purified with a miRNeasy Mini Kit (Qiagen 217084). Quantification was carried out using Nanodrop2000 (Thermo Scientific). For microarray labeling, 100ng of total RNA was taken as starting material, and amplification and hybridization were performed according to Affymetrix standard protocol. 12.5 µg of amplified RNA was hybridized on Mouse Genome 430 version 2.0 arrays (Affymetrix) for 16h at 45°C. The arrays were washed and stained in an Affymetrix Fluidics Station-450, according to the manufacturer's instructions. After staining, arrays were scanned with an Affymetrix Gene-Chip Scanner-3000-7G (257).

Microarray data were processed using the robust multi-array average (RMA) method on the R/Bioconductor platform. Variability between samples was visualized using Principal Component Analysis (PCA), hierarchical clustering, and density plots, implemented in R using the entire poly(A)-RNA datasets. For differential expression analysis, the Bioconductor package *limma (258)* and multivariate empirical Bayes statistics were applied. Gene expression was considered significantly altered when the adjusted p-value was inferior to 0.05 and a positive or negative Logarithm fold change (LogFC) was superior to 1 (259). Upregulated and downregulated differentially expressed genes (DEGS) pathway analysis was performed by Wikipathways conducted by Enrichr (260, 261).

2.2.4 Immunocytochemistry

Immunocytochemistry was performed with *Cited2*$^{fl/fl}$[Cre] ESC treated with EtOH or 4HT at D0 and differentiated for 10 days. At D10, cells were dissociated with trypsin and grown in coverslips, previously coated with gelatine ON. On the next day, cells were washed with PBS (Sigma) and fixed in 4% formaldehyde (Sigma, F8775) for 15 min at 37°C, permeabilized in 0.1% Triton X-100 diluted in PBS for 20 minutes and blocked with 2% Bovine Serum Albumin (BSA) (Nzytech) in PBS for 30 minutes. Samples were then incubated with mouse monoclonal anti-α-ACTININ 1:500 (Sigma, A7811) or mouse monoclonal anti-MYOSIN 1:300 (DSHB, MF20) diluted in PBS with 0.1% Tween 20 (PBS-T) (Sigma) for 2 hours at Room temperature (RT). Afterward, samples were washed three times with PBS-T and incubated with secondary antibody AlexaFluor-594 (Invitrogen, AF594) for 1 hour at RT. The coverslips were then washed three times with PBS-T and incubated with 5µg/mL of DAPI (Sigma, 28718) for 10 minutes. Lastly, coverslips were washed twice with PBS-T and mounted with Mowiol. Fluorescence microscopy was performed using an Axio Imager Z2 Fluorescence microscope (Carl Zeiss) and images obtained at 100x magnification.

2.2.5 Conditioned Medium preparation

To prepare the conditioned medium (CM), $3x10^6$ previously transfected E14T/CAGIP or E14T/FC2 ESC were plated on a 0.1% gelatine-coated 10cm dish and supplemented with GMEM without LIF ON. The following day, cells were washed twice with PBS (Sigma) and 10mL of GMEM without supplements was added ON. On the next morning (approximately 16 hours), the medium was collected and filtered through 0.45µm. At the onset of differentiation, *Cited2*$^{fl/fl}$[Cre] ESC were treated with half CM and half differentiation medium with 10% total FBS. After D2, cells were treated with normal differentiation medium for the remaining of the differentiation.

2.2.6 Immunoprecipitation and Western Blot

For immunoprecipitation (IP), 1.5mL of the collected CM was incubated with the 5µg of rat monoclonal anti-WNT5a (R&D Systems, MAB645), rabbit polyclonal anti-WNT11 (Santa Cruz Biotechnology, SC50360) or goat polyclonal anti-FGF10 (Sant Cruz Biotechnology, SC7375) ON at 4°C. On the following day, 30µL of Protein G Sepharose Beads (GE Healthcare), pre-blocked with 1% BSA solution were added to the CM and incubated at 4°C with agitation for 1 hour. Afterward, the CM was centrifuged at 1000g for 5min and both the pellet and the supernatant were recovered.

Proteins immunoprecipitated were separated using SDS-PAGE 10% bisacrylamide-polyacrylamide gel (National Diagnostics™) using the Miniprotean II system (BioRad) along with NZYColour Protein Marker II (NZYTech, MB090) and transferred to PVDF membrane (GE Healthcare) using a semi-dry blotter (20min at 200mA, BioRad). The membrane was blocked for 1 hour at RT with a solution containing 4% milk in PBS-T. The membrane was subsequently incubated with rat monoclonal anti-WNT5a (1:1000), rabbit polyclonal anti-WNT11 (1:200) or goat polyclonal anti-FGF10 (1:200) at RT for 1 hour. Samples were washed three times with PBS-T and incubated with the appropriate secondary antibody horseradish peroxidase (HRP) conjugated for 1 hour at RT (Santa Cruz Biotechnology sc-2313 1:10,000; Santa Cruz Biotechnology sc-2378 1:5,000; Abcam, ab97057 1:5000). The HRP activity was

revealed by ECL Plus kit (GE Healthcare) according to the manufacturer's instructions and image acquisition was done on the ChemiDoc™ MP Imaging System (BioRad).

2.2.7 Immunodepleted Conditioned Medium and Rescue Assay

For immunodepleted CM, the supernatant of previously immunoprecipitated CM or CM incubated with 5µg/mL of rat monoclonal anti-WNT5a, 2.5µg/mL of rabbit polyclonal anti-WNT11, 2.5µg/mL of goat polyclonal anti-FGF10, or 5µg/mL of polyclonal rabbit IgG, polyclonal (Abcam, ab37415) was added at the onset of differentiation of *Cited2*$^{fl/fl}$[Cre] ESC.

For rescue assay, 100ng of recombinant WNT5a protein (Millipore, GF146), 100ng of recombinant of WNT11 (R&D Systems, 6179-WN), or a combination of 50ng of WNT5a and 50ng of WNT11 was added at the onset of differentiation of *Cited2*$^{fl/fl}$[Cre] ESC.

2.2.8 Luciferase Assay

E14T ESC were plated in 24 well plates at 2.5x10^4 cells per well and transfected the following day using Lipofectamine 2000 (Invitrogen) with 100ng of Wnt11-luc reporter (246), 100ng of CAGIP-FC2 expression or CAGIP control vectors and 100ng of CMV-lacZ plasmid. Cells were maintained under pluripotency conditions and lysed 48h post-transfection and both luciferase and lacZ activities were measured as previously reported in (224), in a Dual Injector GloMax-Multi Detection System (Promega).

2.2.9 Zebrafish Microinjection and Developmental Study

The night before the injection, male and female zebrafishes were set up in breeding tanks with dividers to increase total egg production. To achieve *Cited2* depletion, 1-cell stage zebrafish eggs were injected with 4.6nl of 5ng of custom anti-*Cited2* Morpholino (MO) designed to bind to the translation staring site (UAG-MO) (5'-CCATCATGCGGTCTACCATTCCC-3') with 3'- Carboxyfluorescein end modification

and/or anti-*Cited2* MO designed to the splicing site of the 1st intron (Splicing-MO) (5´-AACTTTGTAACCTTTACCTCTCCGC-3') with 3'-Lissamine end modification (GeneTools) prepared in Danieau's solution (262). To control the procedure, 1-cell stage zebrafish eggs were injected with 5ng of a standard control oligo (Control MO) (5'-CCTCTTACCTCAGTTACAATTTATA-3') (GeneTools) also prepared in Danieau's solution. To perform the rescue assays, Danieau's solution with 5ng of *Cited2* MO was co-injected with 500pg of 8R-CITED2 or 5-10pg of WNT5a and/or WNT11. Previous dialysis of 8R-CITED2 in SnakeSkin® Dialysis Tubing 3.5k MWCO (Thermofisher) was performed at 4°C ON with constant agitation, against PBS, to ensure the removal of phenylmethylsulfonyl fluoride (PMSF) from the solution.

Zebrafish embryos were kept in embryo medium (263) at 28.5°C with a photoperiod of 14hours light and 10 hours dark. The medium was changed every day and the dead embryos discarded. For heart rate determination, the beating per minute (bpm) were counted from 10-second videos of hearts acquired from randomly picked embryos at 48hpf. Live imaging and photography were captured on a Leica MZ 7.5 stereomicroscope (Leica Microsystems) at RT. All experiments were conducted in accordance with the regulation of the Directive 2010/63/EU (EU, 2010).

2.2.10 Statistical Analysis

Statistical Analysis Statistical significance was determined by two-tailed Student's t-tests assuming unequal variance or Fisher's Exact test of independence when we had two nominal variables. P-values were considered significant when $p<0.05$.

CHAPTER 3

Cited2 depletion impairs cardiac differentiation

3.1 Introduction

In mice, the transcriptional modulator Cited2 is required for normal embryogenesis. KO of *Cited2* in the epiblast results in embryonic lethality associated with multiple cardiovascular defects (194-196). In humans, mutations in the gene encoding CITED2 are associated with CHD (197-201).

To better understand the role of *Cited2* in the early stages of mESC differentiation, our group employed a CITED2 gain of function approach to examine its role during cardiac differentiation (224). CITED2 overexpression, in undifferentiated ESC, stimulates the expression of transcription factors important for cardiac lineage commitment and differentiation, promoting cardiac cell emergence upon differentiation (264).

Previous data also showed that CITED2 expression is highly associated with CPC populations, particularly CPC of the SHF and that CITED2 is recruited to the promoter of the *Isl1* gene (264). We also provided evidence that the human CITED2 and ISL1 proteins physically interact and synergize to promote cardiogenesis from ESC (264) (Figure 3.1).

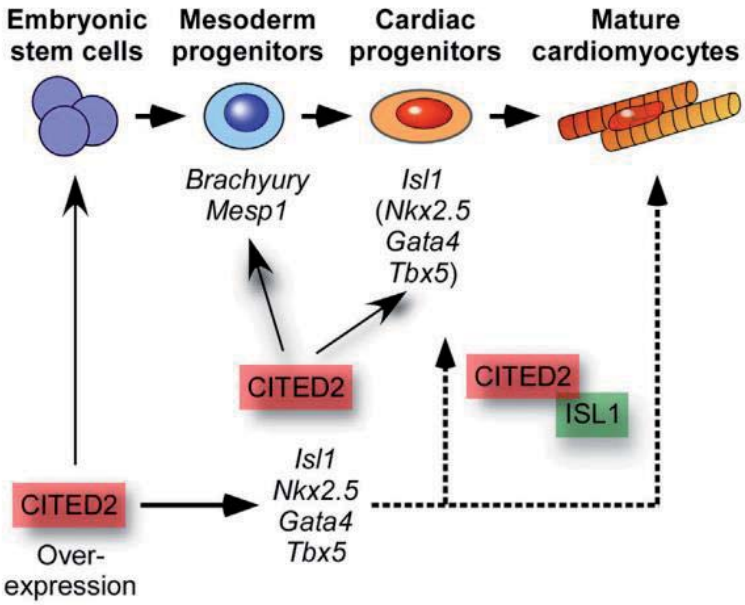

Figure 3.1. Model of the role of Cited2 during cardiogenesis of ESC. CITED2 is required for the normal expression of mesoderm markers such as Brachyury and Mesp1 and cardiac mesoderm markers such as Isl1, Nkx2.5, Gata4, and Tbx5. The overexpression of CITED2 in ESC triggers an increase of Isl1, Nkx2.5, Gata4, and Tbx5 which favours cardiac differentiation. Lastly, CITED2 and ISL1 proteins physically interact and cooperatively promote cardiac differentiation (264).

3.2 Chapter Objectives and experimental strategy

To better understand the role of Cited2 at the early stages of mESC differentiation, we employed a CITED2 loss and gain of function approaches to examine the role of *Cited2* during cardiac differentiation.

3.3 *Cited2* is expressed throughout cardiac differentiation

To further investigate the role of Cited2 in cardiac differentiation we used *Cited2*$^{fl/fl}$[Cre], which allows the conditional KO of *Cited2* by supplementation of 4HT to the culture medium. First, we analysed *Cited2* kinetic expression by qPCR, during the differentiation of *Cited2*$^{fl/fl}$[Cre] ESC (Figure 3.2). The pattern of *Cited2* expression in control ESC (EtOH treated) is biphasic. *Cited2* transcripts decrease from the onset of differentiation, D0 to D2 of differentiation, followed by an elevation from D3 onward.

Next, we examined *Cited2* expression in *Cited2*$^{fl/fl}$[Cre] ESC treated with 4HT (Figure 3.2). In cells treated with 4HT, *Cited2* expression decreases at a similar rate as control ESC from day D0 to D2 of differentiation. However, from D3 onwards *Cited2* transcripts were significantly lower in cells treated with 4HT when compared to those where EtOH was used as a vehicle. This decrease of *Cited2* expression from D3 onwards is due to cells impaired ability to produce *Cited2* transcripts indicative of a partial *Cited2* KO.

The increase in *Cited2* transcripts levels on control ESC matches *Cited2* expression *in vivo*. In mice, *Cited2* expression is detected post gastrulation in the cardiogenic mesoderm and later in CPC of both FHF and SHF (234).

Cited2 depletion was incomplete during the time course of differentiation since *Cited2* transcripts remained detectable in cells treated with 4HT. Even so, these levels were significantly reduced in comparison to the EtOH treated cells, especially from day 3 onwards. This decrease should still result in phenotypic changes since *Cited2* haploinsufficiency is sufficient to result in CHD in mouse and human (242).

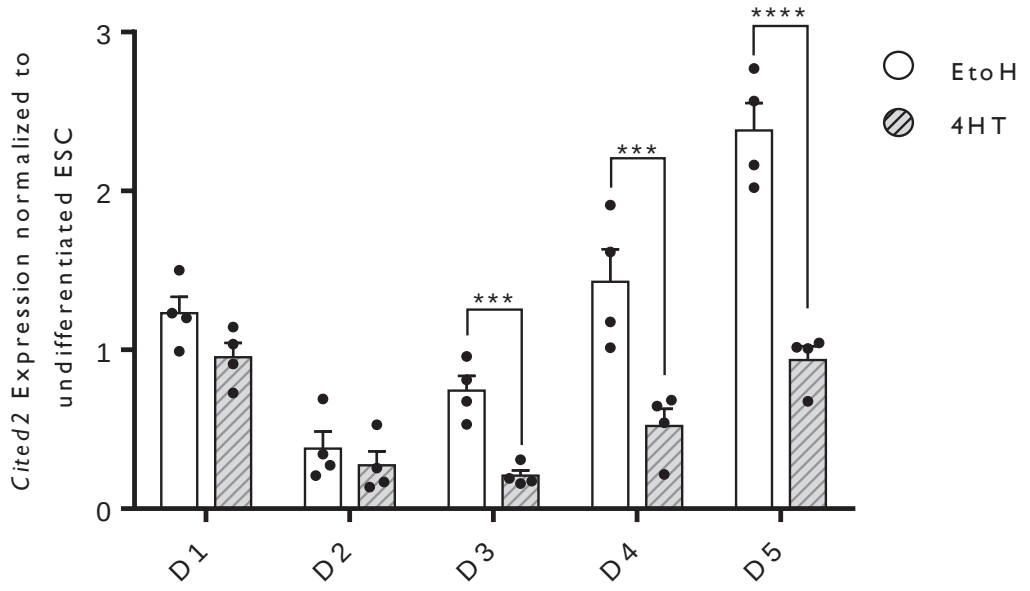

Figure 3.2. Cited2 expression in mESC differentiation. The expression of *Cited2* was determined by qPCR of *Cited2*$^{fl/fl}$[Cre] ESC treated either with EtOH or 4HT at the onset of differentiation. Samples were taken every 24h during the initial 5 days of differentiation. *Cited2* expression was normalized to the expression of undifferentiated *Cited2*$^{fl/fl}$[Cre] ESC. Each dot represents the expression per sample and mean ±SEM of four independent experiments. (*** p<0.005; **** p<0.001).

3.4 Cited2 is required for cardiomyocytes differentiation

To determine if Cited2 depletion impairs the cardiac cell fate decision of ESC, we counted the number of EB that originated spontaneous beating foci at D10 of differentiation. Noticeably, the number of beating foci was reduced in cell cultures treated with 4HT at D0 compared with cell cultures treated with EtOH (Figure 3.3). Indeed, in comparison to control cells, the number of beating colonies arising from *Cited2* depleted cells reduced in half.

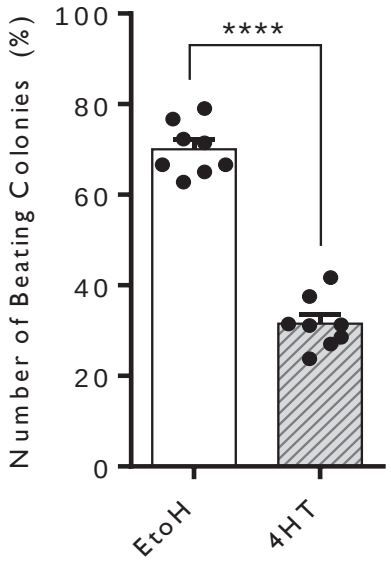

Figure 3.3. *Cited2* depletion impairs cardiac differentiation. *Cited2*$^{fl/fl}$[Cre] ESC were treated either with EtOH or 4HT at the onset of differentiation and the average number of beating colonies was determined at D8 of differentiation. The percentage of beating colonies was determined by the number of colonies that express a beating colony divided by the total number of colonies. Each dot represents an independent experiment and mean ±SEM of eight independent experiments. (**** $p<0.001$),

To further support and validate these observations, we analysed the expression of cardiomyocyte-specific markers through immunocytochemistry (ICC) at D10 of differentiation (Figure 3.4). Approximately 25% to 30% of *Cited2*$^{fl/fl}$[Cre] ESC treated with EtOH were positive for α-ACTININ and MF20. *Cited2*$^{fl/fl}$[Cre] ESC treated with 4HT resulted in the decline of α-ACTININ or MF20 protein detection and in the diminution of the number of cells stained positive α-ACTININ and MF20 in comparison with control ESC (Figure 3.5a). Interestingly, when we investigated the sarcomere organization of *Cited2* depleted ESC we observed that they were largely unorganized. Indeed, α-ACTININ and MF20 positive control ESC had the majority of their sarcomeric region well organized. In comparison, 4HT treated cells had most of their sarcomeric region disorganized (Figure 3.5b).

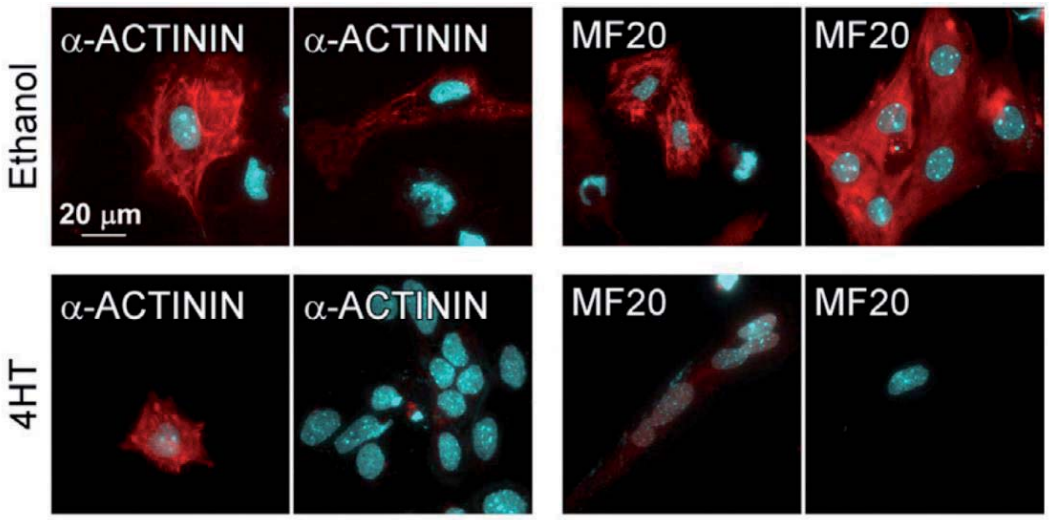

Figure 3.4. Immunofluorescence detection of sarcomeric proteins in cardiomyocytew. *Cited2*$^{fl/fl}$[Cre] ESC treated either with Ethanol or 4HT at the onset of differentiation were stained for α-ACTININ (left panels, red staining) or MF20 (right panels, red staining). Nuclei wer stained with DAPI and cells were analysed at 100X magnification.

Both actin (thin) and myosin (thick) filaments expression were reduced, most notably, myosin filaments which were almost non-existent in *Cited2* depleted ESC. Smaller sarcomere length is typically found in immature cardiomyocytes (265) This suggests that *Cited2* depleted ESC do not differentiate efficiently resulting in very immature cardiomyocytes.

3.5 A recombinant Cited2 protein rescues Cited2 depletion defects

To confirm that the cardiogenic differentiation defects observed in *Cited2* depleted cells were caused by the loss of CITED2 expression, *Cited2*$^{fl/fl}$[Cre] ESC, treated with 4HT, were supplemented with 5-10μg of a recombinant human CITED2 protein, hereafter known as 8R-CITED2. The recombinant 8R-CITED2 has the CITED2 N-terminal domain with a stretch of eight arginine's, that allow proteins to pass the intracellular membrane and translocate into the nucleus (266).

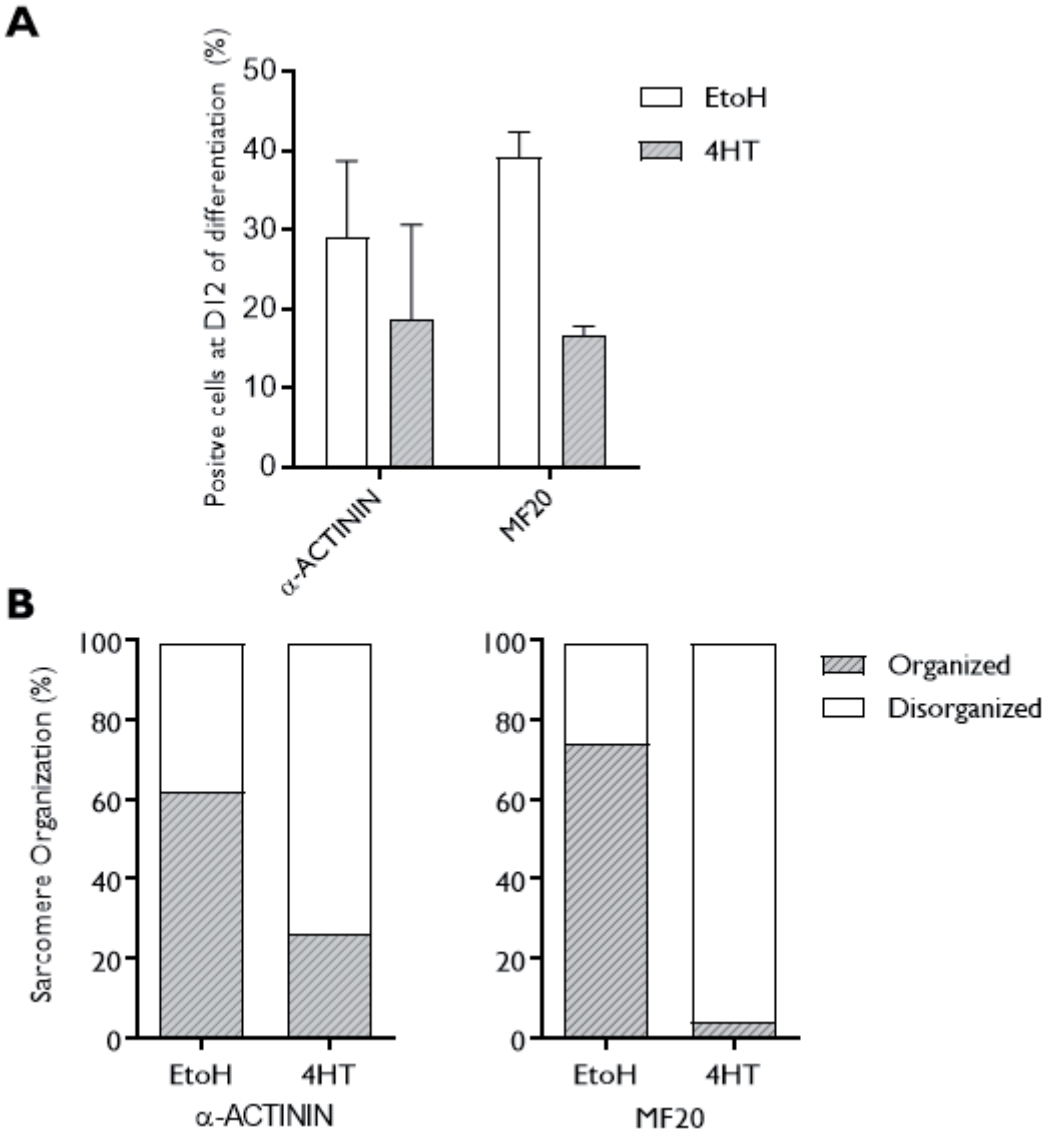

Figure 3.5 Expression and organization of sarcomeric proteins in cardiomyocytes. A) Percentage of positive cells stained at D12 of differentiation for α-ACTININ or MF20 in *Cited2*$^{fl/fl}$[Cre] ESC treated either with EtOH (white bars) or 4HT (grey bars) at the onset of differentiation. B) Sarcomeric organization of α-ACTININ or MF20 positive cells. A) Bars represent the mean ±SEM of two independent experiments.

We first supplemented 8R-CITED2, in combination with 4HT, to the culture medium of *Cited2*$^{fl/fl}$[Cre] ESC at D0. Surprisingly, the average number of beating colonies did not change between cells treated with 4HT and 4HT+8R-CITED2 (Figure 3.6a). Interestingly, the supplementation of 8R-CITED2 at D2 of differentiation in the culture medium of ESC treated with 4HT at D0 restored the emergence of beating colonies to control levels, further confirming that the cardiac defects observed are caused by *Cited2* depletion (Figure 3.6b).

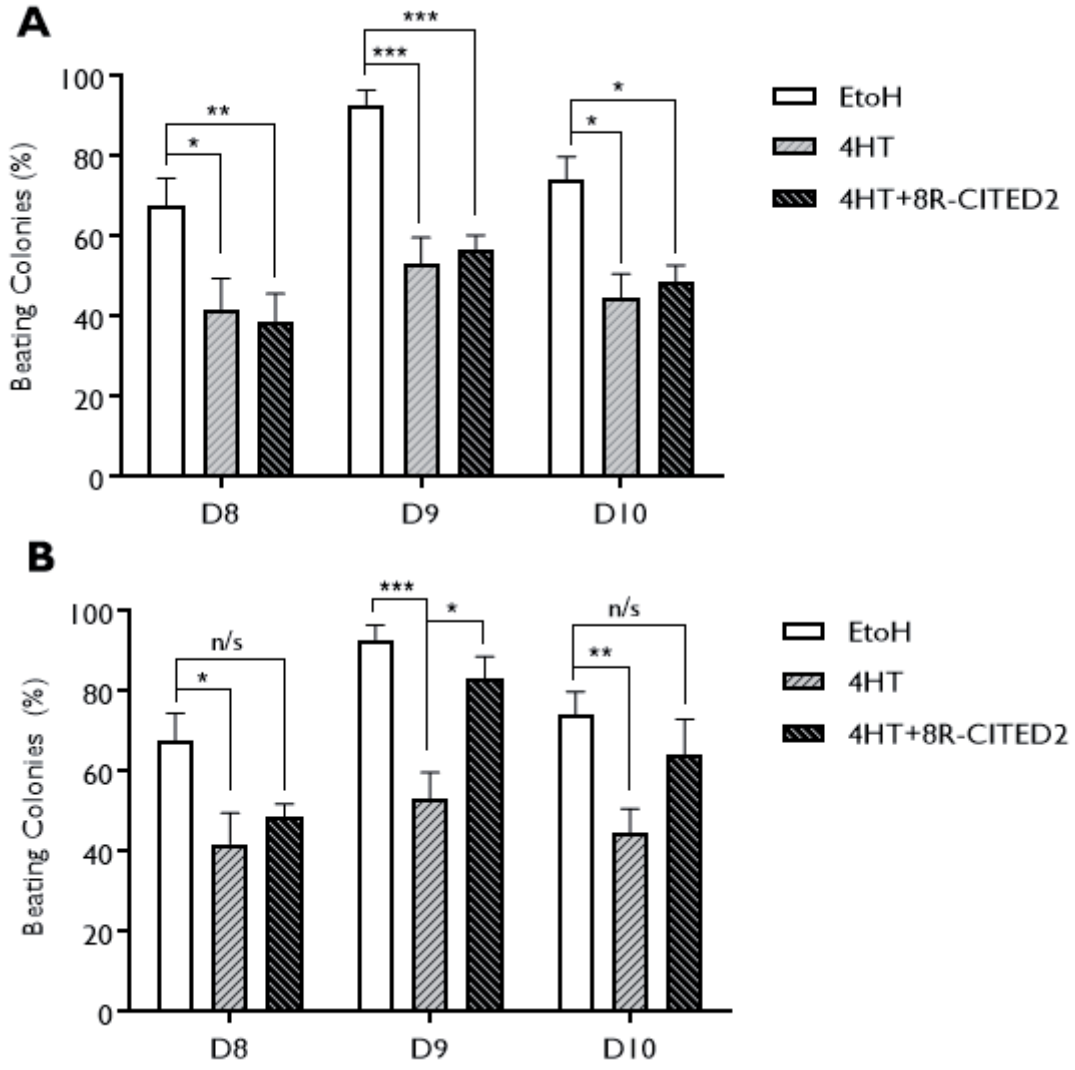

Figure 3.6 Recombinant CITED2 protein can rescue cardiac defects caused by *Cited2* depletion. A) *Cited2*$^{fl/fl}$[Cre] ESC were treated at the onset of differentiation with EtOH, 4HT or 4HT with 5-10 μg/mL of 8R-CITED2. The percentage of beating colonies was determined at D8, D9 or D10 of differentiation. B) *Cited2*$^{fl/fl}$[Cre] ESC were treated at the onset of differentiation with EtOH or 4HT at the onset of differentiation. At D2 of differentiation, some of the 4HT treated cells were then supplemented with 5-10 μg/mL of 8R-CITED2, while the rest was maintained under normal conditions. The percentage of beating colonies was determined at D8, D9 or D10 of differentiation. Bars represent the mean ±SEM of four independent experiments. Non-significant (n/s); (* $p<0.05$); (** $p<0.01$); (*** $p<0.005$).

Next, we supplemented 8R-CITED2 to *Cited2*$^{\Delta/\Delta}$ ESC, which complete lack CITED2 expression and do not differentiate well into cardiomyocytes (264). *Cited2*$^{\Delta/\Delta}$ ESC were treated with 8R-CITED2 at D2 of differentiation and the number of beating cells determined at D10. Even with supplementation of 8R-CITED2, we failed to increase the number of beating cells.

As such, we investigated if 8R-CITED2 supplementation could increase the expression of mesoderm and cardiac mesoderm transcription factors.

At D5 of differentiation *Cited2*$^{\Delta/\Delta}$ ESC, express less mesoderm and cardiac mesoderm transcription factors compared to *Cited2*$^{fl/fl}$ ESC. Indeed, while *Gata4* expression was similar in both cell types, *Cited2*$^{\Delta/\Delta}$ ESC express lower levels of *Brachyury, Mesp1*, *Tbx5, Isl1,* and *Nkx2.5* when compared to *Cited2*$^{fl/fl}$ ESC. However, when *Cited2*$^{\Delta/\Delta}$ ESC were treated with 8R-CITED2 at D2 of differentiation, the expression of *Brachyury, Mesp1*, *Tbx5, Isl1,* and *Nkx2.5* increased. While this increase in expression matched the expression levels of *Cited2*$^{fl/fl}$ ESC, only *Isl1* expression was significantly different when compared to non-treated *Cited2*$^{\Delta/\Delta}$ ESC (Figure 3.7).

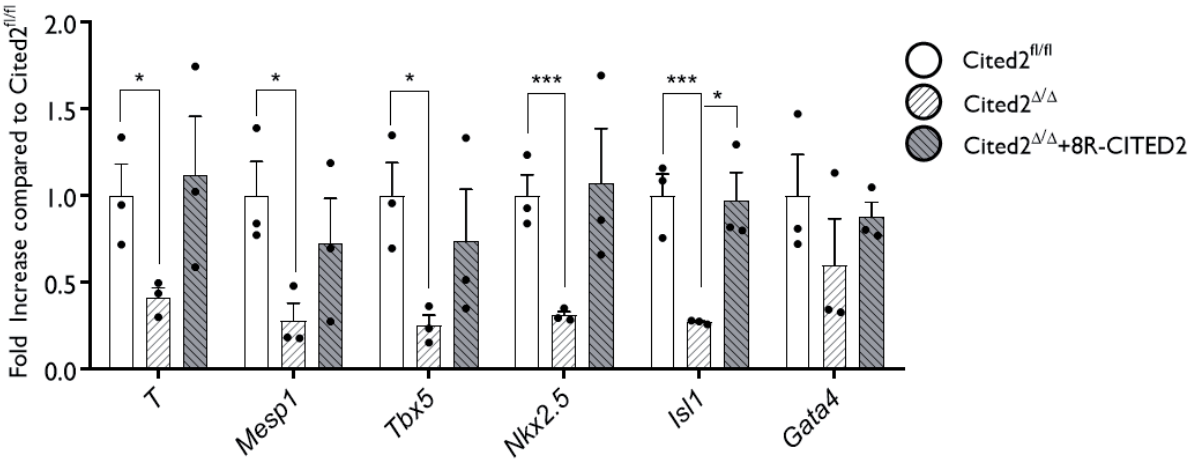

Figure 3.7 8R-CITED2 can partially rescue *Cited2* null ESC. The expression of *T, Mesp1, Tbx5, Nkx2.5, Isl1,* and *Gata4,* were determined at D5 of differentiation in *Cited2*$^{fl/fl}$, *Cited*$^{\Delta/\Delta}$ and *Cited*$^{\Delta/\Delta}$ ESC treated at D2 of differentiation with 5-10 μg/mL of 8R-CITED2 through qPCR. The expression of each gene was normalized to the levels obtained in *Cited2*$^{fl/fl}$ ESC at D5 of differentiation. Each dot represents the expression per sample and mean ±SEM of three independent experiments. (* $p<0.05$); (*** $p<0.005$).

3.6 Decrease of Cited2 expression during mesoderm is required for proper cardiac differentiation.

Previous data showed that CITED2 overexpression, in mESC, promotes cardiac cell emergence upon differentiation (264). However, both *Cited2* kinetic expression, as well rescue with 8R-CITED2, made us hypothesize that *Cited2* expression needs to go down, during the

initial days of differentiation, to allow ESC to go into a state permissive to their differentiation. To test this hypothesis, we used A2UpC2 ESC that enable the temporal overexpression of *Cited2* upon addition of doxycycline into the medium at different time points of differentiation.

Doxycycline was added at different time points of differentiation and renewed every two days until D10 of differentiation and the number of beating colonies was determined between D7 to D9. The addition of doxycycline every two days ensures that the levels of *Cited2* remain high throughout the process of differentiation (Figure 3.8).

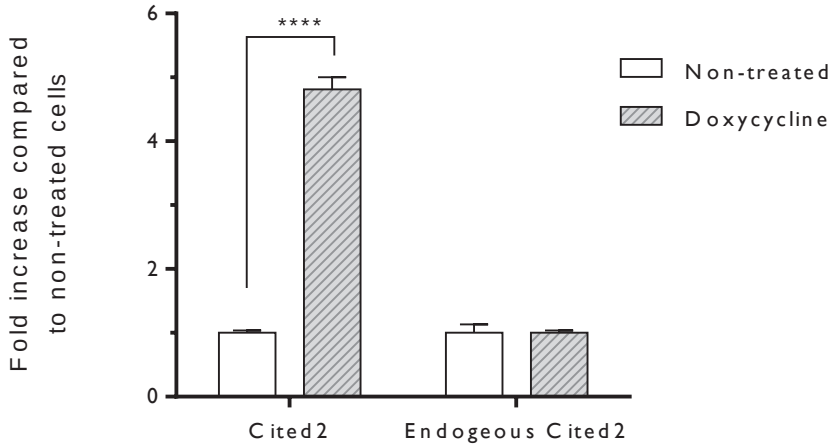

Figure 3.8 Inducible *Cited2* overexpression system. The expression of *Cited2* was determined in A2UpC2 ESC, treated or non-treated, with 1µg/mL of doxycycline for two days through qPCR. The expression of Cited2 was normalized to the levels of non-treated cells. Error bars represent the mean ±SEM of three independent experiments. (**** p<0.001).

When doxycycline was added from D0 onward, the differentiation into cardiomyocytes was severely compromised. Indeed, continuous overexpression of *Cited2* from D0 results in almost no beating colonies when compared to non-treated A2UpC2 ESC. Interestingly, continuous addition of doxycycline at a later time point of differentiation did not affect the ability of A2UpC2 to differentiate into cardiomyocytes when compared to non-treated cells (Figure 3.9).

Thus, *Cited2* expression needs to go down to ensure a proper cardiac differentiation. To some extent, this result contradicts what we had previously reported (264). However, contrary to the previously mentioned experiment where *Cited2* was overexpressed prior to differentiation, in this experiment we continuously maintained *Cited2* levels high throughout differentiation.

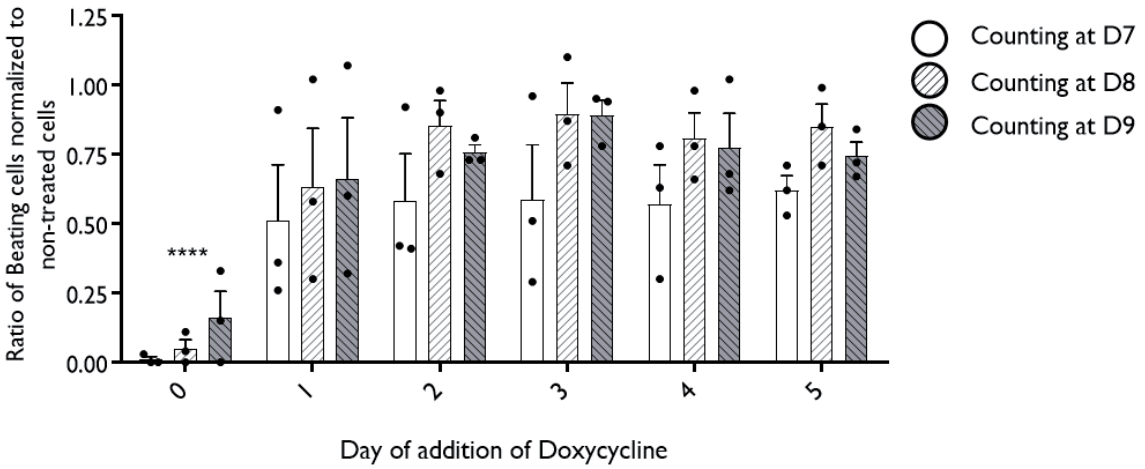

Figure 3.9 Continuous Cited2 Overexpression at the onset of differentiation impairs cardiac differentiation. 2µg/mL of doxycycline was added to A2UpC2 ESC at different days of differentiation and renewed every two days until D9 of differentiation. The average number of beating colonies was assessed at D7, D8 and D9 of differentiation and normalized to non-treated A2UpC2 at D7, D8 and D9 of differentiation. Each dot represents the expression per sample and mean ±SEM of three independent experiments. Statistical analysis was performed for the countings at D8 of differentiation. (**** $p<0.001$).

3.7 Conclusion

Cited2 is expressed throughout the process of cardiac differentiation but its expression is minimal at D2 of differentiation. Depletion of *Cited2* at the onset of differentiation impairs the ability of ESC to give rise to cardiomyocytes. This was observed through a decrease in the average number of beating cells and the decrease of cardiomyocyte-specific markers. To demonstrate that the cardiac defects observed were caused by *Cited2* depletion we treated ESC with a recombinant CITED2 protein that can revert cardiac defects when added at D2 of differentiation. We also provide evidence that continuous expression of *Cited2*, from the onset of differentiation, impairs cardiac differentiation. This indicates that the expression of *Cited2* must decrease to ensure proper cardiac differentiation.

CHAPTER 4

Gene Profile of Cited2 depleted ESC

4.1 Introduction

We previously reported that Cited2 contributes to the expression of a subset of key cardiopoietic genes involved in mesoderm and CPC specification (264). During mouse embryonic development CITED2 expression was detected in early mesodermal cardiac-derived structures (233).

Surprisingly, using a *Brachyury*-CRE or a *Mesp1*-CRE conditional *Cited2* KO only resulted in minor heart developmental defects of mouse embryos, while *Cited2* KO in the epiblast consistently resulted in embryonic lethality and heart defects (242). Similarly, we reported that *Cited2* depletion at the onset of differentiation of ESC causes the most severe impact on cardiac differentiation (264). On the other hand, *Cited2* depletion from D2 onwards had little to no effect on cardiogenesis. Together, with the results from the previous chapter, indicate that *Cited2* function is important for the early commitment of ESC to mesoderm and cardiac specification.

4.2 Experimental Strategy

To further investigate the mechanisms underlying the loss of Cited2, in pluripotency and early differentiation, we compared the gene expression profiles of *Cited2* depleted cells at D4 of differentiation, to control cells at D4 of differentiation or undifferentiated. For that, we extracted RNA and performed microarray analysis, of *Cited2*$^{fl/fl}$[Cre] ESC, treated with EtOH or 4HT, at the onset of differentiation, at D0 and D4 of differentiation (Figure 4.1).

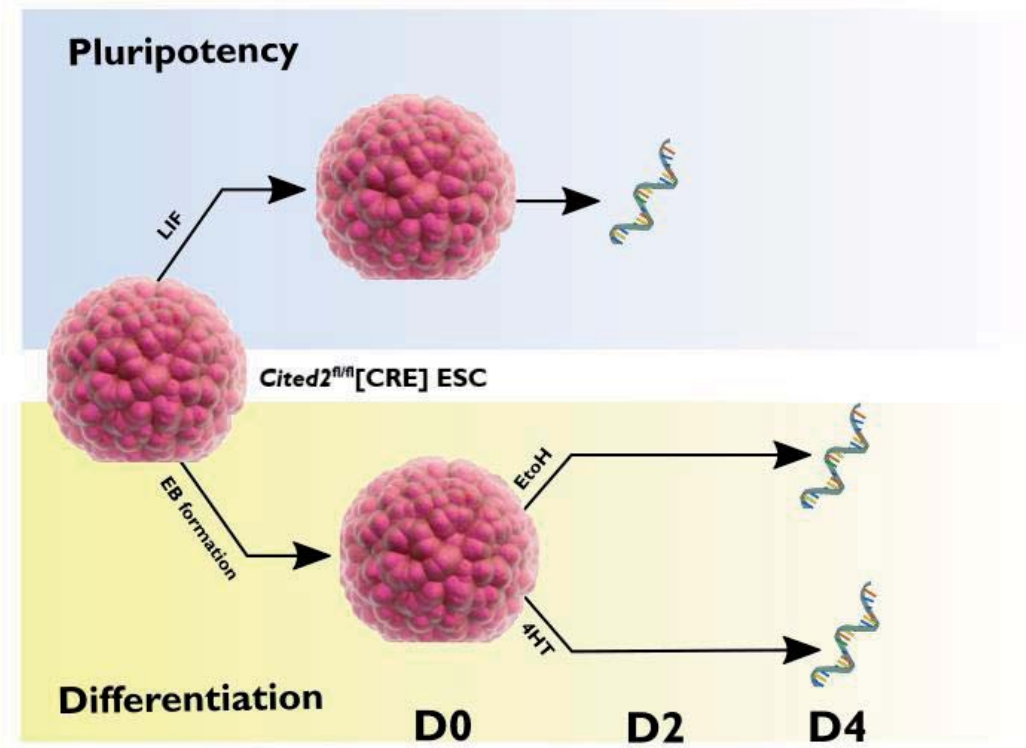

Figure 4.1 Microarray experimental strategy. *Cited2*$^{fl/fl}$[Cre] ESC were treated with EtOH or 4HT and maintained under pluripotent conditions or differentiated. Total RNA of cells maintained under pluripotency conditions was extracted at D2, whereas total RNA of cells used for differentiation was extracted at D4. Samples were later sent for microarray analysis.

4.3 Transcriptional differences between control cells and *Cited2* depleted cells.

To understand the molecular differences between *Cited2* depleted cells and control cells we first performed a PCA. PCA is a statistical procedure that simplifies the complexity in high dimensional data while retaining trends and patterns. PCA analysis indicated that patterns of expression of undifferentiated and differentiated *Cited2*$^{fl/fl}$[Cre] ESC are very distinct (Figure 4.2). Interestingly, the transcriptomic profile of *Cited2* depleted cells at D4 of differentiation clustered closer to those of undifferentiated ESC than to control ESC at D4 of differentiation.

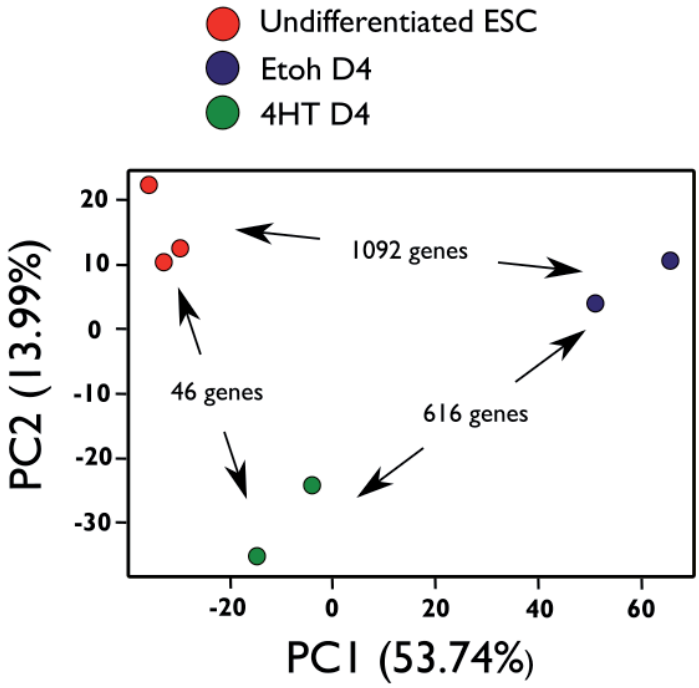

Figure 4.2 Principal Component Analysis. PCA analysis of *Cited2*$^{fl/fl}$[Cre] ESC undifferentiated (red dots), control cells at D4 of differentiation (blue dots) and *Cited2* depleted at D4 of differentiation (green dots). The number of differentially expressed genes is indicated. Each dot represents an individual sample.

Next, we analysed the gene expression differences between undifferentiated ESC and control cells at D4 of differentiation. We considered the expression values significantly altered when adjusted p-value was inferior to 0.05 and the absolute LogFC was greater than 1. We found 546 genes differentially expressed genes (DEGS) upregulated while 546 DEGS were downregulated in *Cited2*$^{fl/fl}$[Cre] ESC at D4 when compared with *Cited2*$^{fl/fl}$[Cre] ESC at D0. Amongst the most upregulated genes, we identified genes important for different cell fate acquisition including *Kdr, Eomes* or *Mixl1* (Figure 4.3A). On the other hand, amongst the most downregulated genes, we identified genes important for pluripotency such as *Sox2*, *Dppa5a,* and *Klf4* (Figure 4.3B)

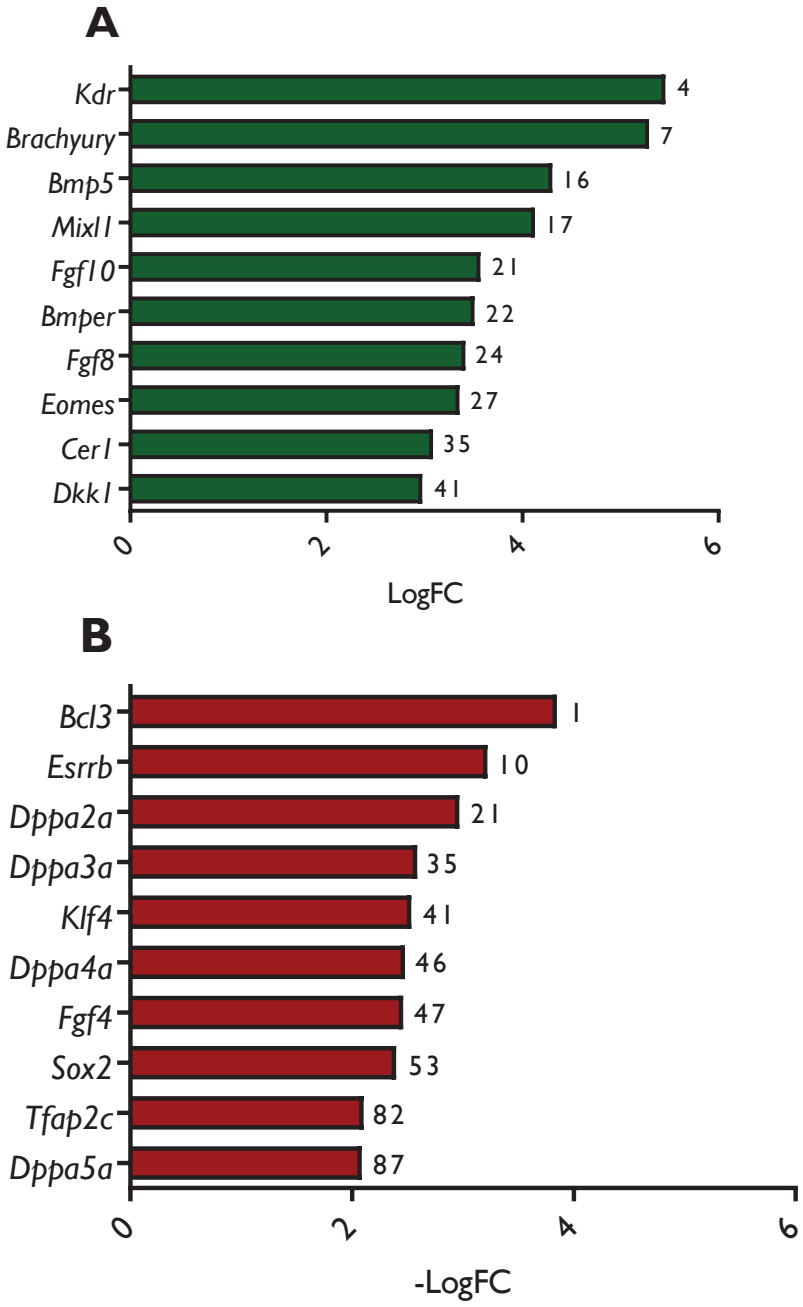

Figure 4.3 Top DEGS between differentiated and undifferentiated cells. Bars represent the top 10 upregulated and downregulated DEGS important for pluripotency or cell fate commitment in *Cited2*$^{fl/fl}$[Cre] ESC at D4 of differentiation compared to *Cited2*$^{fl/fl}$[Cre] ESC undifferentiated. A) DEGS upregulated. B) DEGS Downregulated. The number ahead of the bars indicates the ranking position in all DEGS found.

For upregulated and downregulated DEGS we performed functional enrichment analysis on basis of Wikipathways conducted by Enrichr web-tool (260, 261). Wikipathways is an open, collaborative platform for capturing and disseminating biological pathways for data

visualization and analysis (267, 268). Pathway enrichment analysis with the upregulated DEGS indicated that the gene expression profile fits the initial process of fate acquisition during ESC differentiation and early embryonic development (Table 4.1). Likewise, pathway analysis of the downregulated DEGS indicated that the gene expression profile is related with pluripotent network and pre-implantation epiblast (Table 4.2).

Table 4.1 Upregulated pathways in differentiated cells compared to undifferentiated cells. Pathway analysis was conducted using Enrichr for the 546 DEGS upregulated in *Cited2*$^{fl/fl}$[Cre] ESC at D4 of differentiation compared to *Cited2*$^{fl/fl}$[Cre] ESC undifferentiated.

Index	Pathway	P-value
1	Mesodermal Commitment	4.159e-14
2	Endoderm Differentiation	6.196e-13
3	Heart Development	1.127e-11
4	Cardiac Progenitor Differentiation	3.553e-11
5	Neural Crest Differentiation	6.938e-10
6	Ectoderm Differentiation	1.509e-8
7	Differentiation Pathway	2.218e-4
8	Adipogenesis	2.307e-4
9	Wnt Signalling Pathway	7.980e-4
10	ESC Pluripotency Pathways	8.137e-4

On the other hand, only 8 DEGS were found upregulated and 37 were found downregulated in differentiated *Cited2* depleted cells at D4 of differentiation in comparison to undifferentiated control cells. Interestingly, the most upregulated gene was *Brachyury* (LogFc 2.95), indicative of initial stages of differentiation. Amongst the 37 DEGS downregulated, we identified *Dppa3a* (LogFC -1.58), a gene expressed in PSC and important for their maintenance. Interestingly, we also identified *Prdm1* (LogFC -1.99), *Pcgf5* (Log FC -1,39), genes responsible for blocking neuronal cell fate decision, amongst the downregulated DEGS (269, 270).

Table 4.2. Downregulated pathways in differentiated cells compared to undifferentiated cells. Pathway analysis was conducted using Enrichr for the 546 DEGS downregulated in *Cited2*$^{fl/fl}$[Cre] ESC at D4 of differentiation compared to *Cited2*$^{fl/fl}$[Cre] ESC undifferentiated.

Index	Pathway	P-value
1	Pluripotency Network	2.712e-11
2	Preimplantation Embryo	1.516e-04
3	Nuclear Receptors	9.862e-04
4	TGF Beta Signalling Pathway	2.648e-03
5	p53 signalling	4.769e-03
6	Focal Adhesion-PI3K-Akt-mTOR-signalling pathway	5.540e-03
7	Endoderm Differentiation	6.370e-03
8	Mesodermal Commitment Pathway	7.687e-03
9	Prostaglandin Synthesis and Regulation	1.099e-02
10	IL-4 Signalling Pathway	3.330e-02

Lastly, we found 366 DEGS upregulated and 250 DEGS downregulated in control cells compared to *Cited2* depleted cells at D4 of differentiation. Intriguingly, we found that most of the top DEGS, previously associated with ESC maintenance or differentiation, were similar to the ones found in differentiated and undifferentiated cells, but in different ranking positions (Figure 4.4). Conversely, pathway analysis of the upregulated DEGS indicated that heart development, endoderm and mesoderm cell fate commitment, were the most affected pathways upon *Cited2* depletion, at D4 of differentiation (Table 4.3). On the other hand, loss of *Cited2* resulted in an incomplete decrease in the expression of genes important for pluripotency maintenance (Table 4.4).

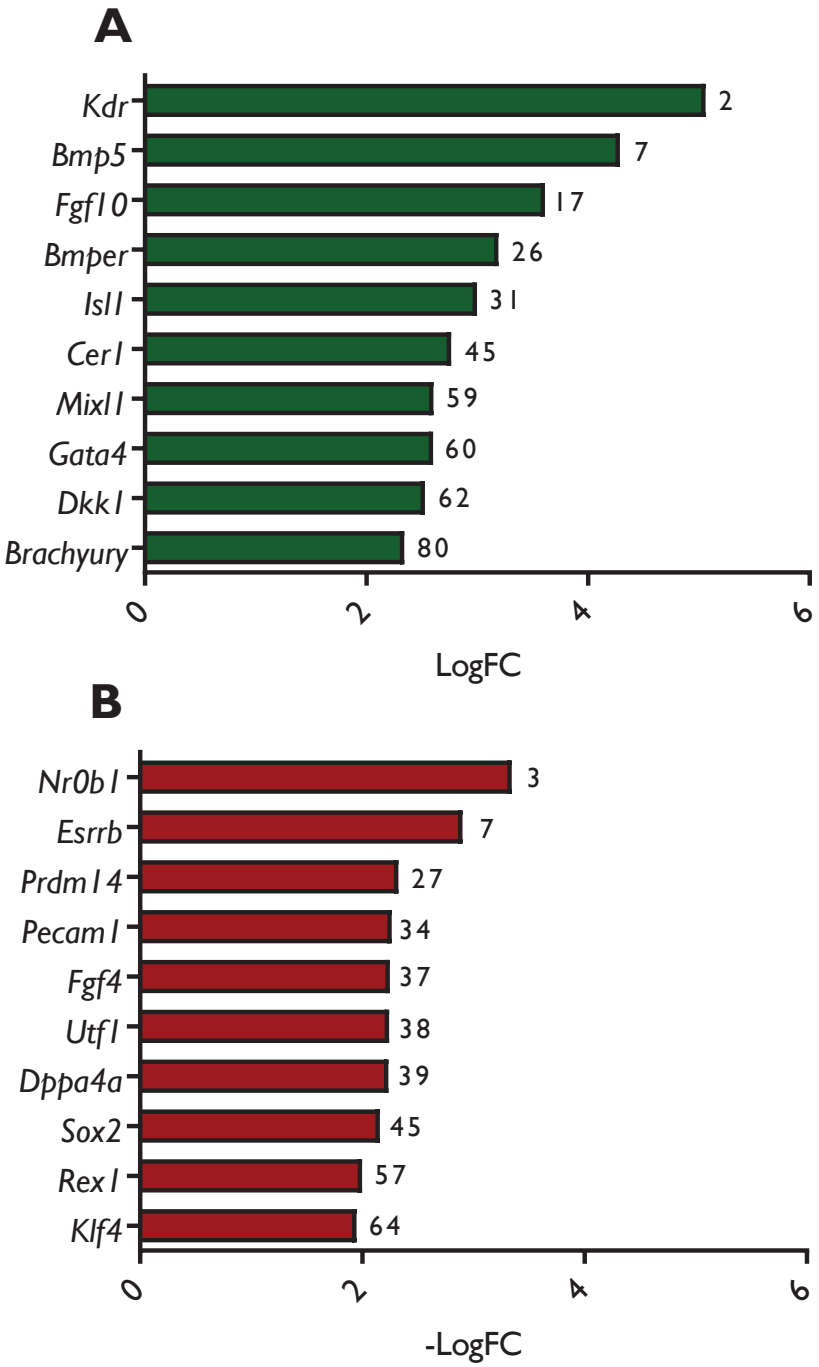

Figure 4.4 Top DEGS between control cells and *Cited2* depleted cells at D4 of differentiation. Bars represent the top 10 upregulated and downregulated DEGS important for pluripotency or cell fate commitment in *Cited2*$^{fl/fl}$[Cre] ESC at D4 of differentiation compared to *Cited2*$^{fl/fl}$[Cre] ESC treated with 4HT at D4 of differentiation. A) DEGS upregulated. B) DEGS Downregulated. The number ahead of the bars indicates the ranking position in all DEGS found.

Table 4.3 Upregulated pathways in control cells compared to *Cited2* depleted cells at D4 of differentiation. The pathway analysis was conducted using Enrichr for the 366 DEGS upregulated in *Cited2*$^{fl/fl}$[Cre] ESC at D4 of differentiation compared to *Cited2*$^{fl/fl}$[Cre] ESC undifferentiated.

Index	Pathway	P-value
1	Heart Development	1.469e-11
2	Endoderm Differentiation	3.456e-11
3	Mesodermal Commitment	9.083e-11
4	Cardiac Progenitor Differentiation	1.602e-10
5	Neural Crest Differentiation	4.643e-10
6	Adipogenesis	1.703e-06
7	TGF-beta Signalling Pathway	1.609e-04
8	Wnt Signalling Pathway	3.300e-04
9	Ectoderm Differentiation	6.580e-04
10	ESC Pluripotency Pathways	1.470e-03

Table 4.4 Downregulated pathways in control cells compared to *Cited2* depleted cells at D4 of differentiation. The pathway analysis was conducted using Enrichr for the 250 DEGS downregulated in *Cited2*$^{fl/fl}$[Cre] ESC at D4 of differentiation compared to *Cited2*$^{fl/fl}$[Cre] ESC undifferentiated.

Index	Pathway	P-value
1	Pluripotency Network	1.419e-12
2	Statin Pathway	5.751e-04
3	Preimplantation Embryo	8.469e-04
4	PPAR Alpha Pathway	4.057e-03
5	Nuclear Receptors	1.096e-02
6	Endoderm Differentiation	1.204e-02
7	Mesodermal Commitment Pathway	1.516e-02
8	TGF Beta Signalling Pathway	2.721e-02
9	ErbB Signalling Pathway	3.144e-02
10	Wnt Signalling Pathway	3.917e-02

4.4 *Cited2* depletion impairs the expression of mesoderm and endoderm genes

The major differences found between undifferentiated cells and *Cited2* depleted cells at D4, when compared to control differentiated cells, was the absence of DEGS important for ectoderm cell fate, in *Cited2* depleted cells. Indeed, the ectoderm pathway was heavily downregulated in undifferentiated cells (p-value 1.509e-8) but, in *Cited2* depleted cells, the ectoderm pathway was less affected (p-value 6.580e-04).

As such we hypothesized that *Cited2* depletion impairs the expression of genes important for mesoderm and endoderm transition. To test our hypothesis, we investigated a reference list of genes specific of each primary embryonic lineage (Supplementary Table 10.1). This list includes 20 ectoderm specific genes, 36 endoderm specific genes, 20 mesoderm specific genes and 30 genes common to both mesoderm and endoderm cell fate (Adapted from (271)).

We identified 12 out of 36 endoderm genes, 4 out of 20 mesoderm genes and 12 out of 30 mesoderm/endoderm genes significantly upregulated, whereas only 1 out of 20 ectoderm genes was found significantly upregulated in D4 control cells compared to *Cited2* depleted cells (Figure 4.5). We then decided to calculate the statistical differences of these observations. For that, we compared the number of upregulated mesoderm and endoderm genes to the number of upregulated ectoderm genes using Fisher's exact test. We found a statistically significant difference between these two groups (p=0.0119), further emphasizing that loss of *Cited2* impairs the expression of mesoderm and endoderm genes without affecting the expression of ectoderm-specific genes.

On the other hand, we only identified two genes significantly upregulated in *Cited2* depleted cells. Curiously, one of the genes belonged to the ectodermal lineage (*Tfcp2l1),* whereas the other is a gene common to both mesoderm and endoderm cell fate (*Gdf3).*

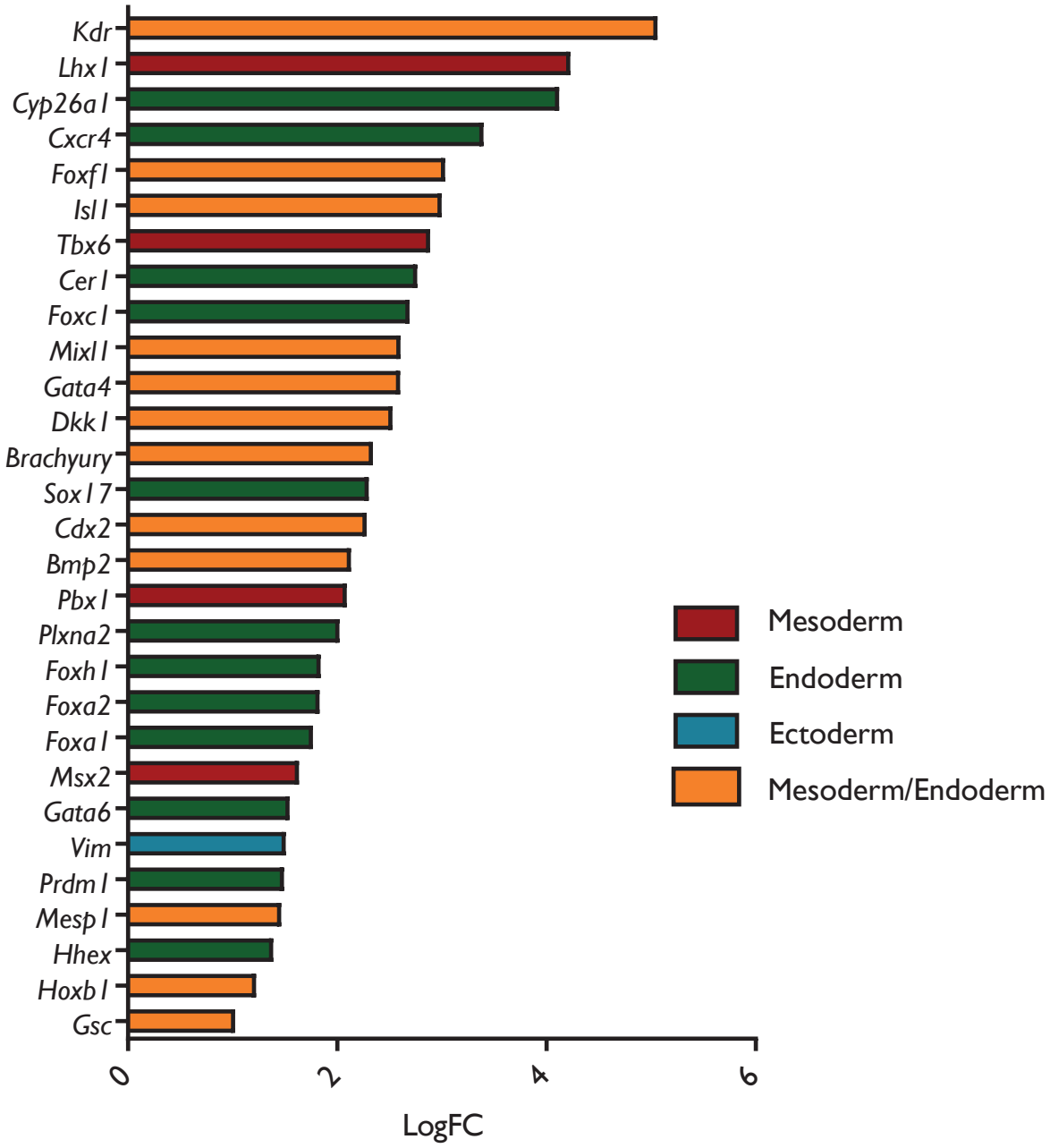

Figure 4.5 Mesoderm and Endoderm commitment is downregulated in *Cited2* depleted cells. Bars represent the DEGS found upregulated in *Cited2*$^{fl/fl}$[Cre] ESC at D4 of differentiation compared to *Cited2*$^{fl/fl}$[Cre] ESC treated with 4HT at D4 of differentiation-specific of ectoderm (blue bars), mesoderm (red bars) and endoderm (green bars) lineages or common to both mesoderm and endoderm (orange bars). Data was obtained according to Supplementary Table 10.1.

4.5 Cited2 depletion delays the expression of mesoderm and cardiac mesoderm transcription factors

As *Cited2* depletion impairs the expression of genes involved in cardiogenesis, we assessed from D1 to D6 of differentiation the expression of genes associated with epiblast (*Fgf5*) and early mesoderm specification (*Brachyury, Mixl1, Mesp1,* and *Eomes)* by qPCR (Figure 4.6).

The expression profile of epiblast marker *Fgf5* expression remained similar between EtOH and 4HT treated cells, from D1 to D4 of differentiation with both presenting peaks of expression occurring at D4. Afterward, *Fgf5* expression decreases on D5 and D6 on EtOH treated cells while in 4HT conditions its expression remains high and similar to the levels observed at D4.

Mesoderm markers *Brachyury*, *Mixl1, Eomes,* and *Mesp1* expression profiles between EtOH and 4HT treated cells were different. In EtOH treated cells the peak of expression happened at D4 and rapidly decreases, while in 4HT treated cells this peak of expression only occurred at D5.

The differences in transcriptional activity are likely to result in the unregulated expression of genes that might favour other cell fate specification. For example, MIXL1 expression is required for mesoderm differentiation, but it's enforced or later expression, suppresses mesoderm and promotes endoderm formation (272).

4.6 Conclusion

Previous results suggested that *Cited2* function is most critical at the early stages of differentiation. To better understand the impact of *Cited2* depletion in ESC cell fate commitment we performed microarray analysis. PCA analysis confirmed that the transcriptomic profile of *Cited2* depleted cells is similar to undifferentiated cells than differentiated cells at D4 of differentiation. The DEGS and the pathway analysis confirmed, that upon *Cited2* depletion, ESC lack the ability to express genes important for endoderm and mesoderm differentiation which results in the impaired ability to give rise to cardiac-derived

cells. Upon further analysis, we identified by qPCR, that cells that lack *Cited2* delay the expression of mesoderm and cardiac mesoderm transcription factors.

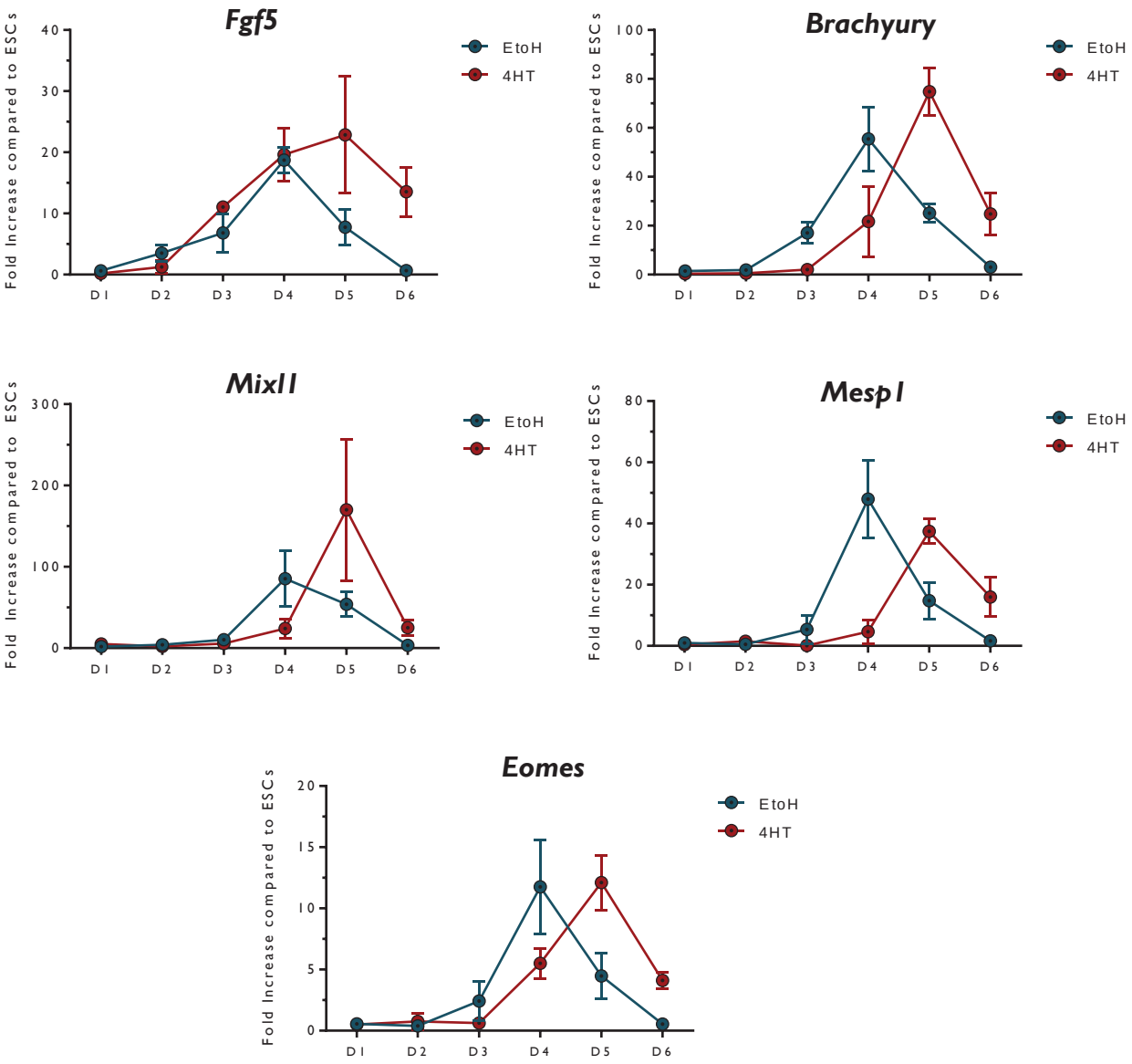

Figure 4.6. *Cited2* depletion delays the expression of mesoderm transcription factors. The expression of *Fgf5, Brachyury*, *Mixl1*, *Mesp1*, and *Eomes* were determined by qPCR of *Cited2*$^{fl/fl}$[Cre] ESC treated either with EtOH or 4HT at the onset of differentiation. Samples were taken every 24h during the initial 5 days of differentiation. Gene expression was normalized to the expression of undifferentiated *Cited2*$^{fl/fl}$[Cre] Sample and mean ±SEM of two (*Mixl1* and *Eomes*) and three (*Fgf5, Brachyury,* and *Mesp1*) independent experiments.

CHAPTER 5

Cited2 induced secretome rescues cardiac defects caused by *Cited2* depletion

5.1 Introduction

During the microarray analysis, we identified that different cardiac signalling pathways were significantly affected by the loss of *Cited2*. Curiously, many of these proteins are proteins secreted outside the cell that act as paracrine factors. For example, we found that *Dkk1* and *Fgf10,* proteins important for proper cardiac cell fate instruction, were significantly downregulated in cells that lack *Cited2*. The decrease in the expression of important cardiac signalling pathways is likely to affect cell differentiation and cardiac commitment. As such, we hypothesized that the cardiogenic deficiency of *Cited2* depleted cells results from the misregulation of extracellular signalling pathways which are precisely regulated during ESC differentiation in order to properly instruct cell fate decisions (273).

Secreted proteins constitute an important class of active molecules that play an important role in several biological processes including cell differentiation and proliferation. The word "secretome" was first introduced by Tjalsma and colleagues in a study dealing with a survey of secreted proteins of *Bacillus subtillis (274).* These secreted proteins including metabolites, amino acids, growth factors, microvesicles or exosomes can be found in the medium where stem cells are cultured (275).

The majority of secretome studies are performed *in vitro*. In general, cells of interest are seeded in serum-supplemented medium to obtain the desired cells. Cells are then washed to remove serum proteins, before incubating them in a serum-free medium for another 12 to 24 hours. CM is then collected and processed for mass spectrometry analysis, protein identification or cellular assays (276).

Few studies have provided evidence of the cardiogenic potential of CM. Treating primary isolated rat cardiomyocytes exposed to hypoxia with CM derived from hypoxic cardiomyocytes increased the number of surviving cardiomyocytes by 40% compared to the control cell (277). In another study, the cardiac defects caused by the KO of Inhibitor of DNA-binding/differentiation proteins, known as ID proteins were rescued through the co-culture experiments in which heart explants were cultured on WNT5a over-expressing MEF (278).

The use of the secretome of the CM has several advantages compared to the use of stem cells. The CM can be manufactured, freeze-dried, packaged and easily transported. Moreover, as it is devoid of cells, there is no need to match the donor and the recipient to

avoid rejection problems. Therefore, stem cell-derived CM has the potential to be produced for regenerative medicine.

5.2 Chapter Objectives and experimental strategy

To determine whether *Cited2* expression promoted the secretion of cardiopoietic factors, we transfected undifferentiated E14/T ESC with a plasmid expressing high levels of CITED2 (E14/T-FC2) and a control plasmid expressing an eGFP protein (E14/T-eGFP). E14/T-FC2 levels of *Cited2* are increased by approximately 10-folds compared to E14/T-eGP (Figure 5.1).

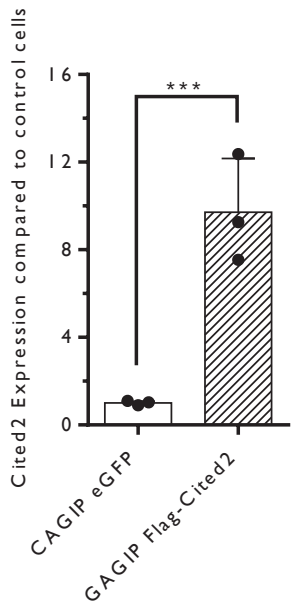

Figure 5.1. *Cited2* overexpression system. E14T ESC were transfected either with a CAGIP-eGFP or CAGIP-FC2 plasmid and *Cited2* expression was determined through qPCR two days post-transfection. Each dot represents an independent experiment and mean ±SEM of three independent experiments. (*** $p<0.005$).

Transfected E14/T ESC were maintained for 1h in a medium deprived of serum and LIF to enrich the medium with factors secreted by ESC. Since the CM is destined to be used in cell differentiation assays, LIF was removed to ensure a better differentiation process of ESC.

The CM collected from E14/T-eGFP (CM-Control) or E14/T-FC2 (CM-FC2) cultures were then supplemented as the differentiation medium of *Cited2*$^{fl/fl}$[Cre] ESC treated either with 4HT or EtOH for the first two days of differentiation. The cardiogenic potential of the CM was then assessed through the ESC ability to generate beating colonies (Figure 5.2).

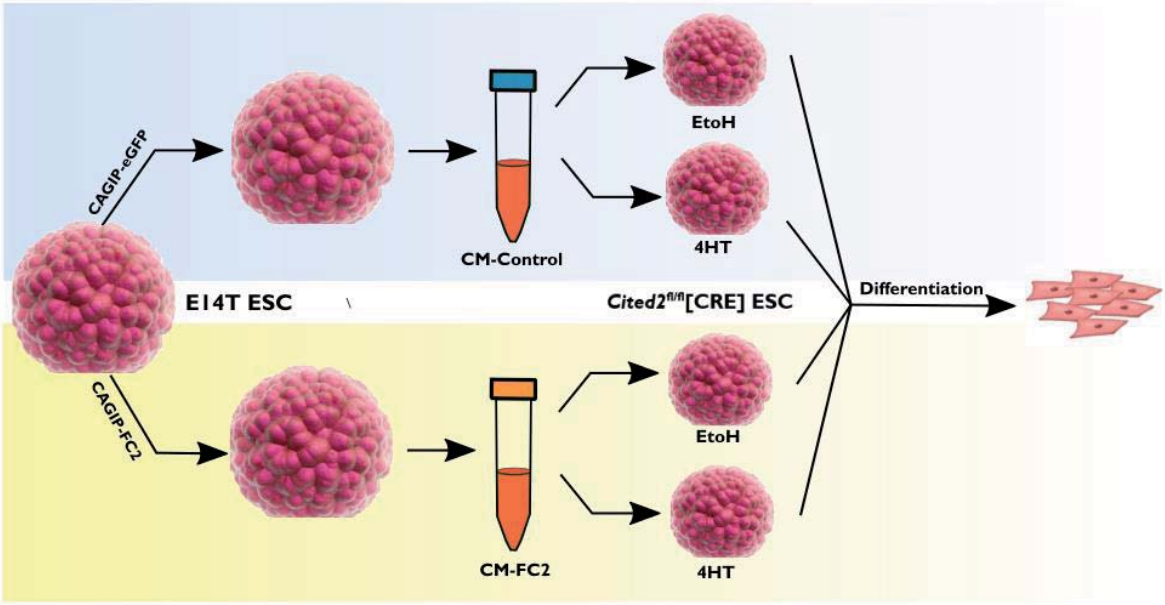

Figure 5.2. Strategy for ESC differentiation with cited2 induced secretome. E14/T ESC were transfected with a control plasmid or a plasmid expressing FC2. The medium of transfected cells was then used in *Cited2*$^{fl/fl}$[Cre] ESC treated either with EtOH or 4HT at the onset of differentiation and the average number of beating colonies was determined at D8 of differentiation.

5.3 Cited2 induced secretome rescues cardiac defects caused by its depletion

Cited2 depletion impairs cardiac cell fate decision of ESC with the number of beating foci being reduced in *Cited2*$^{fl/fl}$[Cre] ESC treated with 4HT at D0 compared to cells treated with EtOH. Supplementing *Cited2* depleted ESC with CM-FC2 significantly increased their ability to generate contractile foci whereas the number of foci in *Cited2* depleted ESC, supplemented with CM-Control, remained low. Interestingly, treating EtOH-treated ESC with either CM-FC2 or CM-Control did not affect their ability to differentiate into cardiomyocytes (Figure 5.3). This indicates that the proteins present in the CM-FC2 compensate or bypass the lack of *Cited2*.

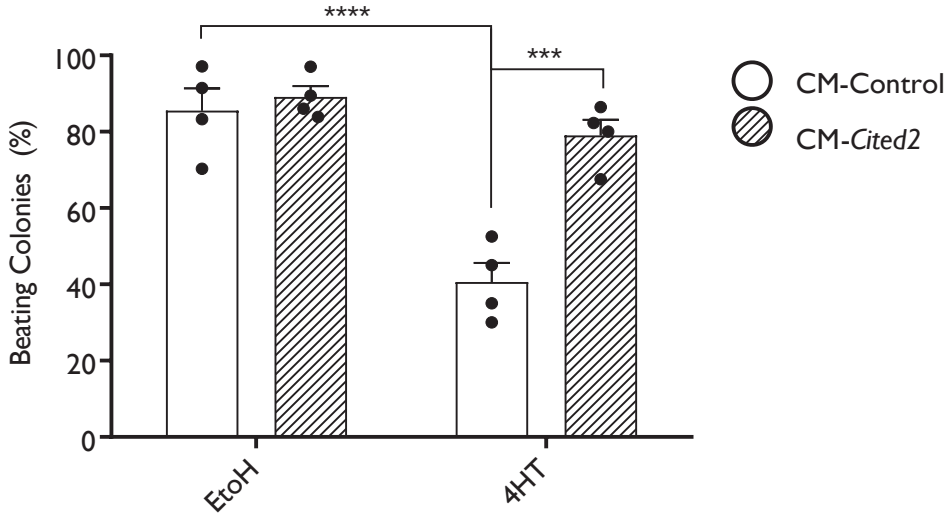

Figure 5.3 *Cited2* Conditioned Medium rescues cardiac defects caused by *Cited2* depletion defects. *Cited2*$^{fl/fl}$[Cre] ESC treated either with EtOH or 4HT and CM-Control or CM-FC2, at the onset of differentiation, and the average number of beating colonies was determined at D8 of differentiation. The percentage of beating colonies was determined by the number of colonies that express a beating foci divided by the total number of colonies. Each dot represents an independent experiment and mean ±SEM of four independent experiments. (*** $p<0.01$; **** $p<0.001$).

5.4 The Conditioned Medium of ESC overexpressing *Cited2* supports ESC transition through mesoderm

To unravel the mechanism by which CM supports cardiac differentiation of *Cited2* depleted ESC, we assessed the transcriptional activity of mesoderm transcription factors *Brachyury* and *Mesp1,* and cardiac mesoderm transcription factors *Nkx2.5* and *Isl1* in *Cited2*$^{fl/fl}$[Cre] ESC treated with 4HT and either CM-Control or CM-FC2 at D5 of differentiation. To exclude possible cell contamination, we also investigated the expression of *Cited2* (Figure 5.4).

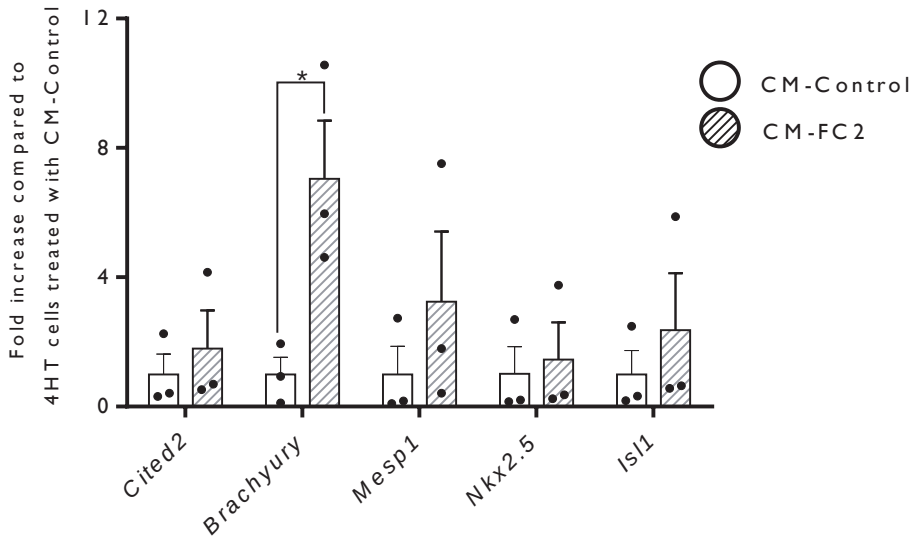

Figure 5.4 The Conditioned medium of ESC overexpressing *Cited2* supports ESC transition through mesoderm. The expression of *Cited2, Brachyury, Mesp1, Nkx2.5,* and *Isl1,* were determined at D5 of differentiation in *Cited2*$^{fl/fl}$[Cre] ESC treated with CM-Control or CM-FC2 for the first two days of differentiation. Each dot represents the expression per sample and mean ±SEM of three independent experiments. (* $p<0.05$).

Cited2 depleted cells treated with CM-FC2 stimulated *Brachyury* expression at D5 of differentiation without affecting significantly the expression of *Mesp1*, *Nkx2.5,* and *Isl1*. In addition, the expression of *Cited2* was not affected by CM-FC2.

The increased expression of *Brachyury* implies that CM-FC2 treatment may restore the differentiation process as early as the mesoderm specification. *Cited2* expression levels remain similar when we compare *Cited2* depleted cells treated with CM-Control or CM-FC2. This indicates that the rescue of cardiac defects was not caused by the reactivation of *Cited2* expression in the presence of E14/T-FC2 ESC. Overall, this indicates that the rescue of Cited2 depletion defects is being caused in a Cited2 independent manner.

5.5 Identification of Cardiopoietic factors present in the Conditioned Medium

Since the CM-FC2 restored the number of beating colonies, caused by *Cited2* depletion, we hypothesized that these defects could result, at least in part, from the

deregulation of the activity of extracellular signalling pathways which are regulated during ESC differentiation to properly instruct cell fate decisions.

Using E14T cells, we assessed by qPCR which secreted factors expression was being affected by the upregulation of *Cited2* levels. We analysed the expression of *Bmp4* and *Cerberus (Cer1)* from the TGF-β signalling pathway; *Wnt3* and *Wnt3a* from the Canonical-Wnt pathway; *Wnt5a, Wnt11,* and *Dkk1* from the non-canonical Wnt pathway; *Nodal*; and *Fgf8* and *Fgf10* from the FGF signalling pathway.

Wnt5a, Wnt11, Dkk1, and *Fgf10* transcripts were found to be significantly upregulated, while *Wnt3a* was the only gene found to be downregulated in E14/T-FC2 cells when compared to E14/T-CAGIP cells. Meanwhile, *Bmp4, Wnt3, Cer1, Nodal* and *Fgf8* expression was not altered upon *Cited2* overexpression (Figure 5.5).

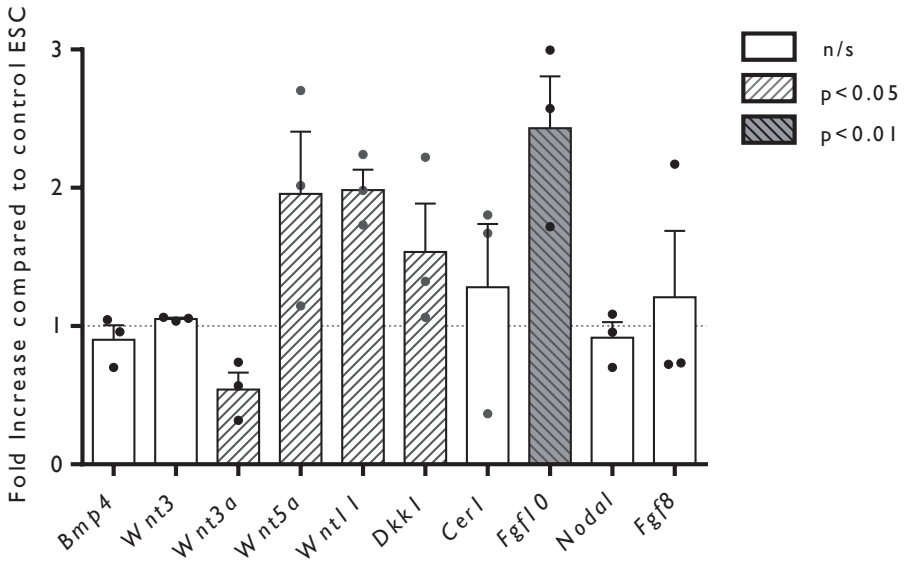

Figure 5.5 Expression level of cardiopoietic factors in *Cited2* overexpressing ESC. The expression of *Bmp4, Wnt3, Wnt3a, Wnt5a, Wnt11, Dkk1, Cer1, Fgf10, Nodal,* and *Fgf8* was determined in E14/T FC2 ESC and normalized to E14/T CAGIP ESC. Each dot represents the expression per sample and mean ±SEM of three independent experiments. The bar pattern is indicative of a significant difference.

Next, we assessed the expression of *Wnt3a, Wnt5a, Wnt11, Fgf8, Fgf10,* and *Cer1,* upon *Cited2* depletion at D4 of differentiation. qPCR analysis of *Cited2*$^{fl/fl}$[Cre] ESC, treated with 4HT at the onset of differentiation leads to a decrease in transcript levels of *Wnt3a, Wnt5a,*

Wnt11 and *Fgf10* compared to control cells. Meanwhile, the expression of *Fgf8* and *Cer1* was not found to be significantly altered (Figure 5.6).

As *Wnt5a, Wnt11* and *Fgf10* expression systematically correlated with the expression of *Cited2*, we decided to pursue further studies with these three secreted factors.

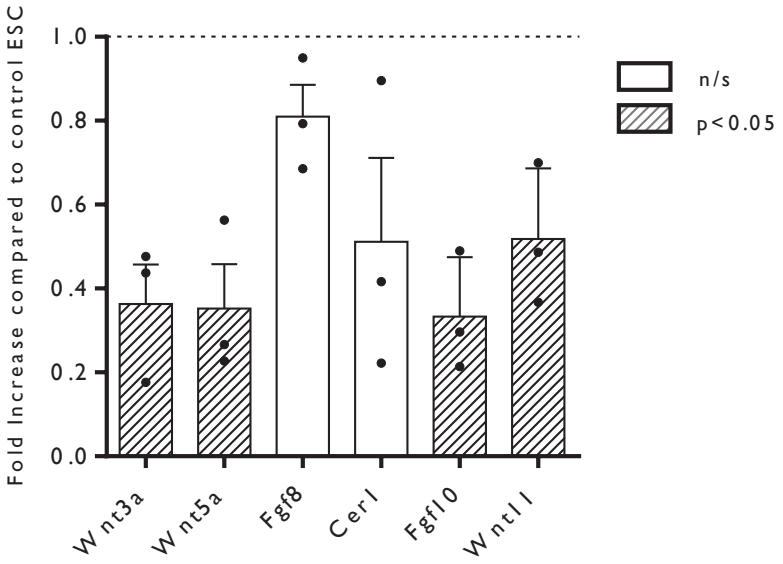

Figure 5.6 Expression level of cardiopoietic factors in *Cited2* depleted cells. The expression of *Wnt3a, Wnt5a, Fgf8, Cer1, Fgf10,* and *Wnt11,* were determined at D4 of differentiation in *Cited2*$^{fl/fl}$[Cre] ESC treated with 4HT at the onset of differentiation and normalized to control cells treated with EtOH. Each dot represents the expression per sample and mean ±SEM of three independent experiments. The bar pattern is indicative of a significant difference.

5.6 The Conditioned medium is enriched with Wnt5a and Wnt11

Since, *Wnt5a, Wnt11,* and *Fgf10* transcripts were upregulated in E14T-FC2 ESC we hypothesized that CM-FC2 is enriched with WNT5a, WNT11, and FGF10 proteins. To test our hypothesis, we performed IP against WNT5a, WNT11, and FGF10, followed by Western Blot (WB) of both CM-Control and CM-FC2.

WB analysis revealed that WNT5a and WNT11 proteins were dramatically increased in the CM-FC2 when compared to CM-Control. Meanwhile, the protein levels of FGF10 were only marginal increased in CM-FC2 (Figure 5.7). This indicates, that FC2 overexpression in ESC stimulated mostly the expression and secretion of particularly WNT5a and WNT11 to the medium.

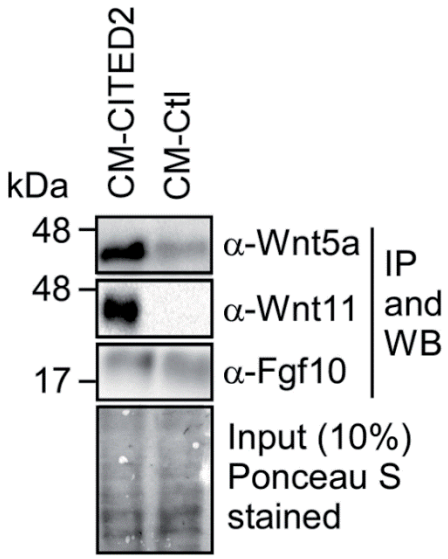

Figure 5.7 The Conditioned Medium is enriched with WNT5a and WNT11. WNT5a, WNT11, and FGF10 protein levels were determined by WB of the Immunoprecipitated CM-Control and CM-FC2. Loading in each lane was monitored by staining Input with Ponceau.

5.7 Removal of WNT5a or WNT11 from the Conditioned Medium impairs its ability to rescue cardiac defects caused by *Cited2* depletion

Since the CM-FC2 was rich in both WNT5a and WNT11, we hypothesized that the ability of the CM to rescue cardiac defects was due to the increase of either WNT5a and/or WNT11. To test this hypothesis, we removed WNT5a and WNT11 from the CM and tested if, the CM, could still rescue cardiac defects caused by *Cited2* depletion. For that, we used two distinct approaches where we depleted WNT5a or WNT11 from the CM.

On the first approach, we immunoprecipitated the CM against WNT5a, WNT11, and FGF10 and used the immuno-depleted CM for differentiation (Figure 5.8). On the second approach, both CM-Control and CM-FC2 were treated with the specific antibody against WNT5a or WNT11 (Figure 5.9).

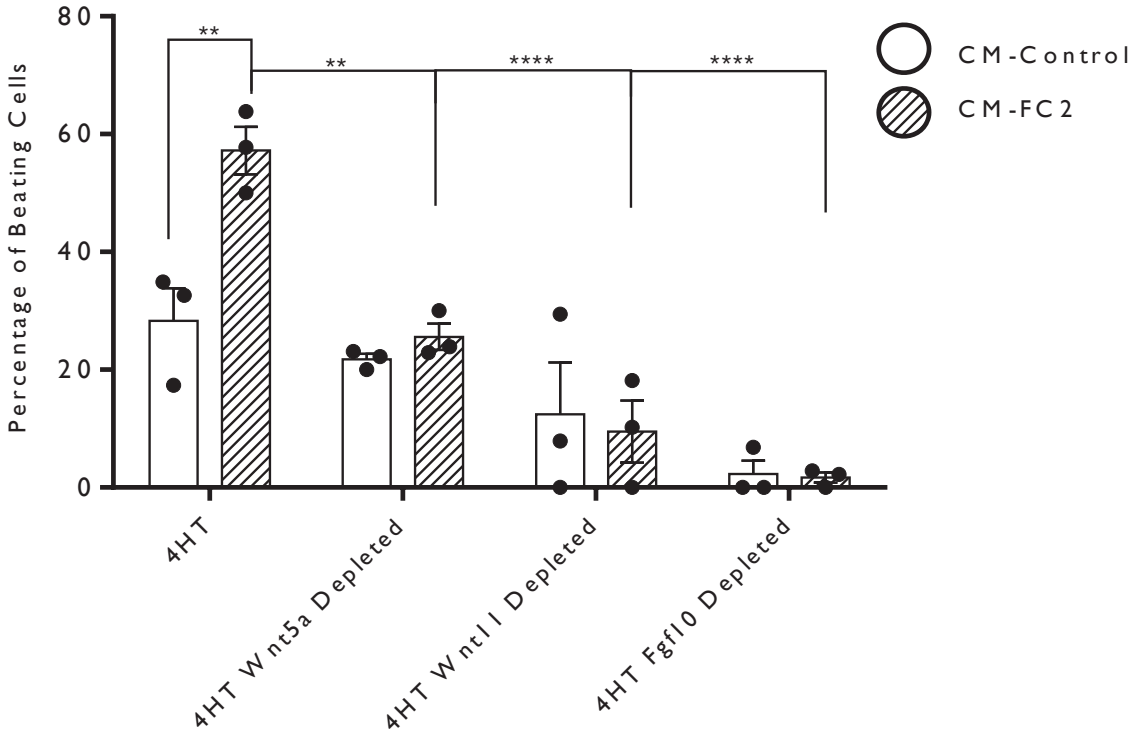

Figure 5.8 *Cited2* immunodepleted medium fails to restore cardiac differentiation. WNT5a and WNT11 immunodepleted CM-Control and CM-FC2 were added to *Cited2*$^{fl/fl}$[Cre] ESC treated with 4HT during the first two days of differentiation. The percentage of beating colonies was determined by the number of colonies that express a beating foci divided by the total number of colonies. Each dot represents an independent experiment and mean ±SEM of three independent experiments. (*** p<0.005; **** p<0.001).

In both experiments, the CM-FC2 WNT5a and WNT11 immuno-depleted failed to restore the emergence of beating colonies while immunodepleted CM-Control ability to generate cardiomyocytes maintained unaltered.

This result indicates that the presence of WNT5a or WNT11 in the CM-FC2 is required to overcome the lack of *Cited2*. As for CM-Control, removal of WNT5a or WNT11 did not affect much the ability to generate beating foci, most likely due to the limited amount of protein in the CM, as was previously demonstrated in the IP of the CM-Control.

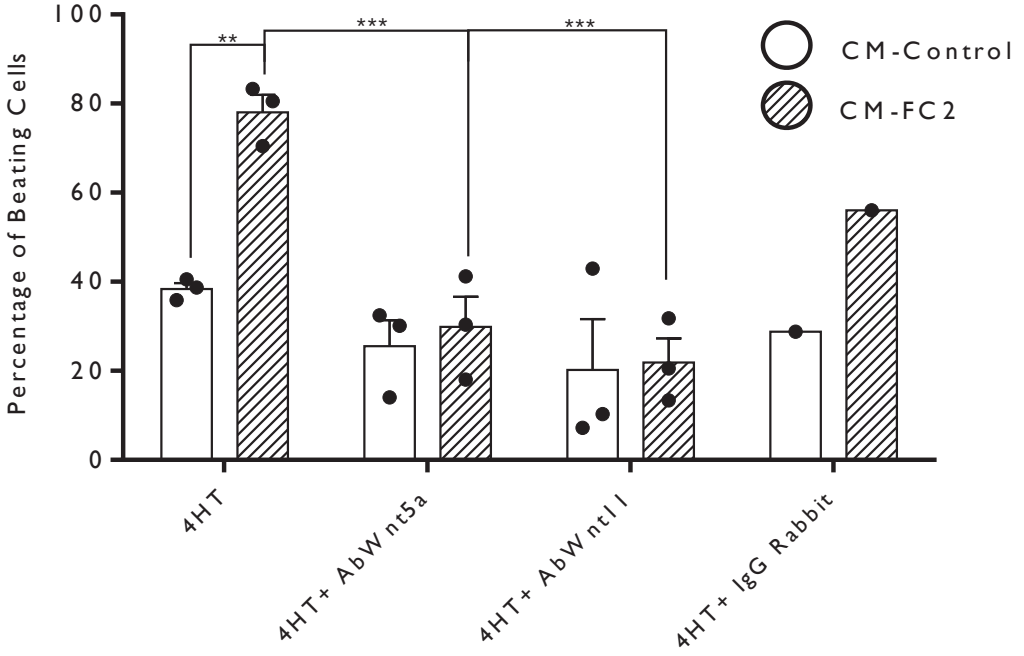

Figure 5.9 *Cited2* conditioned medium fails to restore cardiac differentiation after incubation with specific antibodies. The CM-Control or CM-FC2 was incubated with 5µg/mL of AbWNT5a or 2.5µg/mL of AbWNT11 and added to *Cited2*$^{fl/fl}$[Cre] ESC treated with 4HT during the first two days of differentiation. The percentage of beating colonies was determined by the number of colonies that express a beating foci divided by the total number of colonies. Each dot represents an independent experiment and mean ±SEM of three independent experiments. (** $p<0.01$; *** $p<0.005$).

Contrary to WNT5a and WNT11, removal of FGF10 from the CM totally disrupts cardiac differentiation. This indicates that the proteins immunodepleted by anti-FGF10, are required at the onset of differentiation and are present in both CM-Control and CM-FC2. We decided to pursue further studies only with WNT5a and WNT11 as their depletion impairs CM-FC2 ability to increase the number of beating cells without significantly altering CM-Control ability to generate cardiomyocytes upon their immunodepleting.

To further demonstrate that these defects were being caused by the loss of protein, we incubated both CM-Control and CM-FC2 with an antibody that does not target any mouse protein. As both CM ability to rescue cardiac defects remained, we can suggest that the removal of WNT5a of WNT11 largely impairs CM-FC2 ability to rescue cardiac defects caused by *Cited2* depletion (Figure 5.8).

5.8 Conclusion

Results from gene expression profile suggested that *Cited2* depleted cells impaired ability to differentiate into beating cardiomyocytes might be due to the misregulation of extracellular signalling proteins. Using a CM approach, we observed that the secretome of ESC overexpressing *Cited2* rescued the number of beating colonies caused by *Cited2* depletion. We observed that the CM is critical to the expression of mesoderm key transcription factor *Brachyury* in a *Cited2* independent manner. Trough *Cited2* gain and loss of function, we saw that the transcript expression of *Wnt5a, Wnt11* and *Fgf10* varied according to the levels of *Cited2*. Through IP followed by WB against WNT5a, WNT11 and FGF10 proteins we saw that CM-FC2 is particularly enriched with WNT5a and WNT11. Once we immunodepleted WNT5a or WNT11 from the CM, it loses its ability to rescue cardiac defects caused by *Cited2* depletion.

CHAPTER 6

WNT5a and WNT11 rescues Cited2 cardiac defects *in vitro*

6.1 Introduction

Wnt5a and *Wnt11* were first identified and characterized in *Xenopus* laevis in 1993 (279). WNT5a expression was found to be enriched in both the anterior and posterior regions of embryos at the late stages of development, with lower levels of expression in the mesoderm (280). WNT11 was found to be expressed in the lateral and ventral marginal zone, in the somites and first brachial arch (281).

Both Wnt5a and Wnt11 belong to the Non-canonical Wnt signalling pathway. The first indication that Non-Canonical Wnts were important to cardiac cell fate commitment occurred in 1997, when Eisenberg and colleagues, found that WNT11 was expressed in post gastrulated mesoderm cells of chick embryos (282). Later, they found that chick embryos exposed to WNT11 increased the ability to generate cardiac tissue (283). In 2002, Pandur and colleagues showed that Wnt11 was required for cardiac specification in *Xenopus*. Through a loss of function experiments, using a dominant negative *Xenopus Wnt11* construct that inhibits Wnt11, they found that its inhibition in the cardiac region strongly inhibited the expression of the early cardiac marker NKX2.*5* and the mature cardiomyocyte marker TROPONIN I (284).

The first data connecting Wnt5a to cardiac development was reported in 1999. Transcripts of *Wnt5a* were observed during gastrulation at E6.5 and E7.5 in mice across the three germ layers, with the highest levels expressed in the mesoderm (285). Similar results were also observed in whole-mount *in situ* hybridization of chick embryos at stage 8/9 where *Wnt5a* was found highly expressed in both PS and lateral mesoderm (286).

Microarray analysis of different derived hPSC lines differentiated into cardiomyocytes suggests that both *WNT5a* and *WNT11* expression increases during cardiac mesoderm and that their expression levels maintain high throughout the rest of differentiation until cardiomyocyte maturation (287).

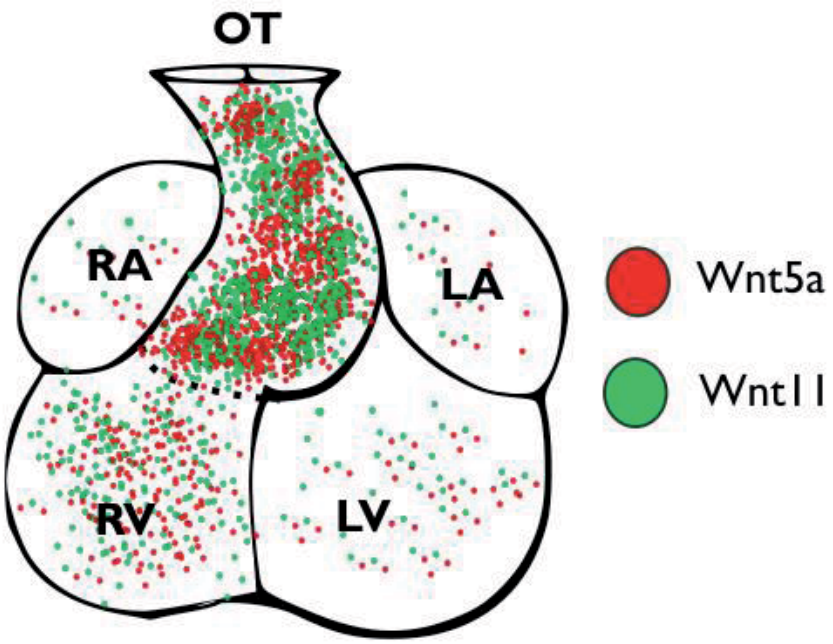

Figure 6.1 Wnt5a and Wnt11 is expressed throughout the heart. Both Wnt5a and Wnt11 are highly expressed in the OT region of the heart. To a lesser extent, their expression can be identified in the RV. Residual expression of the Wnt5a and Wnt11 can be identified in the RA, LA and LV. Information gathered from the following papers (285, 288-290),

In 1999, Yamaguchi and colleagues, described for the first-time a loss-of-function mutation of WNT5a, which was lethal and affected many structures which development requires the extension from the primary body axis (285). It was only in 2007, that *Wnt5a* null mice embryos hearts were first described to have multiple cardiac defects with a 100% penetrance of OT abnormalities (291).

A conditional *Isl1*-Cre induced Rosa26^{Wnt5a} mice, which permits the expression of WNT5a in the SHF progenitors, revealed that the endogenous WNT5a expression is present at a higher level in the caudal SpM and at a lower level in the rostral SpM and OT. Overexpression of WNT5a resulted in its expression across the entire SpM and OT, where the previous expression was low or not detected. However, this ectopic expression of WNT5a in the SHF progenitors disturbs their deployment and causes heart-looping and OT shortening (292, 293).

To explore the role of Wnt11 in mammalian development, Sinha and colleagues developed a *Wnt11*-CreERT transgenic mouse line. Initially, they found that cells transiently

expressing WNT11 at early gastrulation were fated to become progenitors of the endoderm. Then, they observed that sequential activation of WNT11 between E7.0 and E9.0 resulted in a highly dynamic contribution of cells to the ventricular myocardium. Administration of WNT11 at E7.5, contributed extensively to the myocardium in the LV and inter-ventricular septum, suggesting a contribution of WNT11 to the CPC of the FHF. Subsequently, WNT11 activation at E8.0 contributed to both LV and RV formation. On the other hand, its forced expression at E8.5 contributed mostly to RV and OT. Lastly, WNT11 forced expression at E9.5 greatly diminished the contribution to the RV formation. The presence of RV becomes non-existent from E10.5 onwards. This suggests that initial expression of WNT11 contributes to cells of the FHF while, at later stages, the contribution starts shifting to cells of the SHF (294).

Analysis of *Wnt11* null mice revealed abnormal OT development from E9.5 onward. These defects lead to the appearance of CHD such as DORV, TGA and VSD that become apparent from E11.5 onward (295, 296).

Compared to mice lacking either *Wnt5a* or Wnt11, double null-mutants embryos defects are exacerbated suggesting the redundancy of these two signalling molecules. While *Wnt5a* or *Wnt11* null mice embryos hearts undergo normal rightward looping, double null mutants fail to undergo normal rightward looping remaining a linear tube at E9.5 (297). Cohen and colleagues showed an overlapping between WNT5a and WNT11 expression in the OT and RV, and that both proteins are co-required to induce CPC differentiation and proper heart formation. They showed that double null mutants, particularly, affected the SHF progenitors with a severe reduction in the number of *Isl1* positive cells without affecting the number of *Nkx2.5*, *Hand1* and *Hand2* positive cells (288).

6.2 Cited2 control the expression of *Wnt5a* and *Wnt11*.

To further investigate the role of Cited2 in the regulation of Wnt5a and Wnt11, we analysed *Wnt5a* and *Wnt11* kinetic expression by qPCR during the differentiation of *Cited2*$^{fl/fl}$[Cre] ESC treated with EtOH or 4HT.

Wnt5a transcripts were low from the onset of differentiation until D4. From D4 onward, *Wnt5a* expression levels rapidly increase in EtOH treated cells, while in 4HT treated cells *Wnt5a* levels remain low (Figure 6.2).

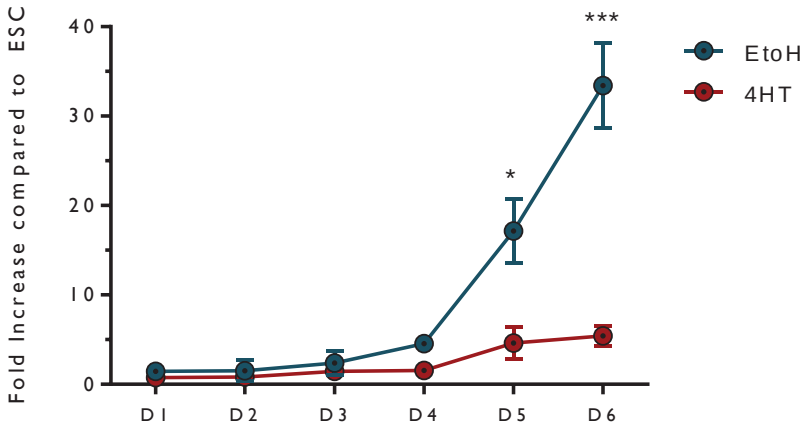

Figure 6.2 *Wnt5a* expression in mESC differentiation. The expression of *Wnt5a* was determined by qPCR of *Cited2*$^{fl/fl}$[Cre] ESC treated either with EtOH or 4HT at the onset of differentiation. Samples were taken every 24h during the initial 6 days of differentiation. *Cited2* expression was normalized to the expression of undifferentiated *Cited2*$^{fl/fl}$[Cre] ESC. Each dot represents the expression per sample and mean ±SEM of three independent experiments. (* $p<0.05$; *** $p<0.005$).

Like Wnt5a, *Wnt11* transcripts are low from the onset of differentiation until D5. At D6, *Wnt11* expression drastically increases in control cells, whereas in *Cited2* depleted cells, this increase is subtler (Figure 6.3).

To investigate the role of Cited2, in the promoter activity of *Wnt11*, we co-transfected E14T cells with vectors expressing FC2 together with a luciferase reporter construct harbouring 1064bp of mouse *Wnt11* promoter proximal region in pGL3-basic (Wnt11-luc) (246). Wnt11-luc was kindly given by Hiroyuki Mori (University of Michigan, USA).

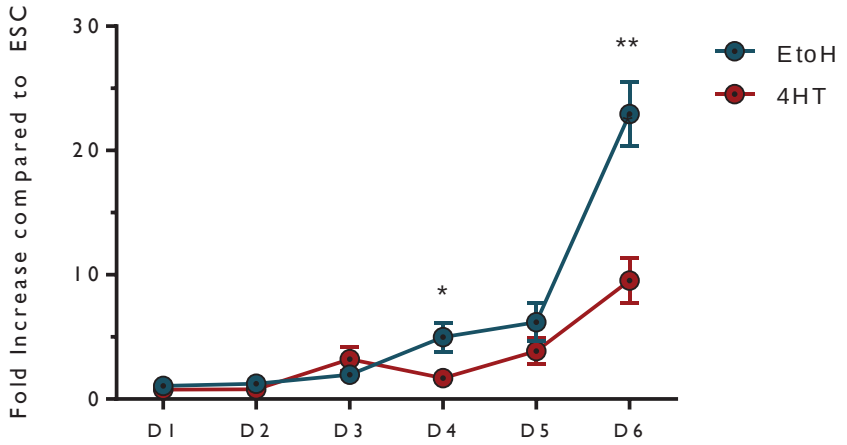

Figure 6.3 *Wnt11* expression in mESC differentiation. The expression of *Wnt11* was determined by qPCR of *Cited2*$^{fl/fl}$[Cre] ESC treated either with EtOH or 4HT at the onset of differentiation. Samples were taken every 24h during the initial 6 days of differentiation. *Cited2* expression was normalized to the expression of undifferentiated *Cited2*$^{fl/fl}$[Cre] ESC. Each dot represents the expression per sample and mean ±SEM of three independent experiments. (* $p<0.05$; ** $p<0.01$).

The co-transfection of CAGIP-FC2 vector increased the reporter gene activity when compared to cells transfected with a control vector (Figure 6.4). These results provide evidence that *Cited2* might be a direct transcriptional activator of *Wnt11*.

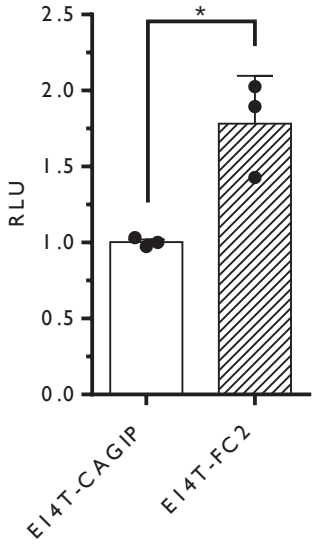

Figure 6.4 *Cited2* increases the promoter activity of *Wnt11*. E14T cells were transiently co-transfected with Wnt11-luc reporter, together with either CAGIP or FC2. The luciferase activity was normalized for the lacZ activity conferred by the CMVlacZ vector. Relative luminescence units (RLU) are presented relative to values of Wnt11-luc transfected with the control vector set at 1. Each dot represents the expression per sample and mean ±SEM of three independent experiments. (* $p<0.05$).

6.3 Wnt5a and Wnt11 can rescue cardiac defects caused by *Cited2* depletion

Next, we sought to understand if Wnt5a and Wnt11 are enough to rescue *Cited2* depletion-caused cardiac defects. For that purpose, we supplemented the differentiation medium at the onset of differentiation with 100ng/mL of WNT5a, 100ng/mL of Wnt11 or 50ng/mL of WNT5a and WNT11. Adding WNT5a or WNT11 to 4HT treated cells significantly increased the number of beating colonies at D8 of differentiation (Figure 6.5). Even though supplementation of WNT5a or WNT11 to 4HT treated cells, was not able to completely rescue the cardiac differentiation defects, when both WNT5a and WNT11 were added together, at the beginning of differentiation, we observed an increase in the number of beating colonies to levels compared to EtOH treated cells (Figure 6.5).

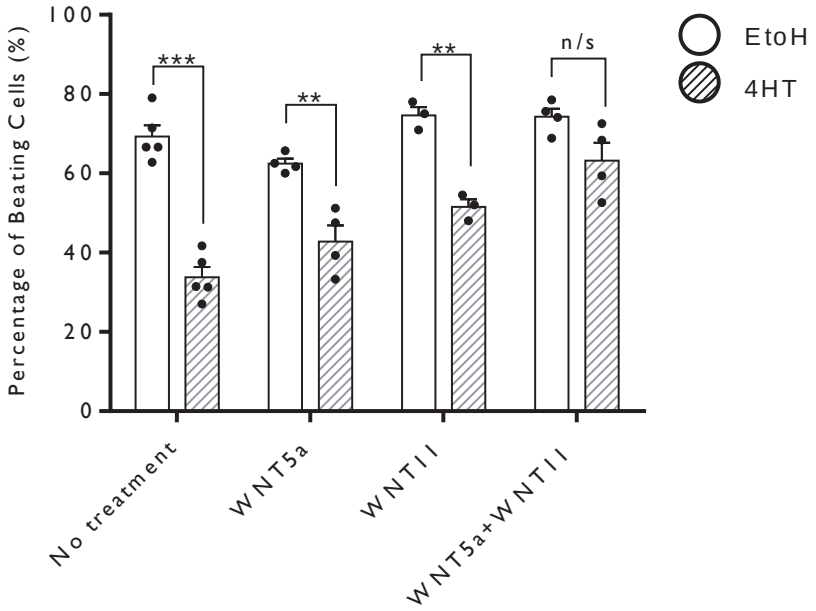

Figure 6.5. WNT5a and WNT11 rescue cardiac defects caused by *Cited2* depletion. *Cited2*$^{fl/fl}$[Cre] ESC were treated either with EtOH or 4HT with WNT5a and/or WNT11 at the onset of differentiation and the average number of beating colonies was determined at D8 of differentiation. The percentage of beating cells was determined by the number of colonies that express a beating colony divided by the total number of colonies. Each dot represents an independent experiment and mean ±SEM of three or more independent experiments. (** $p<0.01$; *** $p<0.005$).

Next, we investigated whether WNT5a and/or WNT11 supplementation could increase the expression of mesoderm and cardiac mesoderm transcription factors. For that, we assessed by qPCR, at D4 of differentiation, the expression of *Cited2* and the expression of genes associated with mesoderm (*Brachyury* and *Mesp1*) and CPC (*Nkx2.5, Isl1* and *Tbx5*) (Figure 6.6).

At D4 of differentiation, EtOH treated cells express significantly more *Cited2* than *Cited2* depleted cells. This indicates that WNT supplementation does not affect *Cited2* transcripts levels.

When we analysed the expression of mesodermal markers, cells treated with only 4HT express significantly less *Brachyury* and *Mesp1* than control cells. The addition of WNT5a significantly increases the expression of *Brachyury* and *Mesp1*. Compared to control cells, cells treated with 4HT and WNT5a restore the expression of *Brachyury* and further increases the expression of *Mesp1*. Treatment with WNT11 also restores the expression of *Brachyury* but fails to restore the expression of *Mesp1*. Whereas *Cited2* depleted cells treated with both WNT5a and WNT11 completely restore the expression of *Mesp1* and further enhances the expression of *Brachyury* when compared to control cells.

Analyses of the expression of CPC markers showed that *Cited2* depleted cells express less *Isl1* and *Tbx5*. The addition of WNT5a restores the expression of *Isl1* but fails in increasing the expression of *Tbx5*. On the other hand, WNT11 is unable to restore either the expression of *Isl1* and *Tbx5*, whereas the addition of both WNT5a and WNT11 restores the expression of *Tbx5* and *Isl1*. The expression of *Nkx2.5* was not found to be altered.

Overall, the addition of WNT5a or WNT11 to the differentiation medium significantly increased the expression of most mesoderm and CPC markers in a *Cited2* independent manner. Even though, only the addition WNT5a and WNT11 resulted in mesodermal and cardiac transcripts levels similar to control cells.

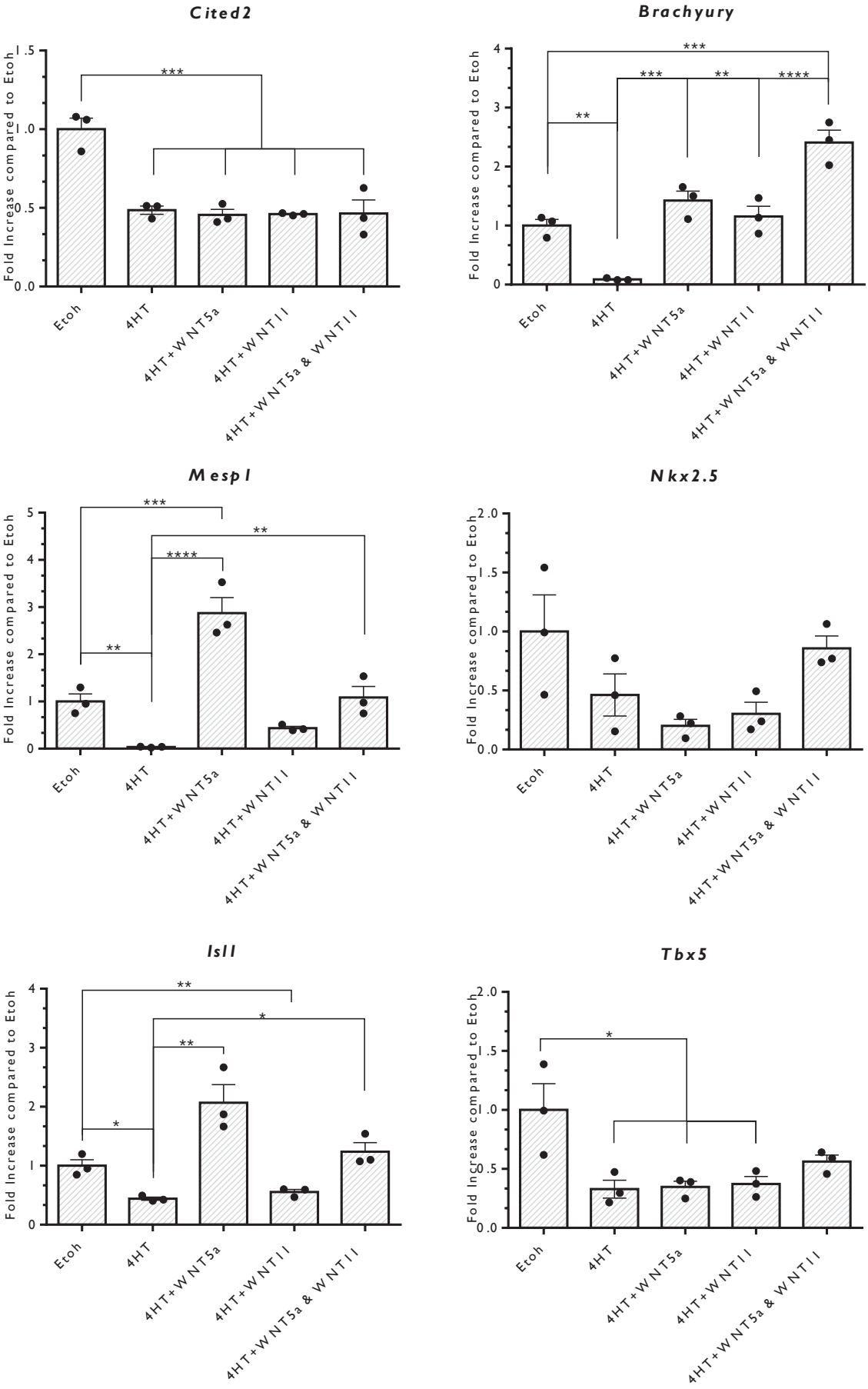
Cited2
Brachyury
Mesp1
Nkx2.5
Isl1
Tbx5
Fold Increase compared to Etoh
Etoh
4HT
4HT+WNT5a
4HT+WNT11
4HT+WNT5a & WNT11

Figure 6.6 WNT5a and WNT11 supports ESC transition through mesoderm. The expression of *Cited2, Brachyury, Mesp1, Nkx2.5, Isl1* and *Tbx5* were determined at D4 of differentiation, by qPCR, in *Cited2*$^{fl/fl}$[Cre] ESC treated with EtOH or 4HT at the onset of differentiation. 4HT treated cells were either not supplemented or supplemented with 100ng/µL of WNT5a, 100ng/µL of WNT11 or 50ng/µL WNT5a and 50ng/µL of WNT11 at the onset of differentiation. Each dot represents the expression per sample and mean ±SEM of three independent experiments. (* p<0.05; ** p<0.01; *** p<0.005; **** p<0.001).

6.4 Wnt5a and Wnt11 can partially rescue *Cited2* null ESC

Lastly, we supplemented WNT5a and WNT11 to *Cited2*$^{\Delta/\Delta}$ ESC, which completely lack CITED2 expression and do not differentiate well into cardiomyocytes (Figure 6.7) (264). Addition of WNT5a or WNT11, individually, to *Cited2*$^{\Delta/\Delta}$ ESC, at the onset of differentiation, does not enhance the appearance of beating foci. However, supplementation of both WNT5a and WNT11 at the onset of differentiation significantly increases the percentage of beating colonies. This indicates that there is a synergistic effect of WNT5a and WNT11 in correcting cardiac defects caused by *Cited2* depletion.

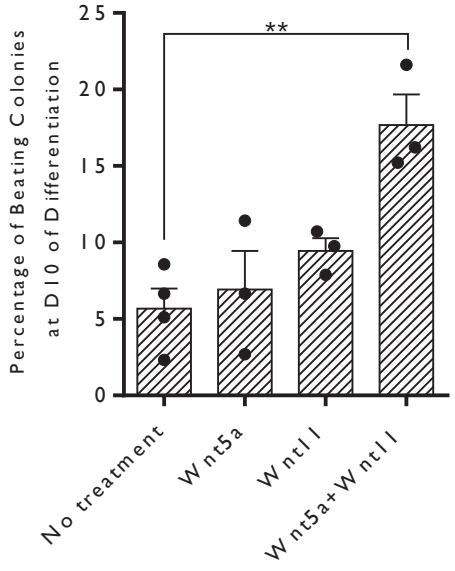

Figure 6.7 WNT5a and WNT11 can partially rescue *Cited2* null ESC cardiovascular defects. *Cited*$^{\Delta/\Delta}$ ESC were either non-treated or treated at the onset of differentiation with either 100ng/µL of WNT5a, 100ng/µL WNT11 or 50ng/µL of WNT5a plus 50ng/µL of WNT11 and the percentage of beating colonies accessed at 10 of Differentiation. Each dot represents the percentage of beating colonies per sample and mean ±SEM of three independent experiments. (** p<0.01).

6.5 Conclusion

Previous result from the CM, showed that CITED2 expression was important to the release of WNT5a and WNT11 outside the cell. We started by showing, that *Cited2* depletion directly impairs the expression of *Wnt5a* and *Wnt11* throughout differentiation. Moreover, we provide evidence that the increased expression of *Cited2* promotes the activity of *Wnt11* proximal promoter region. While the molecular mechanisms behind *Cited2* and *Wnt5a* or *Wnt11* are still unknown, our results point to *Cited2* being a transcriptional activator of both genes.

Since the presence of WNT5a and WNT11 in the CM was required to rescue cardiac defects caused by Cited2 depletion, we hypothesized that these two proteins, alone, rescued cardiac defects caused by *Cited2* depletion. We showed that WNT5a and WNT11 synergize together to correct *Cited2* depletion defects *in vitro,* not only in terms of cell differentiation and the emergence of beating foci but also restores the correct expression of mesoderm and cardiac mesoderm transcription factors.

CHAPTER 7

In vivo rescue of Cited2 depletion defects

7.1 Introduction

The zebrafish, *Danio renio*, is a tropical freshwater fish native to North Indian Rivers. It is approximately 3.5 to 4.5 cm in length and immediately identified by its distinctive striped scales pattern. Zebrafish as a model system presents many advantages. They are vertebrates that have at least one orthologue for approximately 70% of human genes (298). Moreover, zebrafish embryonic development is external, fast and the transparency of the eggs and early embryos provide optically accessible means to visualise development. Furthermore, the zebrafish is practically and economically advantageous, given that large numbers of animals can be kept in a relatively small space at a low cost.

Like in mammals, the zebrafish heart is the first organ to fully develop and function during vertebrate embryogenesis, a process that occurs in 2 days in zebrafish, 12 days in mice and 35 days in humans (299). Most cardiac developmental processes and cardiac structural features are conserved between all vertebrate species and thus, zebrafish have been used to model cardiac development in humans (Figure 7.1) (146). Moreover, the optical clarity allows easy access and detailed imaging of the developing heart. Interestingly, zebrafish embryos can survive for up to 5 dpf with severe cardiac phenotypes because they are able to obtain oxygen by passive diffusion (300). This feature enables large-scale forward and reverse genetic screening and phenotypic characterisation of genes influencing cardiac development, to an advanced stage, that would otherwise be embryonic lethal in mammals.

Several approaches to modify the genome have been successfully applied to the zebrafish. The use of MO remains one of the preferred methods to carry out a loss of function approaches in the zebrafish. The MO technology induces gene silencing via antisense complementarity oligonucleotides to disrupt target protein synthesis. MO contain a methylene morpholine ring in place of a ribose or deoxyribose sugar in the macromolecule backbone. The MO can be designed to bind near the AUG translation start site or splicing to elicit target gene Knockdown (KD) (301).

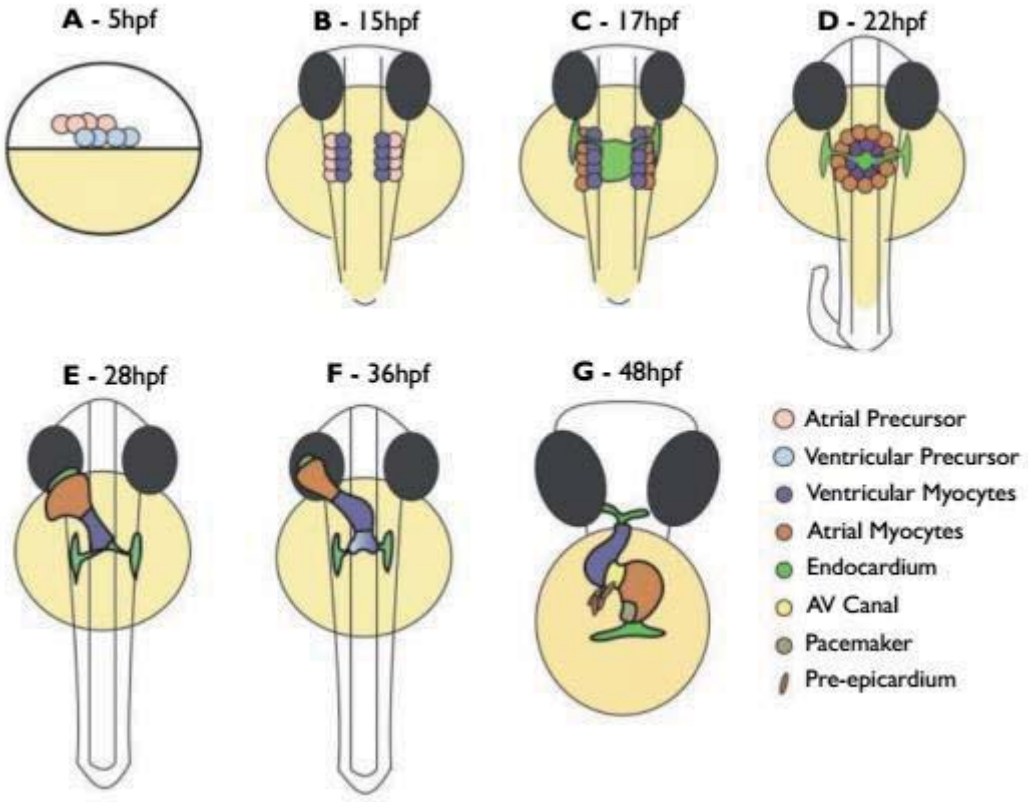

Figure 7.1 Schematic representation of heart development in zebrafish. A) CPC are identified 5hpf, located in the lateral marginal zone. B) At 15hpf cardiac primordia are bilaterally aligned at the lateral plate mesoderm. C) & D) Endocardial progenitors are established at the midline before migrating towards the midline and fusing to form the primitive heart with ventricular cells at the apex and atrial cells at the base. E) The heart starts elongating and the primitive heart tube begins to contract. F) The heart tube undergoes looping and the distinct atria and ventricle compartments become evident. G) Cardiac maturation occurs, AV valve is formed and the proepicardium adheres to the heart surface. Image adapted from. (146).

The ortholog of *Cited2* in zebrafish is in chromosome 20. Information regarding *Cited2* in zebrafish is scarce. Thisse *et al.* in 2004 reported, through *in situ* hybridization, that Cited2 was expressed across all development stages similar to what had been reported in mice. At 5hpf, pre-gastrulation, *Cited2* expression can already be detected, but specific tissues cannot yet be identified. At 15hpf, its expression is mostly found in the somites and the eyes. At 17hpf, its expression can also be detected in the branchial arches, and at 30hpf *Cited2* expression can also be detected in the hindbrain. Expression in the eyes, branchial arches and the hindbrain can be detected until hatching (302). Other than that, there is no evidence of further studies relating zebrafish and *Cited2*.

7.2 Experimental strategy

To perform *Cited2* depletion in zebrafish, two MO were designed to target *Cited2* transcripts. A custom MO oligo with 3'-Carboxyfluorescein end modification, designed to block the translation initiation complex of CITED2, hereafter termed AUG MO and, a custom MO oligo with 3'-Lissamine end modification, designed to block sites involved in splicing *Cited2* pre-mRNA, hereafter termed SPL MO. To control all the procedure, we used a standard control MO with no described biological activity, hereafter known as Control MO.

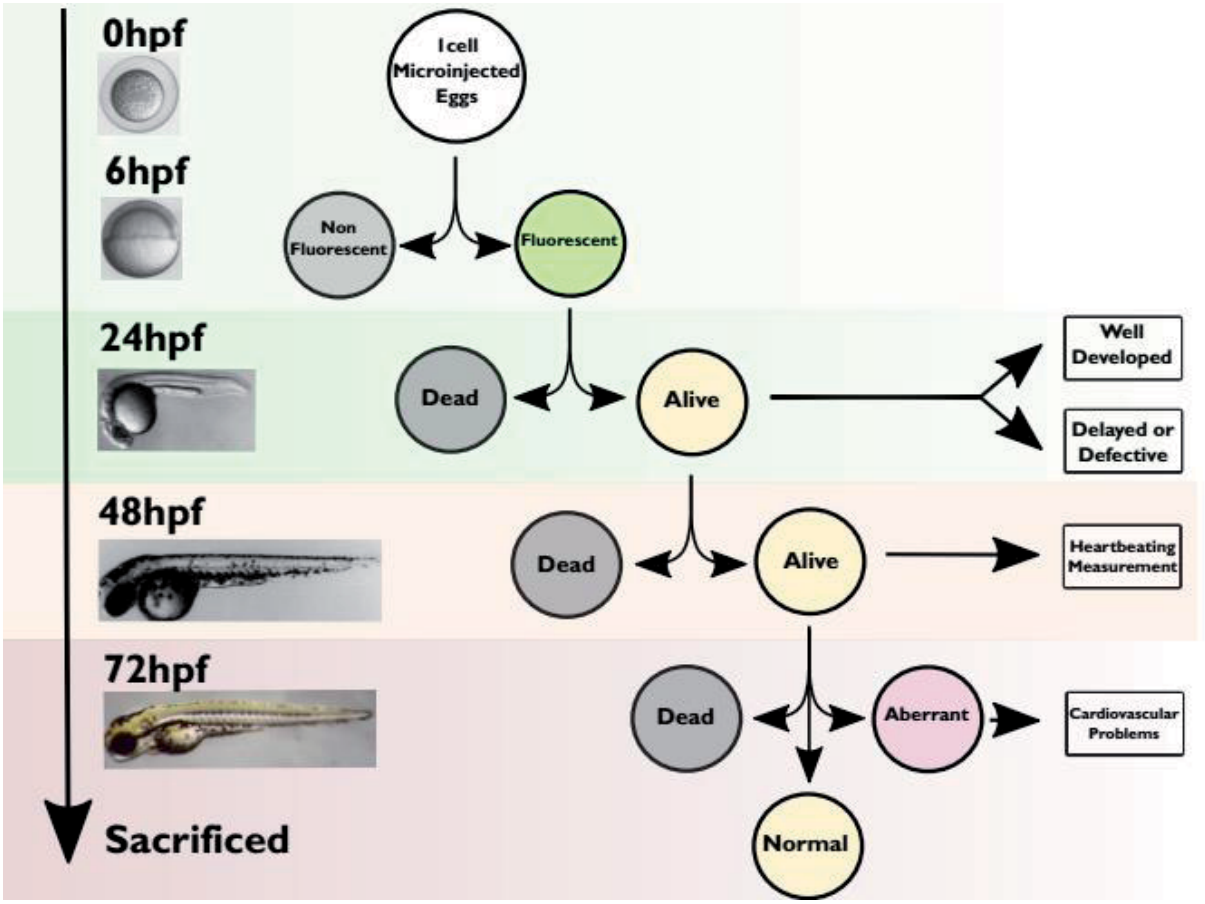

Figure 7.2 Schematic representation of the experimental setting. 1cell stage embryos were injected and at 6hpf fluorescent embryos were selected. At 24hpf dead embryos were removed and the remaining evaluated if they were well developed. At 48hpf dead embryos were removed and heart beating was measured. At 72hpf larvae were separated in dead, normal or aberrant. Aberrant larvae were assessed for possible cardiac problems. Larvae were sacrificed at 72hpf. Embryos and larvae photos were obtained from (303).

An experimental strategy for all the steps regarding zebrafish experiments is described in Figure 7.2. In summary, approximately, 5ng of MO was injected at 1-cell stage embryo and fluorescence was accessed at 6hpf. Only the fluorescent embryos were kept for further observations, and the non-fluorescent were disposed of. Embryonic lethality was accessed every 24h, until the end of the experiment, and dead embryos were disposed of. At 24hpf, embryo morphology was observed and developmental delay was accessed. At 48pf, the zebrafish average heart rate was also determined with a resource to 10sec videos of the heart. At 72hpf the remaining zebrafish were separated and classified as presenting a normal or aberrant morphology. Aberrant zebrafishes were individually analysed to identify potential cardiovascular defects. All zebrafish larvae were sacrificed at 72hpf.

7.3 *Cited2* depletion increases embryo lethality and delays proper development

The first individual parameter we assessed was the efficiency of our microinjections. As both Cited2 MO have fluorescent tags we easily detected the embryos that successfully integrated the MO. The fluorescence was detected as soon as 6hpf and distributed ubiquitously throughout the embryo, suggesting a proper delivery at 1-cell stage (Figure 7.3). On average, 60% of the injected embryos were fluorescent. Non-fluorescent embryos were disposed of (Figure 7.4).

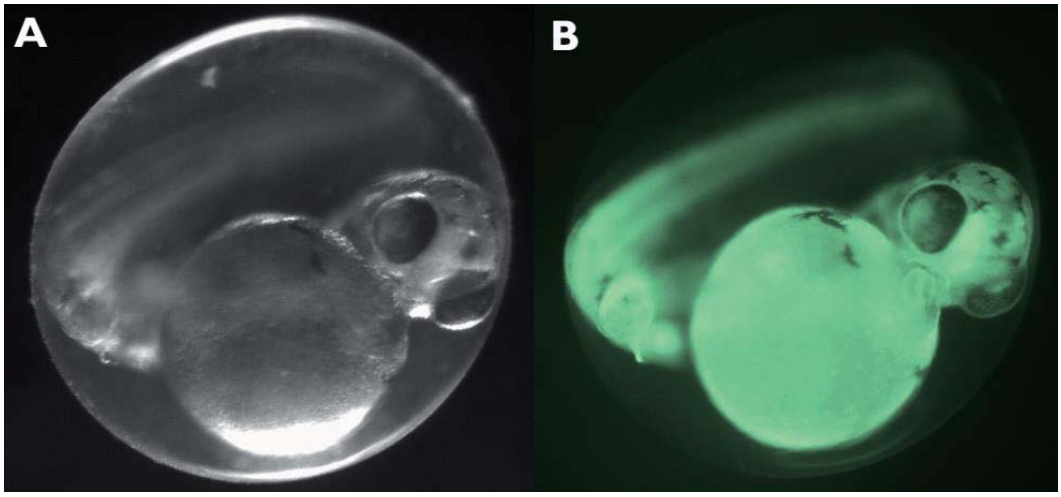

Figure 7.3 Live imaging of fluorescent embryos. Representative fluorescent image of 1 cell-stage egg embryo injected with custom MO with 3'-Carboxyfluorescein 48hpf. Images were obtained at 100x magnification.

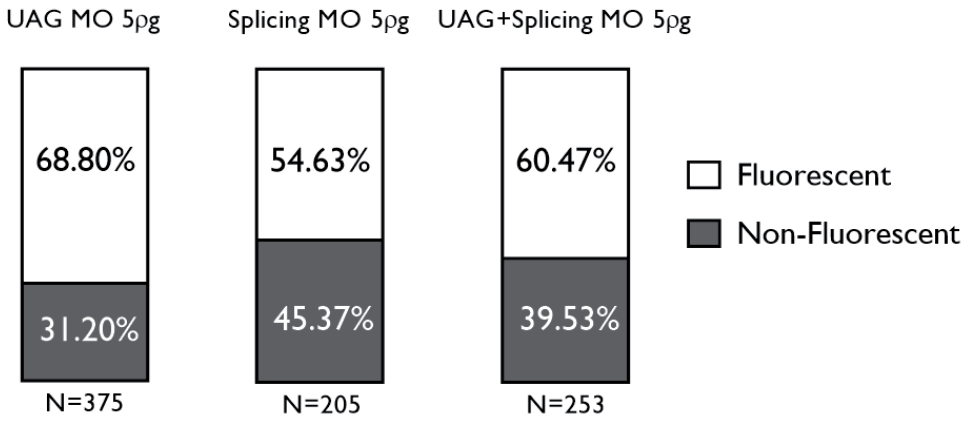

Figure 7.4 Percentage of fluorescent embryos at 6h post-fertilization. 1cell-stage egg embryos were injected either with UAG MO 5ng, SPL MO 5ng or UAG+SPL MO 5ng and the fluorescent embryos determined at 6hpf. The total number of counted embryos is indicated at the bottom across three independent days of injections.

To further investigate the effect of *Cited2* depletion on zebrafish development, we analysed zebrafish embryo death at 24hpf (Figure 7.5). Dead embryos were easily identified by the blue staining caused by the penetration of blue methylene contained in the medium. We observed that non-injected and Control MO-injected embryo death rate was very similar, indicating that the process of microinjection was not directly affecting embryo viability. Next, we compared non-injected to Cited2 MO-injected embryos. AUG or SPL MO microinjected embryos died more frequently, but the co-injection of both Cited2 MO was the most lethal (Figure 7.5). The increased lethality in embryo injected with both AUG and SPL MO is likely due to a more efficient KD of *Cited2* as both MO have different target sites.

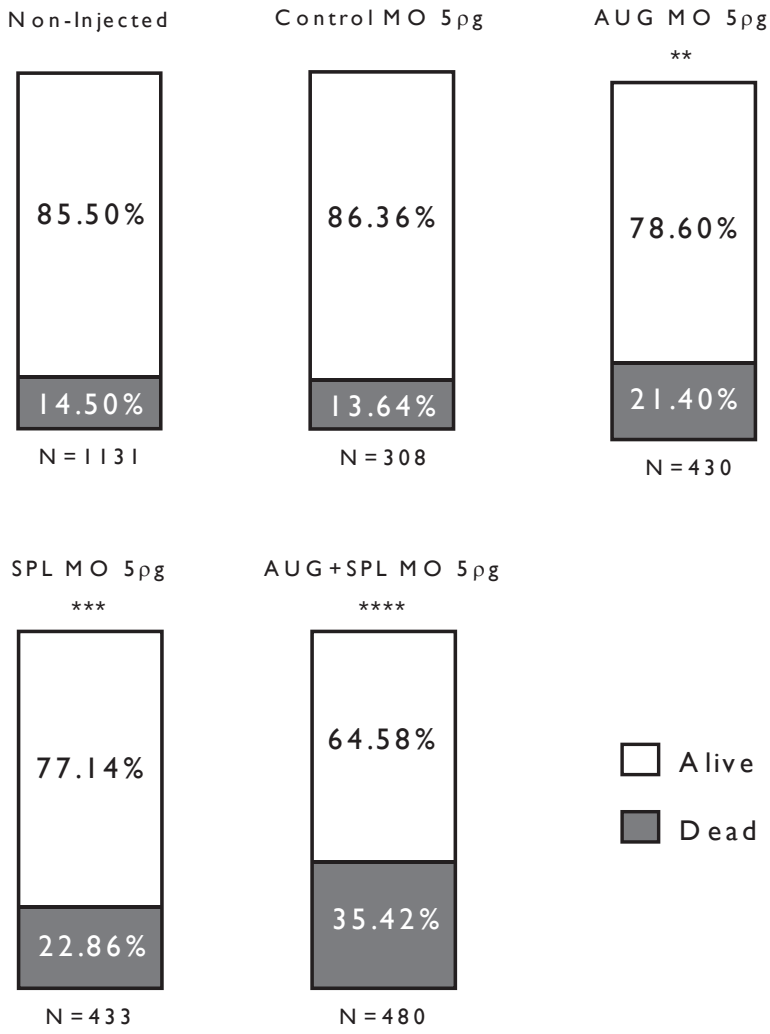

Figure 7.5 Percentage of death at 24h post-fertilization. Percentage of alive or dead embryos non-injected or injected with indicated MO 24hpf. The total number of counted embryos is indicated at the bottom with three or more independent days of injections. (** p<0,01; *** p<0.005; **** p<0.001).

At 24hpf we checked embryo development. Surprisingly, we detected two distinct phenotypes at 24hpf. We identified normal looking embryos with their tail clearly separated from the yolk and an evident head structure (Figure 7.6A&B), and embryos roundly shaped with their body completely attached to the yolk (Figure 7.6C&D). While the first group resembles a normal zebrafish embryo at 24hpf, the second group resembles a 12hpf embryo rather than a 24hpf embryo. Therefore, we decided to classify embryos that match Figure 7.6A&B as well developed, whereas embryos that resemble Figure 7.6C&D we classified them as delayed or aberrant.

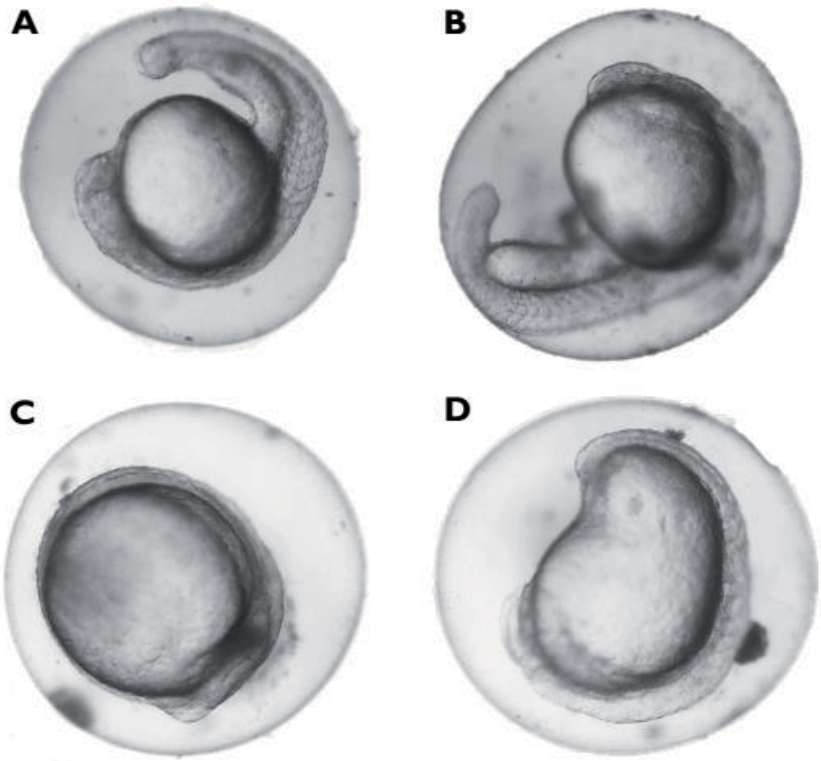

Figure 7.6 Morphology of the zebrafish eggs at 24hours post-fertilization. Photos represent the two distinct phenotypes observed a 24hpf A) and B) Well developed embryos. C) and D) Delayed or aberrant embryos. Embryos were examined at 50X magnification.

Next, we quantified embryos according to their morphology (Figure 7.6). Almost all embryos non-injected or injected with Control MO were well developed. On the other hand, the number of delayed or aberrant embryos drastically increased in Cited2 MO-injected embryos (Figure 7.7). This supports the idea of the importance of Cited2 during early embryo development alike what happens in mice in which, only *Cited2* KO in the epiblast consistently resulted in embryonic lethality and heart defects (242).

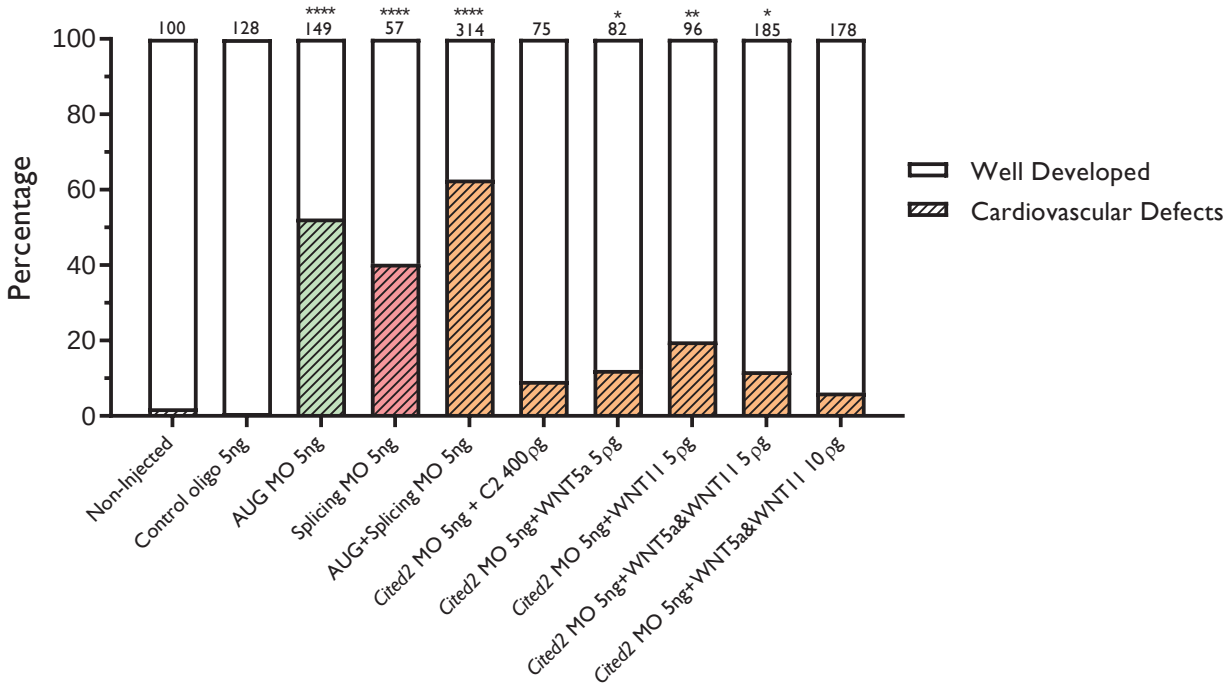

Figure 7.7 Development state of zebrafish egg at 24h post-fertilization. Percentage of well-developed or delayed/abnormal embryos non-injected or injected with respective MO at 24hpf. Some *Cited2* MO-injected embryos were also co-injected with 8R-CITED2 or WNT5a and/or WNT11. Green bars injected with AUG MO, red bars injected Splicing MO, orange bars injected with both *Cited2* MO. The total number of assessed embryos is indicated in the top of the graphs. (* $p<0.05$; ** $p<0.01$; **** $p<0.005$).

7.4 *Cited2* depletion impairs proper heart development

At 48hpf the heart is fully formed while the zebrafish larvae are still in the egg. As most of the larvae have yet to hatch, looking into the heart becomes much easier as they are mostly static. We took this opportunity to record videos of the larvae heart to determine if *Cited2* depletion could have an effect in the heart-beating of the zebrafish. Control larvae had an average heartbeat of approximately 180 beatings per minute (bpm), while *Cited2*-depleted larvae bpm were lower. On average the heartbeat of AUG and/or SPL MO-injected larvae ranged between 120-130 bpm (Figure 7.8).

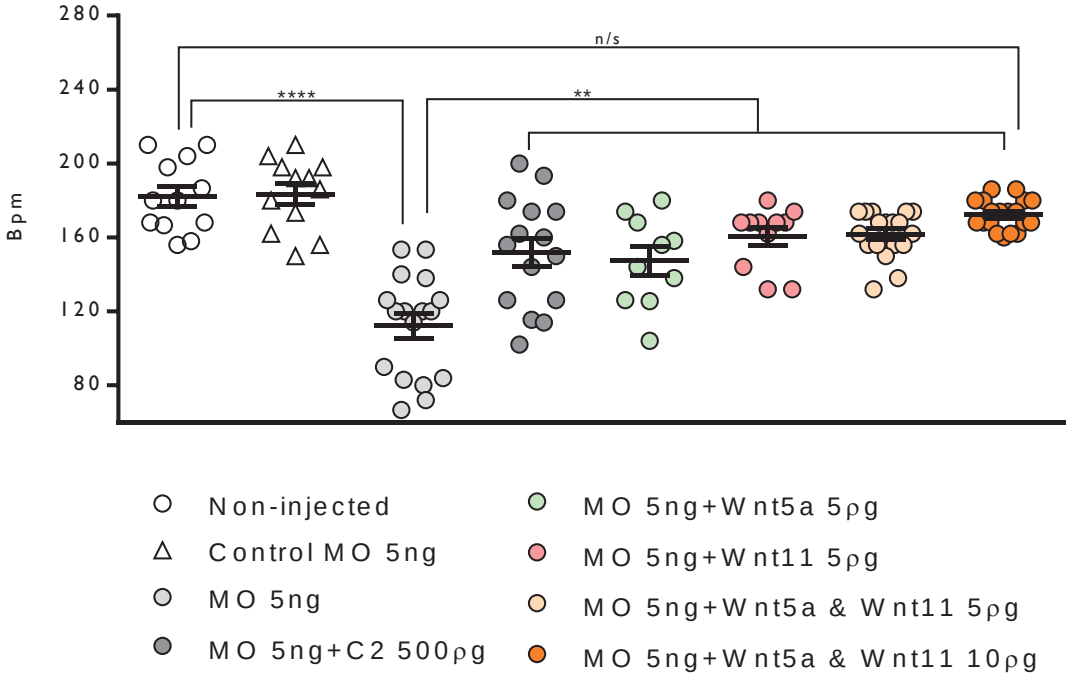

Figure 7.8 Zebrafish average heartbeat at 48h post-fertilization. 10-second videos of zebrafish heart were recorded and average beating per minute (bpm) was determined. All recordings were performed at RT. Each symbol represents the bpm of a randomly selected zebrafish. (** p<0.01; **** p<0.001).

A slower rhythm than normal, also known as bradycardia, in Cited2 MO embryos, suggested a decline in overall cardiac performance in which myocardial contractile function might be compromised. As a decreased bpm is likely to be associated with heart problems and CHD, we looked at larvae, post-hatching, for potential cardiovascular defects. At 72hpf, we separated embryos according to normal, aberrant and dead. Aberrant larvae refer to those that while alive, had clear developmental defects. Typical defects observed included: larvae that had yet to hatch, presenting low mobility, the presence of edema and abnormal back curvature (Figure 7.9).

Interestingly, in all zebrafish larvae that had clear developmental defects, cardiovascular defects were also observed. The most common and obvious defects observed were: the presence of edema, slow beating heart, heart hypotrophy and heart hypertrophy (Figure 7.10).

We also observed other cardiovascular defects such as a linear heart or a failure in the ventricle-atria separation.

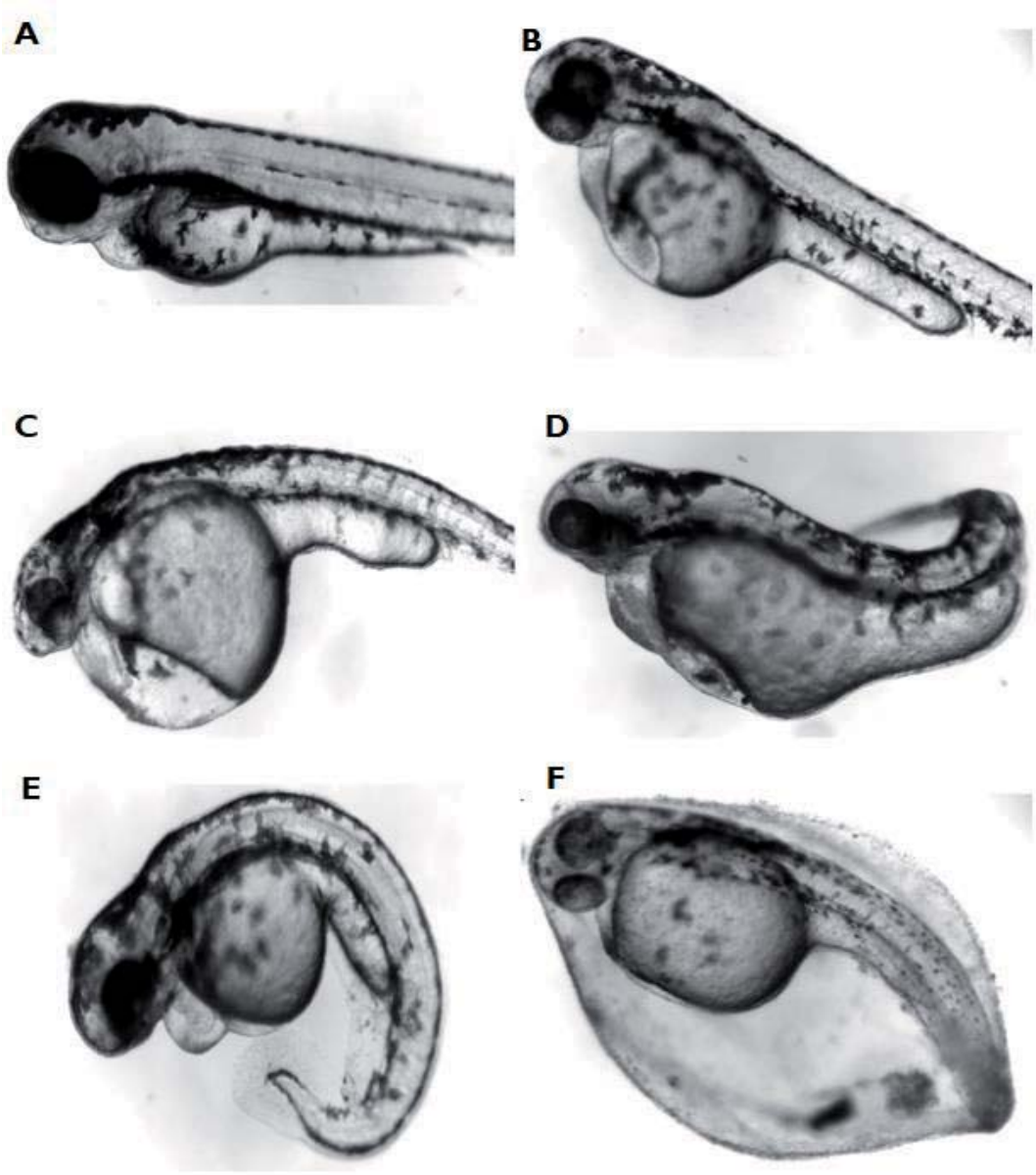

Figure 7.9 Development defects identified in Zebrafish at 72h post-fertilization. The developmental defects identified in zebrafish embryos 72hpf. A) Normal larvae, B) & C) Edema, D) & E) Abnormal Curvature, F) Not hatched.

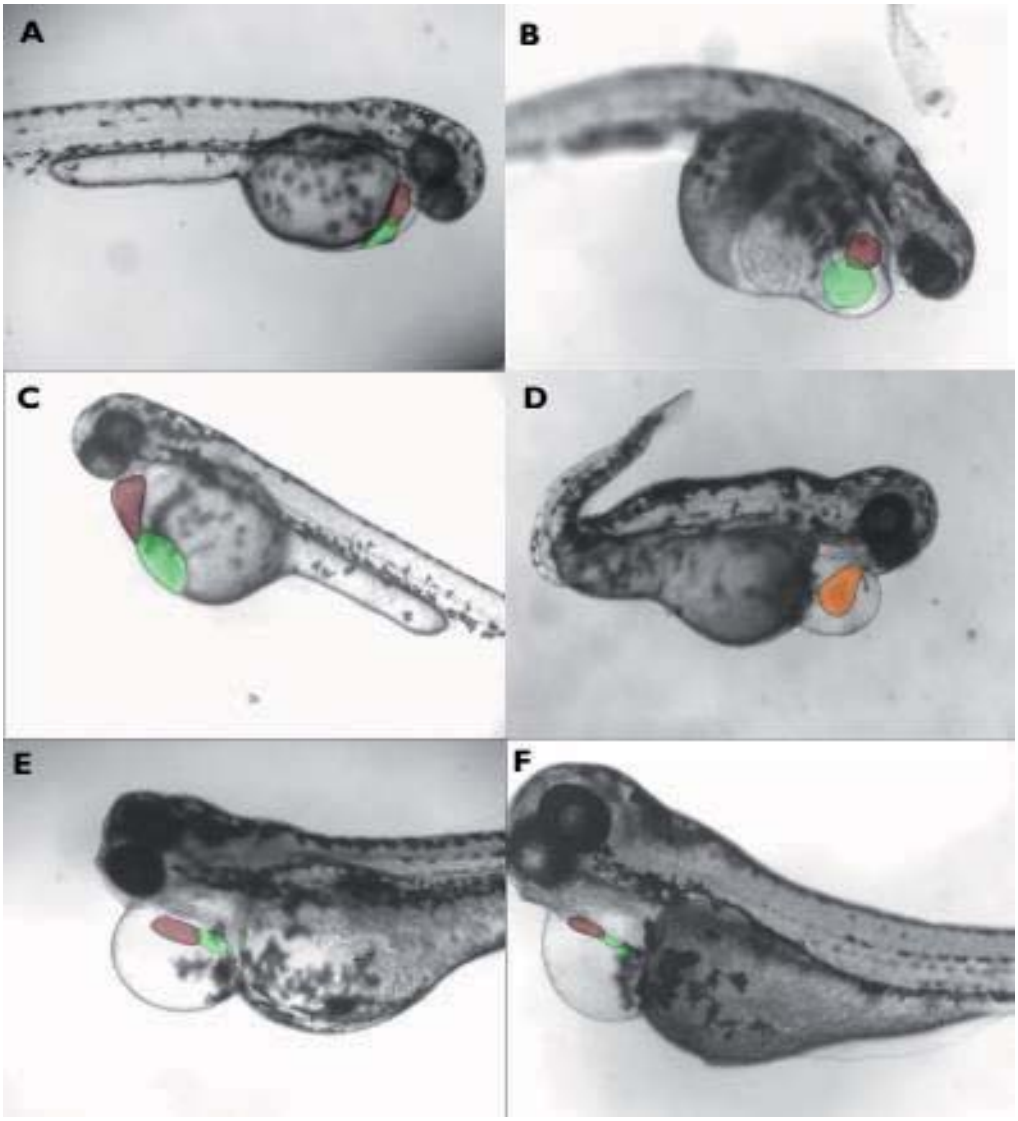

Figure 7.10 Cardiovascular defects observed in zebrafish embryos at 72h post-fertilization. Cardiovascular defects identified in zebrafish larvae at 72hpf. A) Normal larvae; B) & C) Cardiac hypertrophy; D) Edema and one single chamber; E) & F) Linear Heart, Hypotrophy and Edema. Auriculum (red area), Ventricle (green area), a single compartment (orange area).

At 72hpf we separated embryos according to normal, presenting cardiac defects and dead (Figure 7.11). Most of the control larvae showed a normal appearance, and only a few died throughout development and a very small fraction of them had cardiovascular defects. On the other hand, most of the Cited2 MO-injected larvae died and, more cardiovascular defects were observed when compared to control larvae. The co-injection of both MO resulted in the most severe phenotype. On the other hand, while MO injection resulted in an

increased number of larvae with cardiovascular defects, we did not find a specific correlation between *Cited2* depletion and cardiovascular specific defects (Figure 7.11).

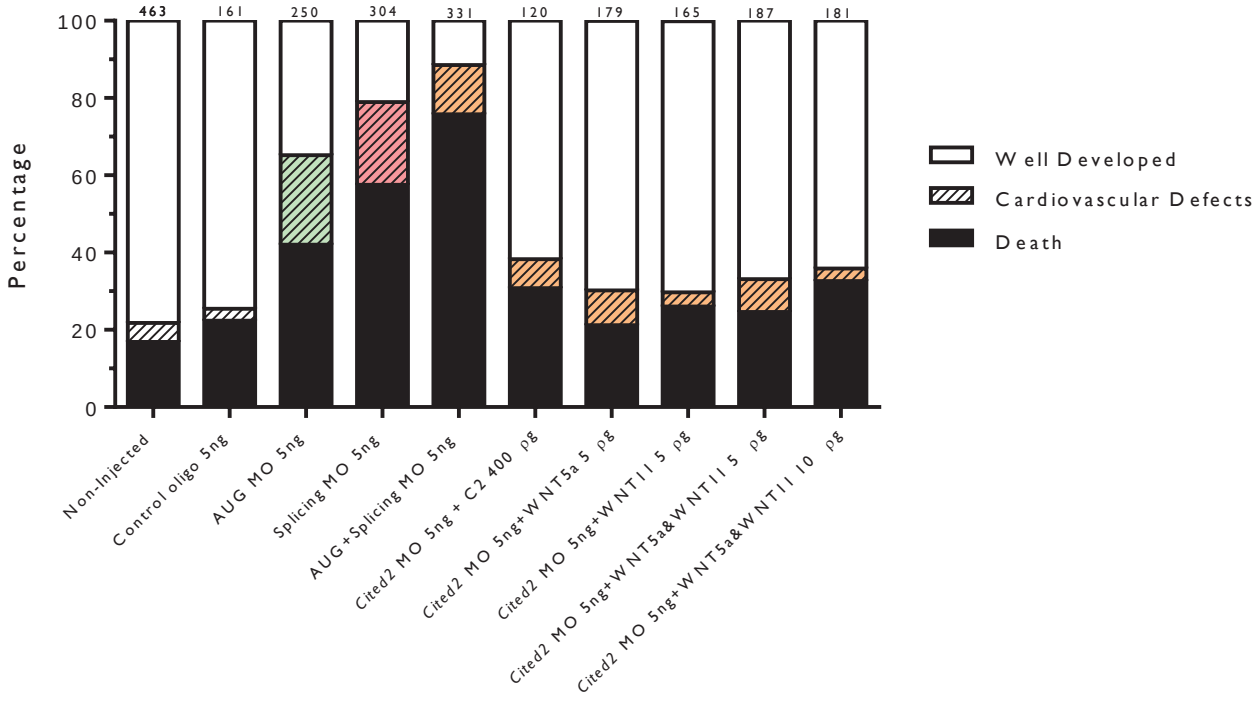

Figure 7.11 *Cited2* depletion induces zebrafish lethality and the appearance of cardiovascular defects at 72h post-fertilization. At 72hpf we separated embryos according to well developed, cardiovascular defects and dead. Green bars injected with AUG MO, red bars injected Splicing MO, orange bars injected with both *Cited2* MO. Zebrafish embryos were either non-injected or injected with *Cited2* MO. Some *Cited2* MO-injected embryos were also co-injected with 8R-CITED2 or WNT5a and/or WNT11. The total number of assessed embryos is indicated in the top of the graphs.

7.5 A *Cited2* recombinant protein can rescue *Cited2* morpholino defects

We next sought to understand if developmental problems found in Cited2 MO were being specifically caused by *Cited2* depletion. For that purpose, we co-injected the MO with 500pg of recombinant CITED2 protein (8R-CITED2) that, in vitro, can translocate towards the nucleus and rescue cardiovascular defects caused by *Cited2* depletion (264).

8R-CITED2 co-injected with Cited2 MO rescued most of the problems caused by *Cited2* depletion. At 24hpf the average number of delayed embryos decreased substantially

(Figure 7.7). Most notably were both SPL MO and AUG+SPL MO that when co-injected with 8R-CITED2 decreased the number of delayed embryos by more than 6 folds. Next, we assessed the heart rate of 8R-CITED2 treated embryos. There was a significant increase in the bpm of embryos injected with 8R-CITED2 compared to embryos only injected with Cited2 MO (Figure 7.8). Though, this increase in average bpm was not sufficient to match the average bpm of control embryos.

Lastly, we investigated if cardiovascular defects and cumulative deaths at 72hpf could be rescued by 8R-CITED2. On average, the percentage of dead larvae at 72hpf reduced on Cited2 MO when treated with 8R-CITED2. Interestingly, 8R-CITED2 treatment largely decreased the number of larvae with cardiovascular defects, to levels of defects observed in control embryos (Figure 7.11).

The overall improvements in terms of viability and cardiovascular function, strongly suggests that the defects caused by the MO were being caused by *Cited2* depletion.

7.6 WNT5a and WNT11 rescues *Cited2* depletion defects *in vivo*

As the last goal of the thesis, we hypothesized that WNT5a and/or WNT11 rescued zebrafish *Cited2* depletion defects, similar to what occurs *in vitro*. For that purpose, we co-injected AUG+SPL MO with either 5-10pg of WNT5a and/or WNT11.

At 24hpf, the number of delayed embryos due to the MO, greatly reduced in embryos treated with WNTs. The best results were obtained when AUG+SPL MO embryos were co-injected with 5pg of WNT5a and 5pg of WNT11 (Figure 7.8).

At 48hpf, *Cited2* depleted embryos treated with WNTs significantly increase zebrafish bpm compared to embryos injected only with Cited2 MO. Interestingly, co-injection of Cited2 MO with a combination of 5pg of WNT5a and 5pg of WNT11 increases the average bpm to the same levels of control embryos (Figure 7.9).

Lastly, we observed whether WNT5a or WNT11 could rescue embryo lethality and cardiovascular defects at 72hpf. Co-injection of WNT5a and/or WNT11 largely increased the number of well-developed larvae and decreased the number of dead larvae and larvae with cardiovascular defects (Figure 7.11).

Overall, this indicates that WNT5a and WNT11 can bypass most developmental defects caused by *Cited2* depletion.

7.7 Conclusion

We started by establishing a *Cited2* KD system *in vivo,* using zebrafish as a model system. We demonstrated that Cited2 is required for proper embryo development in this novel model. As previously reported for mouse KO embryos, we identified more lethality and more cardiac defects in *Cited2*-depleted zebrafish embryos. We also identified that *Cited2* depletion results in a delay of the developmental processes. We were able to rescue *Cited2* depletion defects using a recombinant CITED2 protein, which indicates that developmental defects were *Cited2* depletion-specific. Like *in vitro*, WNT5a and/or WNT11 rescued *Cited2* depletion defects *in vivo*.

CHAPTER 8

Conclusion, discussion and future perspectives

The importance of Cited2 in heart development and CHD had been previously established but its role and mechanisms were largely unknown. In our laboratory, we used ESC as a model system since they can differentiate into all the cells that comprise the heart while sharing the same mechanisms. But most importantly, because *Cited2* null mice embryos die in utero which makes it difficult to fully understand the impact of Cited2 in cardiac development.

Previously, we demonstrated in mESC that CITED2 and ISL1 proteins interact and synergize together to promote cardiogenesis. However, in that study, we did not answer why Cited2 is so critical at the onset of differentiation or development (242, 264).

As the first goal of this thesis, we started by establishing the impact of *Cited2* depletion on ESC differentiation and cardiac commitment (264). *Cited2* expression was still detected in *Cited2*$^{fl/fl}$ [Cre], treated with 4HT, suggesting an incomplete *Cited2* KO. The incomplete deletion by Cre recombinase is not uncommon in cells when two copies of floxed sequences need to be targeted (244). This effect is even more notorious, in situations where 4HT addition and plasmid transfection are involved. Even though we have an incomplete *Cited2* KO, the decrease of *Cited2* expression resulted in phenotypic changes as *Cited2* haploinsufficiency is sufficient to result in CHD in mice and humans (242).

We determined that *Cited2* transcripts expression are biphasic during ESC differentiation. Since *Cited2* expression is both required for ESC pluripotency and cardiac differentiation, we hypothesize that the decline of *Cited2* expression is required for cells to switch from a pluripotent to a cardiac differentiation permissive state. This hypothesis is corroborated by the experiments that we performed, where we attempted the rescue cardiac differentiation defects in *Cited2* depleted ESC with the supplementation of 8R-CITED2 and the results obtained with A2UpC2 ESC. We have shown that 8R-CITED2 only rescued cardiac defects at D2 of differentiation whereas continuous overexpression of *Cited2* at D0 or D1 impaired cardiac differentiation. One possible explanation is the fact that high levels of *Cited2* result in an increased expression of *Nanog.* The increase of *Nanog* expression is likely to result in pluripotency maintenance or induction of endoderm differentiation by inhibiting mesoderm and ectoderm. As such, it is possible that *Cited2* levels are required to go down, to ensure that the levels of *Nanog* also decrease, to ensure that ESC differentiate into mesoderm cell lineages. We opted for adding doxycycline every 48h because the half-life of doxycycline is approximately 18h-24h (304). Furthermore, since *Cited2* protein has a half-life of 1h (305),

adding doxycycline every 48h ensures that the levels of *Cited2* remained high throughout the differentiation process.

On the other hand, it would be interesting to understand the cell fate decision of A2UpC2 ESC treated with Doxycycline at D0. It is very unlikely, that these cells remained pluripotent, as, by D8 onwards, they phenotypically resembled differentiated cells rather than ESC (data not shown). Since *Cited2* null mESC have been reported to have defective ability to differentiate into hematopoietic or neuronal lineages (224, 225), we hypothesize that CITED2 overexpression prior to differentiation may favour one of these two cell fate decisions rather than cardiac lineage.

We observe, that *Cited2* depletion impairs cardiac differentiation and the emergence of beating colonies. These results were also confirmed by the lack of organization of the sarcomere of *Cited2* depleted cardiomyocytes. This phenotype is typically found in immature cardiomyocytes which indicates that ESC that lack *Cited2* do not differentiate well resulting in very immature cardiomyocytes.

To further investigate the mechanisms underlying the loss of pluripotency and differentiation of *Cited2*-depleted cells, we compared the gene expression profiles of control cells and *Cited2* depleted cells at D4 of differentiation. We opted for analysing the transcriptomic impact of *Cited2* depletion at D4 because, our previous observations, indicated that *Cited2* function is the most critical during early mesoderm commitment (264).

We observed that *Cited2* depleted cells at D4 of differentiation are transcriptionally similar to undifferentiated cells than control cells at the same day. Curiously, the biggest difference between differentiated cells that lack *Cited2*, and undifferentiated cells, is the fact that these cells start to express genes important for gastrulation and cell differentiation, such as *Brachyury*. This resembles the expression profile of mEpiSC which lead us to believe that these cells are likely stuck or delayed in the epiblast transition at D4 of differentiation.

We corroborated these findings by the analysis of different mesodermal transcripts and observed that their transcripts peak of expression is always one day earlier in control cells than *Cited2* depleted cells. Interestingly, our results suggest that the delay in the expression of mesodermal genes in *Cited2* depleted cells occurs somewhere between D3 and D4. This is the point where *Cited2* expression starts to increase and the lack of *Cited2* expression becomes evident. As such, it would be interesting to further understand the

molecular function of *Cited2* at D3 and D4 and identify and validate new transcriptional targets. The unregulated expression of mesodermal genes is likely to favour other cell fates specification.

Interestingly, ectoderm cell fate commitment does not seem to be as affected as the endoderm or mesoderm. Indeed, the epiblast marker *Fgf5* expression, which has been also strongly associated with ectoderm cell fate commitment (306), is similar between EtOH and 4HT treated cells, from D1 to D4, and even remains high in *Cited2* depleted cells from D4 onwards.

The pathway analysis revealed that *Cited2* depletion may strongly affect the cardiopoietic factors. We hypothesize that the decrease in the expression of important cardiac signalling pathways delayed cell differentiation and cardiac commitment.

We showed, that the secretome of *Cited2* overexpressing ESC rescues the emergence of beating colonies in *Cited2* depleted ESC. The increase of the expression of *Brachyury* implies that the CM of ESC overexpressing *Cited2* supports ESC transition to mesoderm. However, the exact mechanism by which Cited2 contributes to mesoderm specification is still unknown. Our observations point that Cited2 might be a transcriptional activator of *Brachyury*, or at least, positively affect its expression. Since early activation of *Brachyury,* is responsible for activating early cardiac mesoderm genes including *Mesp1 (307),* the lack of *Cited2* expression, around D3, is likely to reduce the proper expression of *Brachyury,* ultimately resulting in a reduction of cardiac cell fate commitment and an increase of other mesoderm or endoderm derivatives. Furthermore, this would also explain why the secretome of *Cited2* overexpressing cells did not increase control ESC ability to differentiate into cardiomyocytes, as these cells already correctly express *Brachyury* at the proper time window.

We identified WNT5a, WNT11, and FGF10 as proteins potentially upregulated in the *Cited2* induced CM. To identify if these proteins were upregulated in the CM, we performed a WB with untreated CM-Control and CM-FC2 using specific WNT5a, WNT11, and FGF10 antibodies. However, we failed in detecting WNT5a, WNT11, and FGF10 proteins. It is likely that these secreted proteins were present in a very low quantity in the CM. Therefore, to obtain enriched WNT5a, WNT11 and FGF10 proteins from the CM, we immunoprecipitated WNT5a, WNT11 and FGF10 from the media.

However, only WNT5a and WNT11 proteins were found substantially altered in the CM and crucial for rescuing cardiovascular defects caused by *Cited2* depletion. Interestingly, immunodepletion of FGF10 from the CM drastically reduced the ability of ESC to spontaneously generate cardiomyocytes. This indicates a very promising role of FGF10 on initial stages of differentiation and worthy to study in the future. In the following work, we were only able to scratch the surface of the CM of *Cited2* overexpressing ESC. It is likely that there are other proteins with a high cardiogenic potential present in the CM-FC2. To understand which proteins are present in the CM, we are currently trying to perform proteomic analysis, through mass spectrometry analysis of the CM of *Cited2* enriched cells. This will also help us understand better the role of *Cited2* in cell signalling.

While we were not able to establish the molecular mechanism behind Cited2 and the expression of both Wnt5a and Wnt11, our results indicated that Cited2 is a likely transcriptional activator of *Wnt5a* and *Wnt11*. Interestingly, in the hematopoietic context, *Cited2* null murine fetal liver also showed a huge decrease in the expression of *Wnt5a* (249). Furthermore, since *Cited2* is co-factor that does not bind into DNA, we need to identify the transcription factor responsible for interacting with CITED2 to cooperatively activate *Wnt5a* and *Wnt11* transcription. A candidate we have in mind is *Tbx1,* which has an important role in determining the fate of SHF derivatives and previously demonstrated to transcriptionally activate *Wnt5a* and *Wnt11* (308-310).

Treating cells with either WNT5a or WNT11 increased the number of beating colonies in *Cited2* depleted cells, however, only the combination of both proteins was able to match control cells number of beating colonies. Indeed, WNT5a and WNT11 have been implicated in many different cell fate decisions, For example, WNT5a is required for normal hematopoiesis (256, 311), whereas WNT11 is required for osteogenesis differentiation (312, 313). This means that WNT5a and WNT11 must be temporally regulated to ensure proper cardiac differentiation. Interestingly, while independently, WNT5a and WNT11 might promote different cell fate decisions, different authors indicate that WNT5a and WNT11 synergistically interact to promote cardiogenesis (288, 314, 315). Our results point in the same direction, with the addition of WNT5a and WNT11 being the key to rescue cardiac defects caused by *Cited2* depletion.

Lastly, we established the importance of Cited2 in zebrafish development. Like what had been previously reported in mice, the lack of *Cited2* results in increased lethality and an

increase in the number of developmental defects and cardiovascular defects in zebrafish compared to control embryos. This indicates that the molecular function of *Cited2* is conserved in vertebrates. Moreover, since the human recombinant CITED2 protein compensates the lack of *Cited2 in vivo,* like what happens with ESC, we can propose the zebrafish as a new model to study the function of Cited2.

Interestingly, no study had yet reported a developmental delay in *Cited2* depleted embryos. We hypothesize that cardiovascular defects are the likely cause of developmental defects. Unfortunately, we lacked specific reporter transgenes to address if the origin of these defects were due to the specification or differentiation of CPC or errors in the heart formation. It is also important to notice that, for the purpose of this work, we have been mostly focusing on the cardiovascular system, but we also noticed back curvature defects and occasional iris coloboma, which are indicative of non-cardiac defects in Cited2 morphants.

We have yet to confirm that CITED2 protein levels are depleted in embryos microinjected with Cited2 MO. However, as we were able to recover most of the developmental and cardiovascular defects with the co-microinjection of recombinant CITED2 protein, it is very likely that these defects are Cited2 specific. With these results, we were also able to confirm that 8R-CITED2 corrects *Cited2* depletion defects in vivo.

Like what was observed *in vitro*, rescuing *Cited2* depletion defects in vivo, with WNT5a and WNT11 corrected most of the developmental delay and cardiovascular defects. The injection of WNT5a and WNT11 with *Cited2* MO also recovered most development defects which further gives evidence on the potential of WNT5a and WNT11 to recover developmental defects caused by *Cited2* depletion.

As future perspectives, we would like to translate this work into a clinical application. 8R-CITED2 is a powerful tool to study and rescue the loss of CITED2 function. This is not only particularly useful to avoid the appearance of CHD, but its application can be widened to adulthood like maintenance of adult HSC function (230), or the study of tumour growth (316).

To better understand the impact of WNT5a and WNT11 in cardiovascular development and their application on CHD patients, we intend to make use of a model system with a cardiovascular system similar to the human such as the mouse. Previous studies provide evidence of the beneficial effect of WNT5a and WNT11 in cardiovascular problems. Providing

WNT5a to Id KO heart explants was able to correct gene expression, especially cardiac MHC which was severely downregulated (278). There are currently available compounds currently used in clinical trials and FDA approved with promising potential for future therapies in humans. Amongst these compounds is Foxy-5 a WNT5a mimicking peptide with positive results in prostate cancer (317) and breast cancer (318).

Our goal is, on the long-term, to successfully develop a new therapeutic option to prevent the appearance of CHD similar to folic acid, a man-made form of B-vitamin, important for the neural tube and proper development of the embryo (319). This newly developed compound would then be available and given to any pregnant woman with the increased potential of transmitting a CHD to the offspring offering a new method to prevent and reduce the number of CHD patients.

CHAPTER 9

References

1. Brand T. Heart development: molecular insights into cardiac specification and early morphogenesis. Dev Biol. 2003;258(1):1-19.
2. Cardiovascular biology: Mutation causes heart disease. Nature. 2017;541(7638):438.
3. Roth GA, Johnson C, Abajobir A, Abd-Allah F, Abera SF, Abyu G, et al. Global, Regional, and National Burden of Cardiovascular Diseases for 10 Causes, 1990 to 2015. J Am Coll Cardiol. 2017;70(1):1-25.
4. Hoffman JI, Kaplan S. The incidence of congenital heart disease. J Am Coll Cardiol. 2002;39(12):1890-900.
5. Bruneau BG. The developmental genetics of congenital heart disease. Nature. 2008;451(7181):943-8.
6. Dalen JE, Alpert JS, Goldberg RJ, Weinstein RS. The epidemic of the 20(th) century: coronary heart disease. Am J Med. 2014;127(9):807-12.
7. Lage K, Greenway SC, Rosenfeld JA, Wakimoto H, Gorham JM, Segre AV, et al. Genetic and environmental risk factors in congenital heart disease functionally converge in protein networks driving heart development. Proc Natl Acad Sci U S A. 2012;109(35):14035-40.
8. Hoffman J. The global burden of congenital heart disease. Cardiovasc J Afr. 2013;24(4):141-5.
9. Pfitzer C, Helm PC, Rosenthal LM, Berger F, Bauer UMM, Schmitt KR. Dynamics in prevalence of Down syndrome in children with congenital heart disease. Eur J Pediatr. 2018;177(1):107-15.
10. Morales-Demori R. Congenital heart disease and cardiac procedural outcomes in patients with trisomy 21 and Turner syndrome. Congenit Heart Dis. 2017;12(6):820-7.
11. Fahed AC, Gelb BD, Seidman JG, Seidman CE. Genetics of congenital heart disease: the glass half empty. Circ Res. 2013;112(4):707-20.
12. Lindsay EA, Vitelli F, Su H, Morishima M, Huynh T, Pramparo T, et al. Tbx1 haploinsufficieny in the DiGeorge syndrome region causes aortic arch defects in mice. Nature. 2001;410(6824):97-101.
13. Merscher S, Funke B, Epstein JA, Heyer J, Puech A, Lu MM, et al. TBX1 is responsible for cardiovascular defects in velo-cardio-facial/DiGeorge syndrome. Cell. 2001;104(4):619-29.
14. van der Linde D, Konings EE, Slager MA, Witsenburg M, Helbing WA, Takkenberg JJ, et al. Birth prevalence of congenital heart disease worldwide: a systematic review and meta-analysis. J Am Coll Cardiol. 2011;58(21):2241-7.
15. Rossant J, Tam PP. Blastocyst lineage formation, early embryonic asymmetries and axis patterning in the mouse. Development. 2009;136(5):701-13.
16. Tam PP, Loebel DA. Gene function in mouse embryogenesis: get set for gastrulation. Nat Rev Genet. 2007;8(5):368-81.
17. Loh KM, Lim B, Ang LT. Ex uno plures: molecular designs for embryonic pluripotency. Physiol Rev. 2015;95(1):245-95.
18. Spater D, Hansson EM, Zangi L, Chien KR. How to make a cardiomyocyte. Development. 2014;141(23):4418-31.
19. Moorman A, Webb S, Brown NA, Lamers W, Anderson RH. Development of the heart: (1) formation of the cardiac chambers and arterial trunks. Heart. 2003;89(7):806-14.
20. Martin-Puig S, Wang Z, Chien KR. Lives of a heart cell: tracing the origins of cardiac progenitors. Cell Stem Cell. 2008;2(4):320-31.
21. Brade T, Pane LS, Moretti A, Chien KR, Laugwitz KL. Embryonic heart progenitors and cardiogenesis. Cold Spring Harb Perspect Med. 2013;3(10):a013847.
22. Zhou B, Ma Q, Rajagopal S, Wu SM, Domian I, Rivera-Feliciano J, et al. Epicardial progenitors contribute to the cardiomyocyte lineage in the developing heart. Nature. 2008;454(7200):109-13.

23. Santini MP, Forte E, Harvey RP, Kovacic JC. Developmental origin and lineage plasticity of endogenous cardiac stem cells. Development. 2016;143(8):1242-58.
24. de la Cruz MV, Sanchez Gomez C, Arteaga MM, Arguello C. Experimental study of the development of the truncus and the conus in the chick embryo. J Anat. 1977;123(Pt 3):661-86.
25. Kelly RG, Brown NA, Buckingham ME. The arterial pole of the mouse heart forms from Fgf10-expressing cells in pharyngeal mesoderm. Dev Cell. 2001;1(3):435-40.
26. Mjaatvedt CH, Nakaoka T, Moreno-Rodriguez R, Norris RA, Kern MJ, Eisenberg CA, et al. The outflow tract of the heart is recruited from a novel heart-forming field. Dev Biol. 2001;238(1):97-109.
27. Waldo KL, Kumiski DH, Wallis KT, Stadt HA, Hutson MR, Platt DH, et al. Conotruncal myocardium arises from a secondary heart field. Development. 2001;128(16):3179-88.
28. Lescroart F, Chabab S, Lin X, Rulands S, Paulissen C, Rodolosse A, et al. Early lineage restriction in temporally distinct populations of Mesp1 progenitors during mammalian heart development. Nat Cell Biol. 2014;16(9):829-40.
29. Cai CL, Liang X, Shi Y, Chu PH, Pfaff SL, Chen J, et al. Isl1 identifies a cardiac progenitor population that proliferates prior to differentiation and contributes a majority of cells to the heart. Dev Cell. 2003;5(6):877-89.
30. Yang L, Cai CL, Lin L, Qyang Y, Chung C, Monteiro RM, et al. Isl1Cre reveals a common Bmp pathway in heart and limb development. Development. 2006;133(8):1575-85.
31. Ma Q, Zhou B, Pu WT. Reassessment of Isl1 and Nkx2-5 cardiac fate maps using a Gata4-based reporter of Cre activity. Dev Biol. 2008;323(1):98-104.
32. Vincent SD, Buckingham ME. How to make a heart: the origin and regulation of cardiac progenitor cells. Curr Top Dev Biol. 2010;90:1-41.
33. Cohen ED, Tian Y, Morrisey EE. Wnt signaling: an essential regulator of cardiovascular differentiation, morphogenesis and progenitor self-renewal. Development. 2008;135(5):789-98.
34. Francou A, Saint-Michel E, Mesbah K, Theveniau-Ruissy M, Rana MS, Christoffels VM, et al. Second heart field cardiac progenitor cells in the early mouse embryo. Biochim Biophys Acta. 2013;1833(4):795-8.
35. Scholer HR, Dressler GR, Balling R, Rohdewohld H, Gruss P. Oct-4: a germline-specific transcription factor mapping to the mouse t-complex. EMBO J. 1990;9(7):2185-95.
36. Ovitt CE, Scholer HR. The molecular biology of Oct-4 in the early mouse embryo. Mol Hum Reprod. 1998;4(11):1021-31.
37. Frum T, Halbisen MA, Wang C, Amiri H, Robson P, Ralston A. Oct4 cell-autonomously promotes primitive endoderm development in the mouse blastocyst. Dev Cell. 2013;25(6):610-22.
38. Nichols J, Zevnik B, Anastassiadis K, Niwa H, Klewe-Nebenius D, Chambers I, et al. Formation of pluripotent stem cells in the mammalian embryo depends on the POU transcription factor Oct4. Cell. 1998;95(3):379-91.
39. Hay DC, Sutherland L, Clark J, Burdon T. Oct-4 knockdown induces similar patterns of endoderm and trophoblast differentiation markers in human and mouse embryonic stem cells. Stem Cells. 2004;22(2):225-35.
40. Niwa H, Miyazaki J, Smith AG. Quantitative expression of Oct-3/4 defines differentiation, dedifferentiation or self-renewal of ES cells. Nat Genet. 2000;24(4):372-6.
41. Chazaud C, Yamanaka Y, Pawson T, Rossant J. Early lineage segregation between epiblast and primitive endoderm in mouse blastocysts through the Grb2-MAPK pathway. Dev Cell. 2006;10(5):615-24.

42. Avilion AA, Nicolis SK, Pevny LH, Perez L, Vivian N, Lovell-Badge R. Multipotent cell lineages in early mouse development depend on SOX2 function. Genes Dev. 2003;17(1):126-40.
43. Masui S, Nakatake Y, Toyooka Y, Shimosato D, Yagi R, Takahashi K, et al. Pluripotency governed by Sox2 via regulation of Oct3/4 expression in mouse embryonic stem cells. Nat Cell Biol. 2007;9(6):625-35.
44. Fong H, Hohenstein KA, Donovan PJ. Regulation of self-renewal and pluripotency by Sox2 in human embryonic stem cells. Stem Cells. 2008;26(8):1931-8.
45. Wang Z, Oron E, Nelson B, Razis S, Ivanova N. Distinct lineage specification roles for NANOG, OCT4, and SOX2 in human embryonic stem cells. Cell Stem Cell. 2012;10(4):440-54.
46. Zhao S, Nichols J, Smith AG, Li M. SoxB transcription factors specify neuroectodermal lineage choice in ES cells. Mol Cell Neurosci. 2004;27(3):332-42.
47. Chambers I, Colby D, Robertson M, Nichols J, Lee S, Tweedie S, et al. Functional expression cloning of Nanog, a pluripotency sustaining factor in embryonic stem cells. Cell. 2003;113(5):643-55.
48. Mitsui K, Tokuzawa Y, Itoh H, Segawa K, Murakami M, Takahashi K, et al. The homeoprotein Nanog is required for maintenance of pluripotency in mouse epiblast and ES cells. Cell. 2003;113(5):631-42.
49. Ivanova N, Dobrin R, Lu R, Kotenko I, Levorse J, DeCoste C, et al. Dissecting self-renewal in stem cells with RNA interference. Nature. 2006;442(7102):533-8.
50. Teo AK, Arnold SJ, Trotter MW, Brown S, Ang LT, Chng Z, et al. Pluripotency factors regulate definitive endoderm specification through eomesodermin. Genes Dev. 2011;25(3):238-50.
51. Chambers I, Silva J, Colby D, Nichols J, Nijmeijer B, Robertson M, et al. Nanog safeguards pluripotency and mediates germline development. Nature. 2007;450(7173):1230-4.
52. Darr H, Mayshar Y, Benvenisty N. Overexpression of NANOG in human ES cells enables feeder-free growth while inducing primitive ectoderm features. Development. 2006;133(6):1193-201.
53. Wang J, Levasseur DN, Orkin SH. Requirement of Nanog dimerization for stem cell self-renewal and pluripotency. Proc Natl Acad Sci U S A. 2008;105(17):6326-31.
54. Faial T, Bernardo AS, Mendjan S, Diamanti E, Ortmann D, Gentsch GE, et al. Brachyury and SMAD signalling collaboratively orchestrate distinct mesoderm and endoderm gene regulatory networks in differentiating human embryonic stem cells. Development. 2015;142(12):2121-35.
55. King T, Beddington RS, Brown NA. The role of the brachyury gene in heart development and left-right specification in the mouse. Mech Dev. 1998;79(1-2):29-37.
56. Costello I, Pimeisl IM, Drager S, Bikoff EK, Robertson EJ, Arnold SJ. The T-box transcription factor Eomesodermin acts upstream of Mesp1 to specify cardiac mesoderm during mouse gastrulation. Nat Cell Biol. 2011;13(9):1084-91.
57. van den Ameele J, Tiberi L, Bondue A, Paulissen C, Herpoel A, Iacovino M, et al. Eomesodermin induces Mesp1 expression and cardiac differentiation from embryonic stem cells in the absence of Activin. EMBO Rep. 2012;13(4):355-62.
58. Saga Y, Miyagawa-Tomita S, Takagi A, Kitajima S, Miyazaki J, Inoue T. MesP1 is expressed in the heart precursor cells and required for the formation of a single heart tube. Development. 1999;126(15):3437-47.
59. Yoshida T, Vivatbutsiri P, Morriss-Kay G, Saga Y, Iseki S. Cell lineage in mammalian craniofacial mesenchyme. Mech Dev. 2008;125(9-10):797-808.

60. David R, Brenner C, Stieber J, Schwarz F, Brunner S, Vollmer M, et al. MesP1 drives vertebrate cardiovascular differentiation through Dkk-1-mediated blockade of Wnt-signalling. Nat Cell Biol. 2008;10(3):338-45.
61. Bondue A, Lapouge G, Paulissen C, Semeraro C, Iacovino M, Kyba M, et al. Mesp1 acts as a master regulator of multipotent cardiovascular progenitor specification. Cell Stem Cell. 2008;3(1):69-84.
62. Lescroart F, Wang X, Lin X, Swedlund B, Gargouri S, Sanchez-Danes A, et al. Defining the earliest step of cardiovascular lineage segregation by single-cell RNA-seq. Science. 2018;359(6380):1177-81.
63. Hiroi Y, Kudoh S, Monzen K, Ikeda Y, Yazaki Y, Nagai R, et al. Tbx5 associates with Nkx2-5 and synergistically promotes cardiomyocyte differentiation. Nat Genet. 2001;28(3):276-80.
64. Durocher D, Charron F, Warren R, Schwartz RJ, Nemer M. The cardiac transcription factors Nkx2-5 and GATA-4 are mutual cofactors. EMBO J. 1997;16(18):5687-96.
65. Dorn T, Goedel A, Lam JT, Haas J, Tian Q, Herrmann F, et al. Direct nkx2-5 transcriptional repression of isl1 controls cardiomyocyte subtype identity. Stem Cells. 2015;33(4):1113-29.
66. Skerjanc IS, Petropoulos H, Ridgeway AG, Wilton S. Myocyte enhancer factor 2C and Nkx2-5 up-regulate each other's expression and initiate cardiomyogenesis in P19 cells. J Biol Chem. 1998;273(52):34904-10.
67. Yamagishi H, Yamagishi C, Nakagawa O, Harvey RP, Olson EN, Srivastava D. The combinatorial activities of Nkx2.5 and dHAND are essential for cardiac ventricle formation. Dev Biol. 2001;239(2):190-203.
68. Maitra M, Schluterman MK, Nichols HA, Richardson JA, Lo CW, Srivastava D, et al. Interaction of Gata4 and Gata6 with Tbx5 is critical for normal cardiac development. Dev Biol. 2009;326(2):368-77.
69. Dai YS, Cserjesi P, Markham BE, Molkentin JD. The transcription factors GATA4 and dHAND physically interact to synergistically activate cardiac gene expression through a p300-dependent mechanism. J Biol Chem. 2002;277(27):24390-8.
70. Dodou E, Verzi MP, Anderson JP, Xu SM, Black BL. Mef2c is a direct transcriptional target of ISL1 and GATA factors in the anterior heart field during mouse embryonic development. Development. 2004;131(16):3931-42.
71. Bodmer R. The gene tinman is required for specification of the heart and visceral muscles in Drosophila. Development. 1993;118(3):719-29.
72. Schott JJ, Benson DW, Basson CT, Pease W, Silberbach GM, Moak JP, et al. Congenital heart disease caused by mutations in the transcription factor NKX2-5. Science. 1998;281(5373):108-11.
73. McCulley DJ, Black BL. Transcription factor pathways and congenital heart disease. Curr Top Dev Biol. 2012;100:253-77.
74. Lyons I, Parsons LM, Hartley L, Li R, Andrews JE, Robb L, et al. Myogenic and morphogenetic defects in the heart tubes of murine embryos lacking the homeo box gene Nkx2-5. Genes Dev. 1995;9(13):1654-66.
75. Kuo CT, Morrisey EE, Anandappa R, Sigrist K, Lu MM, Parmacek MS, et al. GATA4 transcription factor is required for ventral morphogenesis and heart tube formation. Genes Dev. 1997;11(8):1048-60.
76. Moorman AF, Christoffels VM. Cardiac chamber formation: development, genes, and evolution. Physiol Rev. 2003;83(4):1223-67.
77. Holtzinger A, Rosenfeld GE, Evans T. Gata4 directs development of cardiac-inducing endoderm from ES cells. Dev Biol. 2010;337(1):63-73.

78. Takeuchi JK, Bruneau BG. Directed transdifferentiation of mouse mesoderm to heart tissue by defined factors. Nature. 2009;459(7247):708-11.
79. Lin Q, Schwarz J, Bucana C, Olson EN. Control of mouse cardiac morphogenesis and myogenesis by transcription factor MEF2C. Science. 1997;276(5317):1404-7.
80. Edmondson DG, Lyons GE, Martin JF, Olson EN. Mef2 gene expression marks the cardiac and skeletal muscle lineages during mouse embryogenesis. Development. 1994;120(5):1251-63.
81. Li QY, Newbury-Ecob RA, Terrett JA, Wilson DI, Curtis AR, Yi CH, et al. Holt-Oram syndrome is caused by mutations in TBX5, a member of the Brachyury (T) gene family. Nat Genet. 1997;15(1):21-9.
82. Basson CT, Huang T, Lin RC, Bachinsky DR, Weremowicz S, Vaglio A, et al. Different TBX5 interactions in heart and limb defined by Holt-Oram syndrome mutations. Proc Natl Acad Sci U S A. 1999;96(6):2919-24.
83. Bruneau BG, Logan M, Davis N, Levi T, Tabin CJ, Seidman JG, et al. Chamber-specific cardiac expression of Tbx5 and heart defects in Holt-Oram syndrome. Dev Biol. 1999;211(1):100-8.
84. Horb ME, Thomsen GH. Tbx5 is essential for heart development. Development. 1999;126(8):1739-51.
85. Mori AD, Zhu Y, Vahora I, Nieman B, Koshiba-Takeuchi K, Davidson L, et al. Tbx5-dependent rheostatic control of cardiac gene expression and morphogenesis. Dev Biol. 2006;297(2):566-86.
86. Bruneau BG, Nemer G, Schmitt JP, Charron F, Robitaille L, Caron S, et al. A murine model of Holt-Oram syndrome defines roles of the T-box transcription factor Tbx5 in cardiogenesis and disease. Cell. 2001;106(6):709-21.
87. Khattar P, Friedrich FW, Bonne G, Carrier L, Eschenhagen T, Evans SM, et al. Distinction between two populations of islet-1-positive cells in hearts of different murine strains. Stem Cells Dev. 2011;20(6):1043-52.
88. Yuan S, Schoenwolf GC. Islet-1 marks the early heart rudiments and is asymmetrically expressed during early rotation of the foregut in the chick embryo. Anat Rec. 2000;260(2):204-7.
89. Srivastava D, Thomas T, Lin Q, Kirby ML, Brown D, Olson EN. Regulation of cardiac mesodermal and neural crest development by the bHLH transcription factor, dHAND. Nat Genet. 1997;16(2):154-60.
90. VanDusen NJ, Vincentz JW, Firulli BA, Howard MJ, Rubart M, Firulli AB. Loss of Hand2 in a population of Periostin lineage cells results in pronounced bradycardia and neonatal death. Dev Biol. 2014;388(2):149-58.
91. Barnes RM, Firulli BA, VanDusen NJ, Morikawa Y, Conway SJ, Cserjesi P, et al. Hand2 loss-of-function in Hand1-expressing cells reveals distinct roles in epicardial and coronary vessel development. Circ Res. 2011;108(8):940-9.
92. Holler KL, Hendershot TJ, Troy SE, Vincentz JW, Firulli AB, Howard MJ. Targeted deletion of Hand2 in cardiac neural crest-derived cells influences cardiac gene expression and outflow tract development. Dev Biol. 2010;341(1):291-304.
93. Tsuchihashi T, Maeda J, Shin CH, Ivey KN, Black BL, Olson EN, et al. Hand2 function in second heart field progenitors is essential for cardiogenesis. Dev Biol. 2011;351(1):62-9.
94. Sun YM, Wang J, Qiu XB, Yuan F, Li RG, Xu YJ, et al. A HAND2 Loss-of-Function Mutation Causes Familial Ventricular Septal Defect and Pulmonary Stenosis. G3 (Bethesda). 2016;6(4):987-92.
95. Massague J. TGFbeta signalling in context. Nat Rev Mol Cell Biol. 2012;13(10):616-30.
96. Urist MR, Jurist JM, Jr., Dubuc FL, Strates BS. Quantitation of new bone formation in intramuscular implants of bone matrix in rabbits. Clin Orthop Relat Res. 1970;68:279-93.

97. van Wijk B, Moorman AF, van den Hoff MJ. Role of bone morphogenetic proteins in cardiac differentiation. Cardiovasc Res. 2007;74(2):244-55.
98. Yuasa S, Itabashi Y, Koshimizu U, Tanaka T, Sugimura K, Kinoshita M, et al. Transient inhibition of BMP signaling by Noggin induces cardiomyocyte differentiation of mouse embryonic stem cells. Nat Biotechnol. 2005;23(5):607-11.
99. Zhang H, Bradley A. Mice deficient for BMP2 are nonviable and have defects in amnion/chorion and cardiac development. Development. 1996;122(10):2977-86.
100. Rivera-Feliciano J, Tabin CJ. Bmp2 instructs cardiac progenitors to form the heart-valve-inducing field. Dev Biol. 2006;295(2):580-8.
101. Winnier G, Blessing M, Labosky PA, Hogan BL. Bone morphogenetic protein-4 is required for mesoderm formation and patterning in the mouse. Genes Dev. 1995;9(17):2105-16.
102. Bernardo AS, Faial T, Gardner L, Niakan KK, Ortmann D, Senner CE, et al. BRACHYURY and CDX2 mediate BMP-induced differentiation of human and mouse pluripotent stem cells into embryonic and extraembryonic lineages. Cell Stem Cell. 2011;9(2):144-55.
103. Witty AD, Mihic A, Tam RY, Fisher SA, Mikryukov A, Shoichet MS, et al. Generation of the epicardial lineage from human pluripotent stem cells. Nat Biotechnol. 2014;32(10):1026-35.
104. Hendrix MJ, Seftor EA, Seftor RE, Kasemeier-Kulesa J, Kulesa PM, Postovit LM. Reprogramming metastatic tumour cells with embryonic microenvironments. Nat Rev Cancer. 2007;7(4):246-55.
105. Vallier L, Reynolds D, Pedersen RA. Nodal inhibits differentiation of human embryonic stem cells along the neuroectodermal default pathway. Dev Biol. 2004;275(2):403-21.
106. Brons IG, Smithers LE, Trotter MW, Rugg-Gunn P, Sun B, Chuva de Sousa Lopes SM, et al. Derivation of pluripotent epiblast stem cells from mammalian embryos. Nature. 2007;448(7150):191-5.
107. Camus A, Perea-Gomez A, Moreau A, Collignon J. Absence of Nodal signaling promotes precocious neural differentiation in the mouse embryo. Dev Biol. 2006;295(2):743-55.
108. Shen MM. Nodal signaling: developmental roles and regulation. Development. 2007;134(6):1023-34.
109. Schier AF. Nodal signaling in vertebrate development. Annu Rev Cell Dev Biol. 2003;19:589-621.
110. Clevers H, Nusse R. Wnt/beta-catenin signaling and disease. Cell. 2012;149(6):1192-205.
111. Gessert S, Kuhl M. The multiple phases and faces of wnt signaling during cardiac differentiation and development. Circ Res. 2010;107(2):186-99.
112. Ueno S, Weidinger G, Osugi T, Kohn AD, Golob JL, Pabon L, et al. Biphasic role for Wnt/beta-catenin signaling in cardiac specification in zebrafish and embryonic stem cells. Proc Natl Acad Sci U S A. 2007;104(23):9685-90.
113. Staal FJ, Luis TC, Tiemessen MM. WNT signalling in the immune system: WNT is spreading its wings. Nat Rev Immunol. 2008;8(8):581-93.
114. Ornitz DM, Itoh N. The Fibroblast Growth Factor signaling pathway. Wiley Interdiscip Rev Dev Biol. 2015;4(3):215-66.
115. Itoh N, Ohta H, Nakayama Y, Konishi M. Roles of FGF Signals in Heart Development, Health, and Disease. Front Cell Dev Biol. 2016;4:110.
116. Sun X, Meyers EN, Lewandoski M, Martin GR. Targeted disruption of Fgf8 causes failure of cell migration in the gastrulating mouse embryo. Genes Dev. 1999;13(14):1834-46.

117. Rochais F, Sturny R, Chao CM, Mesbah K, Bennett M, Mohun TJ, et al. FGF10 promotes regional foetal cardiomyocyte proliferation and adult cardiomyocyte cell-cycle re-entry. Cardiovasc Res. 2014;104(3):432-42.
118. Kopp JL, Ormsbee BD, Desler M, Rizzino A. Small increases in the level of Sox2 trigger the differentiation of mouse embryonic stem cells. Stem Cells. 2008;26(4):903-11.
119. Yu P, Pan G, Yu J, Thomson JA. FGF2 sustains NANOG and switches the outcome of BMP4-induced human embryonic stem cell differentiation. Cell Stem Cell. 2011;8(3):326-34.
120. Jaenisch R, Young R. Stem cells, the molecular circuitry of pluripotency and nuclear reprogramming. Cell. 2008;132(4):567-82.
121. Silva J, Smith A. Capturing pluripotency. Cell. 2008;132(4):532-6.
122. Beck S, Le Good JA, Guzman M, Ben Haim N, Roy K, Beermann F, et al. Extraembryonic proteases regulate Nodal signalling during gastrulation. Nat Cell Biol. 2002;4(12):981-5.
123. Mossman AK, Sourris K, Ng E, Stanley EG, Elefanty AG. Mixl1 and oct4 proteins are transiently co-expressed in differentiating mouse and human embryonic stem cells. Stem Cells Dev. 2005;14(6):656-63.
124. Suzuki A, Raya A, Kawakami Y, Morita M, Matsui T, Nakashima K, et al. Maintenance of embryonic stem cell pluripotency by Nanog-mediated reversal of mesoderm specification. Nat Clin Pract Cardiovasc Med. 2006;3 Suppl 1:S114-22.
125. Blauwkamp TA, Nigam S, Ardehali R, Weissman IL, Nusse R. Endogenous Wnt signalling in human embryonic stem cells generates an equilibrium of distinct lineage-specified progenitors. Nat Commun. 2012;3:1070.
126. Davidson KC, Adams AM, Goodson JM, McDonald CE, Potter JC, Berndt JD, et al. Wnt/beta-catenin signaling promotes differentiation, not self-renewal, of human embryonic stem cells and is repressed by Oct4. Proc Natl Acad Sci U S A. 2012;109(12):4485-90.
127. Sumi T, Oki S, Kitajima K, Meno C. Epiblast ground state is controlled by canonical Wnt/beta-catenin signaling in the postimplantation mouse embryo and epiblast stem cells. PLoS One. 2013;8(5):e63378.
128. Xu RH, Peck RM, Li DS, Feng X, Ludwig T, Thomson JA. Basic FGF and suppression of BMP signaling sustain undifferentiated proliferation of human ES cells. Nat Methods. 2005;2(3):185-90.
129. Aulehla A, Wiegraebe W, Baubet V, Wahl MB, Deng C, Taketo M, et al. A beta-catenin gradient links the clock and wavefront systems in mouse embryo segmentation. Nat Cell Biol. 2008;10(2):186-93.
130. Schneider VA, Mercola M. Wnt antagonism initiates cardiogenesis in Xenopus laevis. Genes Dev. 2001;15(3):304-15.
131. Marvin MJ, Di Rocco G, Gardiner A, Bush SM, Lassar AB. Inhibition of Wnt activity induces heart formation from posterior mesoderm. Genes Dev. 2001;15(3):316-27.
132. Monteiro RM, de Sousa Lopes SM, Bialecka M, de Boer S, Zwijsen A, Mummery CL. Real time monitoring of BMP Smads transcriptional activity during mouse development. Genesis. 2008;46(7):335-46.
133. Tonegawa A, Funayama N, Ueno N, Takahashi Y. Mesodermal subdivision along the mediolateral axis in chicken controlled by different concentrations of BMP-4. Development. 1997;124(10):1975-84.
134. Loh KM, Chen A, Koh PW, Deng TZ, Sinha R, Tsai JM, et al. Mapping the Pairwise Choices Leading from Pluripotency to Human Bone, Heart, and Other Mesoderm Cell Types. Cell. 2016;166(2):451-67.
135. Yang L, Soonpaa MH, Adler ED, Roepke TK, Kattman SJ, Kennedy M, et al. Human cardiovascular progenitor cells develop from a KDR+ embryonic-stem-cell-derived population. Nature. 2008;453(7194):524-8.

136. Lian X, Hsiao C, Wilson G, Zhu K, Hazeltine LB, Azarin SM, et al. Robust cardiomyocyte differentiation from human pluripotent stem cells via temporal modulation of canonical Wnt signaling. Proc Natl Acad Sci U S A. 2012;109(27):E1848-57.
137. Lian X, Zhang J, Azarin SM, Zhu K, Hazeltine LB, Bao X, et al. Directed cardiomyocyte differentiation from human pluripotent stem cells by modulating Wnt/beta-catenin signaling under fully defined conditions. Nat Protoc. 2013;8(1):162-75.
138. Reifers F, Walsh EC, Leger S, Stainier DY, Brand M. Induction and differentiation of the zebrafish heart requires fibroblast growth factor 8 (fgf8/acerebellar). Development. 2000;127(2):225-35.
139. Watanabe Y, Miyagawa-Tomita S, Vincent SD, Kelly RG, Moon AM, Buckingham ME. Role of mesodermal FGF8 and FGF10 overlaps in the development of the arterial pole of the heart and pharyngeal arch arteries. Circ Res. 2010;106(3):495-503.
140. Perrimon N, Pitsouli C, Shilo BZ. Signaling mechanisms controlling cell fate and embryonic patterning. Cold Spring Harb Perspect Biol. 2012;4(8):a005975.
141. Sommer D, Peters AE, Baumgart AK, Beyer M. TALEN-mediated genome engineering to generate targeted mice. Chromosome Res. 2015;23(1):43-55.
142. Yang H, Wang H, Jaenisch R. Generating genetically modified mice using CRISPR/Cas-mediated genome engineering. Nat Protoc. 2014;9(8):1956-68.
143. Bouabe H, Okkenhaug K. Gene targeting in mice: a review. Methods Mol Biol. 2013;1064:315-36.
144. Wittig JG, Munsterberg A. The Early Stages of Heart Development: Insights from Chicken Embryos. J Cardiovasc Dev Dis. 2016;3(2).
145. Hempel A, Kuhl M. A Matter of the Heart: The African Clawed Frog Xenopus as a Model for Studying Vertebrate Cardiogenesis and Congenital Heart Defects. J Cardiovasc Dev Dis. 2016;3(2).
146. Bakkers J. Zebrafish as a model to study cardiac development and human cardiac disease. Cardiovasc Res. 2011;91(2):279-88.
147. Taghli-Lamallem O, Plantie E, Jagla K. Drosophila in the Heart of Understanding Cardiac Diseases: Modeling Channelopathies and Cardiomyopathies in the Fruitfly. J Cardiovasc Dev Dis. 2016;3(1).
148. Piazza N, Wessells RJ. Drosophila models of cardiac disease. Prog Mol Biol Transl Sci. 2011;100:155-210.
149. Louch WE, Sheehan KA, Wolska BM. Methods in cardiomyocyte isolation, culture, and gene transfer. J Mol Cell Cardiol. 2011;51(3):288-98.
150. Ehler E, Moore-Morris T, Lange S. Isolation and culture of neonatal mouse cardiomyocytes. J Vis Exp. 2013(79).
151. Kimes BW, Brandt BL. Properties of a clonal muscle cell line from rat heart. Exp Cell Res. 1976;98(2):367-81.
152. Jaffredo T, Chestier A, Bachnou N, Dieterlen-Lievre F. MC29-immortalized clonal avian heart cell lines can partially differentiate in vitro. Exp Cell Res. 1991;192(2):481-91.
153. Claycomb WC, Lanson NA, Jr., Stallworth BS, Egeland DB, Delcarpio JB, Bahinski A, et al. HL-1 cells: a cardiac muscle cell line that contracts and retains phenotypic characteristics of the adult cardiomyocyte. Proc Natl Acad Sci U S A. 1998;95(6):2979-84.
154. Nagy A, Rossant J, Nagy R, Abramow-Newerly W, Roder JC. Derivation of completely cell culture-derived mice from early-passage embryonic stem cells. Proc Natl Acad Sci U S A. 1993;90(18):8424-8.
155. Evans MJ, Kaufman MH. Establishment in culture of pluripotential cells from mouse embryos. Nature. 1981;292(5819):154-6.

156. Martin GR. Isolation of a pluripotent cell line from early mouse embryos cultured in medium conditioned by teratocarcinoma stem cells. Proc Natl Acad Sci U S A. 1981;78(12):7634-8.
157. Thomson JA, Itskovitz-Eldor J, Shapiro SS, Waknitz MA, Swiergiel JJ, Marshall VS, et al. Embryonic stem cell lines derived from human blastocysts. Science. 1998;282(5391):1145-7.
158. Turksen K, Troy TC. Human embryonic stem cells: isolation, maintenance, and differentiation. Methods Mol Biol. 2006;331:1-12.
159. Takahashi K, Yamanaka S. Induction of pluripotent stem cells from mouse embryonic and adult fibroblast cultures by defined factors. Cell. 2006;126(4):663-76.
160. Tesar PJ, Chenoweth JG, Brook FA, Davies TJ, Evans EP, Mack DL, et al. New cell lines from mouse epiblast share defining features with human embryonic stem cells. Nature. 2007;448(7150):196-9.
161. Nichols J, Smith A. Naive and primed pluripotent states. Cell Stem Cell. 2009;4(6):487-92.
162. Haub O, Goldfarb M. Expression of the fibroblast growth factor-5 gene in the mouse embryo. Development. 1991;112(2):397-406.
163. Conlon FL, Lyons KM, Takaesu N, Barth KS, Kispert A, Herrmann B, et al. A primary requirement for nodal in the formation and maintenance of the primitive streak in the mouse. Development. 1994;120(7):1919-28.
164. Ying QL, Wray J, Nichols J, Batlle-Morera L, Doble B, Woodgett J, et al. The ground state of embryonic stem cell self-renewal. Nature. 2008;453(7194):519-23.
165. Hanna J, Cheng AW, Saha K, Kim J, Lengner CJ, Soldner F, et al. Human embryonic stem cells with biological and epigenetic characteristics similar to those of mouse ESCs. Proc Natl Acad Sci U S A. 2010;107(20):9222-7.
166. Sato M, Kimura T, Kurokawa K, Fujita Y, Abe K, Masuhara M, et al. Identification of PGC7, a new gene expressed specifically in preimplantation embryos and germ cells. Mech Dev. 2002;113(1):91-4.
167. Daheron L, Opitz SL, Zaehres H, Lensch MW, Andrews PW, Itskovitz-Eldor J, et al. LIF/STAT3 signaling fails to maintain self-renewal of human embryonic stem cells. Stem Cells. 2004;22(5):770-8.
168. Williams RL, Hilton DJ, Pease S, Willson TA, Stewart CL, Gearing DP, et al. Myeloid leukaemia inhibitory factor maintains the developmental potential of embryonic stem cells. Nature. 1988;336(6200):684-7.
169. Kurosawa H. Methods for inducing embryoid body formation: in vitro differentiation system of embryonic stem cells. J Biosci Bioeng. 2007;103(5):389-98.
170. Passier R, Oostwaard DW, Snapper J, Kloots J, Hassink RJ, Kuijk E, et al. Increased cardiomyocyte differentiation from human embryonic stem cells in serum-free cultures. Stem Cells. 2005;23(6):772-80.
171. Hwang YS, Chung BG, Ortmann D, Hattori N, Moeller HC, Khademhosseini A. Microwell-mediated control of embryoid body size regulates embryonic stem cell fate via differential expression of WNT5a and WNT11. Proc Natl Acad Sci U S A. 2009;106(40):16978-83.
172. Mohr JC, Zhang J, Azarin SM, Soerens AG, de Pablo JJ, Thomson JA, et al. The microwell control of embryoid body size in order to regulate cardiac differentiation of human embryonic stem cells. Biomaterials. 2010;31(7):1885-93.
173. Laflamme MA, Chen KY, Naumova AV, Muskheli V, Fugate JA, Dupras SK, et al. Cardiomyocytes derived from human embryonic stem cells in pro-survival factors enhance function of infarcted rat hearts. Nat Biotechnol. 2007;25(9):1015-24.

174. Cao N, Liang H, Huang J, Wang J, Chen Y, Chen Z, et al. Highly efficient induction and long-term maintenance of multipotent cardiovascular progenitors from human pluripotent stem cells under defined conditions. Cell Res. 2013;23(9):1119-32.
175. Burridge PW, Matsa E, Shukla P, Lin ZC, Churko JM, Ebert AD, et al. Chemically defined generation of human cardiomyocytes. Nat Methods. 2014;11(8):855-60.
176. Batalov I, Feinberg AW. Differentiation of Cardiomyocytes from Human Pluripotent Stem Cells Using Monolayer Culture. Biomark Insights. 2015;10(Suppl 1):71-6.
177. Lo B, Parham L. Ethical issues in stem cell research. Endocr Rev. 2009;30(3):204-13.
178. Volarevic V, Markovic BS, Gazdic M, Volarevic A, Jovicic N, Arsenijevic N, et al. Ethical and Safety Issues of Stem Cell-Based Therapy. Int J Med Sci. 2018;15(1):36-45.
179. Murry CE, Keller G. Differentiation of embryonic stem cells to clinically relevant populations: lessons from embryonic development. Cell. 2008;132(4):661-80.
180. van Berlo JH, Kanisicak O, Maillet M, Vagnozzi RJ, Karch J, Lin SC, et al. c-kit+ cells minimally contribute cardiomyocytes to the heart. Nature. 2014;509(7500):337-41.
181. Perino MG, Yamanaka S, Li J, Wobus AM, Boheler KR. Cardiomyogenic stem and progenitor cell plasticity and the dissection of cardiopoiesis. J Mol Cell Cardiol. 2008;45(4):475-94.
182. Dey D, Han L, Bauer M, Sanada F, Oikonomopoulos A, Hosoda T, et al. Dissecting the molecular relationship among various cardiogenic progenitor cells. Circ Res. 2013;112(9):1253-62.
183. Hsieh PC, Segers VF, Davis ME, MacGillivray C, Gannon J, Molkentin JD, et al. Evidence from a genetic fate-mapping study that stem cells refresh adult mammalian cardiomyocytes after injury. Nat Med. 2007;13(8):970-4.
184. Senyo SE, Steinhauser ML, Pizzimenti CL, Yang VK, Cai L, Wang M, et al. Mammalian heart renewal by pre-existing cardiomyocytes. Nature. 2013;493(7432):433-6.
185. Zhang Y, Cao N, Huang Y, Spencer CI, Fu JD, Yu C, et al. Expandable Cardiovascular Progenitor Cells Reprogrammed from Fibroblasts. Cell Stem Cell. 2016;18(3):368-81.
186. Birket MJ, Ribeiro MC, Verkerk AO, Ward D, Leitoguinho AR, den Hartogh SC, et al. Expansion and patterning of cardiovascular progenitors derived from human pluripotent stem cells. Nat Biotechnol. 2015;33(9):970-9.
187. Soldner F, Jaenisch R. iPSC Disease Modeling. Science. 2012;338(6111):1155-6.
188. Ebert AD, Liang P, Wu JC. Induced pluripotent stem cells as a disease modeling and drug screening platform. J Cardiovasc Pharmacol. 2012;60(4):408-16.
189. Liu X, Li W, Fu X, Xu Y. The Immunogenicity and Immune Tolerance of Pluripotent Stem Cell Derivatives. Front Immunol. 2017;8:645.
190. Sayed N, Liu C, Wu JC. Translation of Human-Induced Pluripotent Stem Cells: From Clinical Trial in a Dish to Precision Medicine. J Am Coll Cardiol. 2016;67(18):2161-76.
191. Bhattacharya S, Michels CL, Leung MK, Arany ZP, Kung AL, Livingston DM. Functional role of p35srj, a novel p300/CBP binding protein, during transactivation by HIF-1. Genes Dev. 1999;13(1):64-75.
192. Freedman SJ, Sun ZY, Kung AL, France DS, Wagner G, Eck MJ. Structural basis for negative regulation of hypoxia-inducible factor-1alpha by CITED2. Nat Struct Biol. 2003;10(7):504-12.
193. José Brança JMAS. Is CITED2 a general regulator of stem cell functions? Stem cell and Translational Investigation. 2015;2(e755).
194. Bamforth SD, Braganca J, Eloranta JJ, Murdoch JN, Marques FI, Kranc KR, et al. Cardiac malformations, adrenal agenesis, neural crest defects and exencephaly in mice lacking Cited2, a new Tfap2 co-activator. Nat Genet. 2001;29(4):469-74.

195. Bamforth SD, Braganca J, Farthing CR, Schneider JE, Broadbent C, Michell AC, et al. Cited2 controls left-right patterning and heart development through a Nodal-Pitx2c pathway. Nat Genet. 2004;36(11):1189-96.
196. MacDonald ST, Bamforth SD, Braganca J, Chen CM, Broadbent C, Schneider JE, et al. A cell-autonomous role of Cited2 in controlling myocardial and coronary vascular development. Eur Heart J. 2013;34(32):2557-65.
197. Sperling S, Grimm CH, Dunkel I, Mebus S, Sperling HP, Ebner A, et al. Identification and functional analysis of CITED2 mutations in patients with congenital heart defects. Hum Mutat. 2005;26(6):575-82.
198. Yang XF, Wu XY, Li M, Li YG, Dai JT, Bai YH, et al. [Mutation analysis of Cited2 in patients with congenital heart disease]. Zhonghua Er Ke Za Zhi. 2010;48(4):293-6.
199. Chen CM, Bentham J, Cosgrove C, Braganca J, Cuenda A, Bamforth SD, et al. Functional significance of SRJ domain mutations in CITED2. PLoS One. 2012;7(10):e46256.
200. Xu M, Wu X, Li Y, Yang X, Hu J, Zheng M, et al. CITED2 mutation and methylation in children with congenital heart disease. J Biomed Sci. 2014;21:7.
201. Xiaoyun W, Min X, Xiaofei Y, Jihua H, Jie T. To Detect and Explore Mechanism of CITED2 Mutation and Methylation in Children with Congenital Heart Disease. In: Nakanishi T, Markwald RR, Baldwin HS, Keller BB, Srivastava D, Yamagishi H, editors. Etiology and Morphogenesis of Congenital Heart Disease: From Gene Function and Cellular Interaction to Morphology. Tokyo2016. p. 377-8.
202. Yin Z, Haynie J, Yang X, Han B, Kiatchoosakun S, Restivo J, et al. The essential role of Cited2, a negative regulator for HIF-1alpha, in heart development and neurulation. Proc Natl Acad Sci U S A. 2002;99(16):10488-93.
203. Xu B, Doughman Y, Turakhia M, Jiang W, Landsettle CE, Agani FH, et al. Partial rescue of defects in Cited2-deficient embryos by HIF-1alpha heterozygosity. Dev Biol. 2007;301(1):130-40.
204. Berlow RB, Dyson HJ, Wright PE. Hypersensitive termination of the hypoxic response by a disordered protein switch. Nature. 2017;543(7645):447-51.
205. Lou X, Sun S, Chen W, Zhou Y, Huang Y, Liu X, et al. Negative Feedback Regulation of NF-{kappa}B Action by CITED2 in the Nucleus. J Immunol. 2011;186(1):539-48.
206. Hui BS. CITED2 mechanoregulation of matrix metalloproteinases. Annals of the New York Academy of Sciences. 2010;1192(Skeletal Biology and Medicine):429-36.
207. Yokota H, Goldring MB, Sun HB. CITED2-mediated Regulation of MMP-1 and MMP-13 in Human Chondrocytes under Flow Shear. Journal of Biological Chemistry. 2003;278(47):47275-80.
208. Wojciak JM, Martinez-Yamout MA, Dyson HJ, Wright PE. Structural basis for recruitment of CBP/p300 coactivators by STAT1 and STAT2 transactivation domains. EMBO J. 2009;28(7):948-58.
209. Bhattacharya S, Michels CL, Leung MK, Arany ZP, Kung AL, Livingston DM. Functional role of p35srj, a novel p300/CBP binding protein, during transactivation by HIF-1. Genes Dev. 1999;13:64-75.
210. Liu Y-C, Chang P-Y, Chao CCK. CITED2 silencing sensitizes cancer cells to cisplatin by inhibiting p53 trans-activation and chromatin relaxation on the ERCC1 DNA repair gene. Nucleic Acids Research. 2015.
211. Mattes K, Berger G, Geugien M, Vellenga E, Schepers H. CITED2 affects leukemic cell survival by interfering with p53 activation. Cell Death Dis. 2017;8:e3132.
212. Bamforth SD, Bragança J, Eloranta JJ, Murdoch JN, Marques FIR, Kranc KR, et al. Cardiac malformations, adrenal agenesis, neural crest defects and exencephaly in mice lacking Cited2, a new Tfap2 co-activator. Nat Genet. 2001;29(4):469-74.

213. Bamforth SD, Bragança J, Farthing CR, Schneider JE, Broadbent C, Michell AC, et al. Cited2 controls left-right patterning and heart development through a Nodal-Pitx2c pathway. Nat Genet. 2004;36(11):1189-96.
214. Bragança J, Eloranta JJ, Bamforth SD, Ibbitt JC, Hurst HC, Bhattacharya S. Physical and Functional Interactions among AP-2 Transcription Factors, p300/CREB-binding Protein, and CITED2. J Biol Chem. 2003;278(18):16021-9.
215. Glenn DJ, Maurer RA. MRG1 binds to the LIM domain of Lhx2 and may function as a coactivator to stimulate glycoprotein hormone alpha -subunit gene expression. J Biol Chem. 1999;274(51):36159-67.
216. Qu X, Lam E, Doughman YQ, Chen Y, Chou YT, Lam M, et al. Cited2, a coactivator of HNF4alpha, is essential for liver development. EMBO J. 2007;26(21):4445-56.
217. Tien ES, Davis JW, Vanden Heuvel JP. Identification of the CREB-binding Protein/p300-interacting protein CITED2 as a peroxisome proliferator-activated receptor alpha coregulator. J Biol Chem. 2004;279(23):24053-63.
218. Gonzalez YR, Zhang Y, Behzadpoor D, Cregan S, Bamforth S, Slack RS, et al. CITED2 Signals through Peroxisome Proliferator-Activated Receptor-{gamma} to Regulate Death of Cortical Neurons after DNA Damage. J Neurosci. 2008;28(21):5559-69.
219. Chou YT, Wang H, Chen Y, Danielpour D, Yang YC. Cited2 modulates TGF-beta-mediated upregulation of MMP9. Oncogene. 2006;25(40):5547-60.
220. Sakai M, Matsumoto M, Tujimura T, Yongheng C, Noguchi T, Inagaki K, et al. CITED2 links hormonal signaling to PGC-1[alpha] acetylation in the regulation of gluconeogenesis. Nat Med. 2012;18(4):612-7.
221. Val P, Martinez-Barbera J-P, Swain A. Adrenal development is initiated by Cited2 and Wt1 through modulation of Sf-1 dosage. Development. 2007;134(12):2349-58.
222. Buaas FW, Val P, Swain A. The transcription co-factor CITED2 functions during sex determination and early gonad development. Human Molecular Genetics. 2009;18(16):2989-3001.
223. Pacheco-Leyva I, Matias Ana C, Oliveira Daniel V, Santos João MA, Nascimento R, Guerreiro E, et al. CITED2 Cooperates with ISL1 and Promotes Cardiac Differentiation of Mouse Embryonic Stem Cells. Stem Cell Reports. 2016;7(6):1037–49.
224. Kranc KR, Oliveira DV, Armesilla-Diaz A, Pacheco-Leyva I, Catarina Matias A, Luisa Escapa A, et al. Acute loss of Cited2 impairs Nanog expression and decreases self-renewal of mouse embryonic stem cells. Stem Cells. 2015;33(3):699-712.
225. Li Q, Ramirez-Bergeron DL, Dunwoodie SL, Yang YC. Cited2 gene controls pluripotency and cardiomyocyte differentiation of murine embryonic stem cells through Oct4 gene. J Biol Chem. 2012;287(34):29088-100.
226. Imakawa K, Dhakal P, Kubota K, Kusama K, Chakraborty D, Karim Rumi MA, et al. CITED2 modulation of trophoblast cell differentiation: insights from global transcriptome analysis. Reproduction. 2016;151(5):509-16.
227. Withington SL, Scott AN, Saunders DN, Lopes Floro K, Preis JI, Michalicek J, et al. Loss of Cited2 affects trophoblast formation and vascularization of the mouse placenta. Dev Biol. 2006;294(1):67-82.
228. Braganca J, Eloranta JJ, Bamforth SD, Ibbitt JC, Hurst HC, Bhattacharya S. Physical and functional interactions among AP-2 transcription factors, p300/CREB-binding protein, and CITED2. J Biol Chem. 2003;278(18):16021-9.
229. Kuckenberg P, Buhl S, Woynecki T, van Furden B, Tolkunova E, Seiffe F, et al. The transcription factor TCFAP2C/AP-2gamma cooperates with CDX2 to maintain trophectoderm formation. Mol Cell Biol. 2010;30(13):3310-20.
230. Kranc KR, Schepers H, Rodrigues NP, Bamforth S, Villadsen E, Ferry H, et al. Cited2 is an essential regulator of adult hematopoietic stem cells. Cell Stem Cell. 2009;5(6):659-65.

231. Du J, Li Q, Tang F, Puchowitz MA, Fujioka H, Dunwoodie SL, et al. Cited2 is required for the maintenance of glycolytic metabolism in adult hematopoietic stem cells. Stem Cells Dev. 2014;23(2):83-94.
232. Korthuis PM, Berger G, Bakker B, Rozenveld-Geugien M, Jaques J, de Haan G, et al. CITED2-mediated human hematopoietic stem cell maintenance is critical for acute myeloid leukemia. Leukemia. 2015;29(3):625-35.
233. Dunwoodie SL, Rodriguez TA, Beddington RS. Msg1 and Mrg1, founding members of a gene family, show distinct patterns of gene expression during mouse embryogenesis. Mech Dev. 1998;72(1-2):27-40.
234. Weninger WJ, Lopes Floro K, Bennett MB, Withington SL, Preis JI, Barbera JP, et al. Cited2 is required both for heart morphogenesis and establishment of the left-right axis in mouse development. Development. 2005;132(6):1337-48.
235. Chen C-m, Bentham J, Cosgrove C, Braganca J, Cuenda A, Bamforth SD, et al. Functional Significance of SRJ Domain Mutations in CITED2. PLoS ONE. 2012;7(10):e46256.
236. Sperling S, Grimm CH, Dunkel I, Mebus S, Sperling H-P, Ebner A, et al. Identification and functional analysis of CITED2 mutations in patients with congenital heart defects. Human Mutation. 2005;26(6):575-82.
237. Li B, Pu T, Liu Y, Xu Y, Xu R. CITED2 Mutations in Conserved Regions Contribute to Conotruncal Heart Defects in Chinese Children. DNA and Cell Biology. 2017.
238. Xu M, Wu X, Li Y, Yang X, Hu J, Zheng M, et al. CITED2 Mutation and methylation in children with congenital heart disease. Journal of Biomedical Science. 2014;21(1):7.
239. Liu Y, Wang F, Wu Y, Tan S, Wen Q, Wang J, et al. Variations of CITED2 Are Associated with Congenital Heart Disease (CHD) in Chinese Population. PLoS ONE. 2014;9(5):e98157.
240. Liu S, Su Z, Tan S, Ni B, Pan H, Liu B, et al. Functional Analyses of a Novel CITED2 Nonsynonymous Mutation in Chinese Tibetan Patients with Congenital Heart Disease. Pediatric Cardiology. 2017.
241. Hu P, Qiao F, Wang Y, Meng L, Ji X, Luo C, et al. Clinical application of targeted next-generation sequencing on fetuses with congenital heart defects. Ultrasound in Obstetrics & Gynecology. 2018;0(ja).
242. MacDonald ST, Bamforth SD, Chen CM, Farthing CR, Franklyn A, Broadbent C, et al. Epiblastic Cited2 deficiency results in cardiac phenotypic heterogeneity and provides a mechanism for haploinsufficiency. Cardiovasc Res. 2008;79(3):448-57.
243. Iacovino M, Roth ME, Kyba M. Rapid genetic modification of mouse embryonic stem cells by Inducible Cassette Exchange recombination. Methods Mol Biol. 2014;1101:339-51.
244. Lee G, Saito I. Role of nucleotide sequences of loxP spacer region in Cre-mediated recombination. Gene. 1998;216(1):55-65.
245. Iacovino M, Bosnakovski D, Fey H, Rux D, Bajwa G, Mahen E, et al. Inducible cassette exchange: a rapid and efficient system enabling conditional gene expression in embryonic stem and primary cells. Stem Cells. 2011;29(10):1580-8.
246. Mori H, Yao Y, Learman BS, Kurozumi K, Ishida J, Ramakrishnan SK, et al. Induction of WNT11 by hypoxia and hypoxia-inducible factor-1alpha regulates cell proliferation, migration and invasion. Sci Rep. 2016;6:21520.
247. Kim B, Kim Y, Sakuma R, Hui CC, Ruther U, Jorgensen JS. Primordial germ cell proliferation is impaired in Fused Toes mutant embryos. Dev Biol. 2011;349(2):417-26.
248. Li L, Liu C, Biechele S, Zhu Q, Song L, Lanner F, et al. Location of transient ectodermal progenitor potential in mouse development. Development. 2013;140(22):4533-43.
249. Chen Y, Haviernik P, Bunting KD, Yang YC. Cited2 is required for normal hematopoiesis in the murine fetal liver. Blood. 2007;110(8):2889-98.

250. Kemp C, Willems E, Abdo S, Lambiv L, Leyns L. Expression of all Wnt genes and their secreted antagonists during mouse blastocyst and postimplantation development. Dev Dyn. 2005;233(3):1064-75.
251. Zhang Y, Wang S, Song Y, Han J, Chai Y, Chen Y. Timing of odontogenic neural crest cell migration and tooth-forming capability in mice. Dev Dyn. 2003;226(4):713-8.
252. Sultana DA, Tomita S, Hamada M, Iwanaga Y, Kitahama Y, Khang NV, et al. Gene expression profile of the third pharyngeal pouch reveals role of mesenchymal MafB in embryonic thymus development. Blood. 2009;113(13):2976-87.
253. Zhong X, Jin Y. Critical roles of coactivator p300 in mouse embryonic stem cell differentiation and Nanog expression. J Biol Chem. 2009;284(14):9168-75.
254. Sachinidis A, Schwengberg S, Hippler-Altenburg R, Mariappan D, Kamisetti N, Seelig B, et al. Identification of small signalling molecules promoting cardiac-specific differentiation of mouse embryonic stem cells. Cell Physiol Biochem. 2006;18(6):303-14.
255. Ogawa K, Saito A, Matsui H, Suzuki H, Ohtsuka S, Shimosato D, et al. Activin-Nodal signaling is involved in propagation of mouse embryonic stem cells. J Cell Sci. 2007;120(Pt 1):55-65.
256. Nemeth MJ, Topol L, Anderson SM, Yang Y, Bodine DM. Wnt5a inhibits canonical Wnt signaling in hematopoietic stem cells and enhances repopulation. Proc Natl Acad Sci U S A. 2007;104(39):15436-41.
257. Acharya A, Brungs S, Henry M, Rotshteyn T, Singh Yaduvanshi N, Wegener L, et al. Modulation of Differentiation Processes in Murine Embryonic Stem Cells Exposed to Parabolic Flight-Induced Acute Hypergravity and Microgravity. Stem Cells Dev. 2018;27(12):838-47.
258. Ritchie ME, Phipson B, Wu D, Hu Y, Law CW, Shi W, et al. limma powers differential expression analyses for RNA-sequencing and microarray studies. Nucleic Acids Res. 2015;43(7):e47.
259. Sabour D, Machado RSR, Pinto JP, Rohani S, Sahito RGA, Hescheler J, et al. Parallel Genome-wide Profiling of Coding and Non-coding RNAs to Identify Novel Regulatory Elements in Embryonic and Maturated Heart. Mol Ther Nucleic Acids. 2018;12:158-73.
260. Kuleshov MV, Jones MR, Rouillard AD, Fernandez NF, Duan Q, Wang Z, et al. Enrichr: a comprehensive gene set enrichment analysis web server 2016 update. Nucleic Acids Research. 2016;44(W1):W90-W7.
261. Chen EY, Tan CM, Kou Y, Duan Q, Wang Z, Meirelles GV, et al. Enrichr: interactive and collaborative HTML5 gene list enrichment analysis tool. BMC Bioinformatics. 2013;14:128-.
262. Danieau solution (300%). Cold Spring Harbor Protocols. 2007;2007(8):pdb.rec11095.
263. Embryo medium for zebrafish. Cold Spring Harbor Protocols. 2011;2011(7):pdb.rec12471.
264. Pacheco-Leyva I, Matias AC, Oliveira DV, Santos JM, Nascimento R, Guerreiro E, et al. CITED2 Cooperates with ISL1 and Promotes Cardiac Differentiation of Mouse Embryonic Stem Cells. Stem Cell Reports. 2016;7(6):1037-49.
265. Bray MA, Sheehy SP, Parker KK. Sarcomere alignment is regulated by myocyte shape. Cell Motil Cytoskeleton. 2008;65(8):641-51.
266. Lundberg M, Wikstrom S, Johansson M. Cell surface adherence and endocytosis of protein transduction domains. Mol Ther. 2003;8(1):143-50.
267. Kutmon M, Riutta A, Nunes N, Hanspers K, Willighagen EL, Bohler A, et al. WikiPathways: capturing the full diversity of pathway knowledge. Nucleic Acids Res. 2016;44(D1):D488-94.
268. Pico AR, Kelder T, van Iersel MP, Hanspers K, Conklin BR, Evelo C. WikiPathways: pathway editing for the people. PLoS Biol. 2008;6(7):e184.

269. Lin IY, Chiu FL, Yeang CH, Chen HF, Chuang CY, Yang SY, et al. Suppression of the SOX2 neural effector gene by PRDM1 promotes human germ cell fate in embryonic stem cells. Stem Cell Reports. 2014;2(2):189-204.
270. Yao M, Zhou X, Zhou J, Gong S, Hu G, Li J, et al. PCGF5 is required for neural differentiation of embryonic stem cells. Nat Commun. 2018;9(1):1463.
271. Maguire CT, Demarest BL, Hill JT, Palmer JD, Brothman AR, Yost HJ, et al. Genome-wide analysis reveals the unique stem cell identity of human amniocytes. PLoS One. 2013;8(1):e53372.
272. Lim SM, Pereira L, Wong MS, Hirst CE, Van Vranken BE, Pick M, et al. Enforced expression of Mixl1 during mouse ES cell differentiation suppresses hematopoietic mesoderm and promotes endoderm formation. Stem Cells. 2009;27(2):363-74.
273. Sahara M, Santoro F, Chien KR. Programming and reprogramming a human heart cell. The EMBO Journal. 2015;34(6):710-38.
274. Tjalsma H, Bolhuis A, Jongbloed JD, Bron S, van Dijl JM. Signal peptide-dependent protein transport in Bacillus subtilis: a genome-based survey of the secretome. Microbiol Mol Biol Rev. 2000;64(3):515-47.
275. Kim HO, Choi S-M, Kim H-S. Mesenchymal stem cell-derived secretome and microvesicles as a cell-free therapeutics for neurodegenerative disorders. Tissue Engineering and Regenerative Medicine. 2013;10(3):93-101.
276. Brown KJ, Formolo CA, Seol H, Marathi RL, Duguez S, An E, et al. Advances in the proteomic investigation of the cell secretome. Expert Rev Proteomics. 2012;9(3):337-45.
277. Gnecchi M, He H, Liang OD, Melo LG, Morello F, Mu H, et al. Paracrine action accounts for marked protection of ischemic heart by Akt-modified mesenchymal stem cells. Nat Med. 2005;11(4):367-8.
278. Fraidenraich D, Stillwell E, Romero E, Wilkes D, Manova K, Basson CT, et al. Rescue of cardiac defects in id knockout embryos by injection of embryonic stem cells. Science. 2004;306(5694):247-52.
279. Clark CC, Cohen I, Eichstetter I, Cannizzaro LA, McPherson JD, Wasmuth JJ, et al. Molecular cloning of the human proto-oncogene Wnt-5A and mapping of the gene (WNT5A) to chromosome 3p14-p21. Genomics. 1993;18(2):249-60.
280. Moon RT, Campbell RM, Christian JL, McGrew LL, Shih J, Fraser S. Xwnt-5A: a maternal Wnt that affects morphogenetic movements after overexpression in embryos of Xenopus laevis. Development. 1993;119(1):97-111.
281. Ku M, Melton DA. Xwnt-11: a maternally expressed Xenopus wnt gene. Development. 1993;119(4):1161-73.
282. Eisenberg CA, Gourdie RG, Eisenberg LM. Wnt-11 is expressed in early avian mesoderm and required for the differentiation of the quail mesoderm cell line QCE-6. Development. 1997;124(2):525-36.
283. Eisenberg CA, Eisenberg LM. WNT11 promotes cardiac tissue formation of early mesoderm. Dev Dyn. 1999;216(1):45-58.
284. Pandur P, Lasche M, Eisenberg LM, Kuhl M. Wnt-11 activation of a non-canonical Wnt signalling pathway is required for cardiogenesis. Nature. 2002;418(6898):636-41.
285. Yamaguchi TP, Bradley A, McMahon AP, Jones S. A Wnt5a pathway underlies outgrowth of multiple structures in the vertebrate embryo. Development. 1999;126(6):1211-23.
286. Baranski M, Berdougo E, Sandler JS, Darnell DK, Burrus LW. The dynamic expression pattern of frzb-1 suggests multiple roles in chick development. Dev Biol. 2000;217(1):25-41.
287. Mehta A, Ramachandra CJ, Sequiera GL, Sudibyo Y, Nandihalli M, Yong PJ, et al. Phasic modulation of Wnt signaling enhances cardiac differentiation in human pluripotent stem cells by recapitulating developmental ontogeny. Biochim Biophys Acta. 2014;1843(11):2394-402.

288. Cohen ED, Miller MF, Wang Z, Moon RT, Morrisey EE. Wnt5a and Wnt11 are essential for second heart field progenitor development. Development. 2012;139(11):1931-40.
289. Kispert A, Vainio S, Shen L, Rowitch DH, McMahon AP. Proteoglycans are required for maintenance of Wnt-11 expression in the ureter tips. Development. 1996;122(11):3627-37.
290. Terami H, Hidaka K, Katsumata T, Iio A, Morisaki T. Wnt11 facilitates embryonic stem cell differentiation to Nkx2.5-positive cardiomyocytes. Biochem Biophys Res Commun. 2004;325(3):968-75.
291. Schleiffarth JR, Person AD, Martinsen BJ, Sukovich DJ, Neumann A, Baker CV, et al. Wnt5a is required for cardiac outflow tract septation in mice. Pediatr Res. 2007;61(4):386-91.
292. Li D, Sinha T, Ajima R, Seo HS, Yamaguchi TP, Wang J. Spatial regulation of cell cohesion by Wnt5a during second heart field progenitor deployment. Dev Biol. 2016;412(1):18-31.
293. Sinha T, Li D, Theveniau-Ruissy M, Hutson MR, Kelly RG, Wang J. Loss of Wnt5a disrupts second heart field cell deployment and may contribute to OFT malformations in DiGeorge syndrome. Hum Mol Genet. 2015;24(6):1704-16.
294. Sinha T, Lin L, Li D, Davis J, Evans S, Wynshaw-Boris A, et al. Mapping the dynamic expression of Wnt11 and the lineage contribution of Wnt11-expressing cells during early mouse development. Dev Biol. 2015;398(2):177-92.
295. van Vliet PP, Lin L, Boogerd CJ, Martin JF, Andelfinger G, Grossfeld PD, et al. Tissue specific requirements for WNT11 in developing outflow tract and dorsal mesenchymal protrusion. Dev Biol. 2017;429(1):249-59.
296. Zhou W, Lin L, Majumdar A, Li X, Zhang X, Liu W, et al. Modulation of morphogenesis by noncanonical Wnt signaling requires ATF/CREB family-mediated transcriptional activation of TGFbeta2. Nat Genet. 2007;39(10):1225-34.
297. Andre P, Song H, Kim W, Kispert A, Yang Y. Wnt5a and Wnt11 regulate mammalian anterior-posterior axis elongation. Development. 2015;142(8):1516-27.
298. Howe K, Clark MD, Torroja CF, Torrance J, Berthelot C, Muffato M, et al. The zebrafish reference genome sequence and its relationship to the human genome. Nature. 2013;496(7446):498-503.
299. Stainier DY. Zebrafish genetics and vertebrate heart formation. Nat Rev Genet. 2001;2(1):39-48.
300. Hu N, Yost HJ, Clark EB. Cardiac morphology and blood pressure in the adult zebrafish. Anat Rec. 2001;264(1):1-12.
301. Nasevicius A, Ekker SC. Effective targeted gene 'knockdown' in zebrafish. Nat Genet. 2000;26(2):216-20.
302. Thisse B, Thisse, C. Fast Release Clones: A High Throughput Expression Analysis. ZFIN Direct Data Submission (http://zfinorg). 2004.
303. Kimmel CB, Ballard WW, Kimmel SR, Ullmann B, Schilling TF. Stages of embryonic development of the zebrafish. Dev Dyn. 1995;203(3):253-310.
304. Tan KR, Magill AJ, Parise ME, Arguin PM, Centers for Disease C, Prevention. Doxycycline for malaria chemoprophylaxis and treatment: report from the CDC expert meeting on malaria chemoprophylaxis. Am J Trop Med Hyg. 2011;84(4):517-31.
305. Chou YT, Yang YC. Post-transcriptional control of Cited2 by transforming growth factor beta. Regulation via Smads and Cited2 coding region. J Biol Chem. 2006;281(27):18451-62.

306. Pankratz MT, Li XJ, Lavaute TM, Lyons EA, Chen X, Zhang SC. Directed neural differentiation of human embryonic stem cells via an obligated primitive anterior stage. Stem Cells. 2007;25(6):1511-20.
307. David R, Jarsch VB, Schwarz F, Nathan P, Gegg M, Lickert H, et al. Induction of MesP1 by Brachyury(T) generates the common multipotent cardiovascular stem cell. Cardiovasc Res. 2011;92(1):115-22.
308. Chen L, Fulcoli FG, Ferrentino R, Martucciello S, Illingworth EA, Baldini A. Transcriptional control in cardiac progenitors: Tbx1 interacts with the BAF chromatin remodeling complex and regulates Wnt5a. PLoS Genet. 2012;8(3):e1002571.
309. Choudhry P, Trede NS. DiGeorge syndrome gene tbx1 functions through wnt11r to regulate heart looping and differentiation. PLoS One. 2013;8(3):e58145.
310. Choe CP, Crump JG. Tbx1 controls the morphogenesis of pharyngeal pouch epithelia through mesodermal Wnt11r and Fgf8a. Development. 2014;141(18):3583-93.
311. Schreck C, Istvanffy R, Ziegenhain C, Sippenauer T, Ruf F, Henkel L, et al. Niche WNT5A regulates the actin cytoskeleton during regeneration of hematopoietic stem cells. J Exp Med. 2017;214(1):165-81.
312. Boyan BD, Olivares-Navarrete R, Berger MB, Hyzy SL, Schwartz Z. Role of Wnt11 during Osteogenic Differentiation of Human Mesenchymal Stem Cells on Microstructured Titanium Surfaces. Sci Rep. 2018;8(1):8588.
313. Zhu JH, Liao YP, Li FS, Hu Y, Li Q, Ma Y, et al. Wnt11 promotes BMP9-induced osteogenic differentiation through BMPs/Smads and p38 MAPK in mesenchymal stem cells. J Cell Biochem. 2018;119(11):9462-73.
314. Bisson JA, Mills B, Paul Helt JC, Zwaka TP, Cohen ED. Wnt5a and Wnt11 inhibit the canonical Wnt pathway and promote cardiac progenitor development via the Caspase-dependent degradation of AKT. Dev Biol. 2015;398(1):80-96.
315. Cha SW, Tadjuidje E, Tao Q, Wylie C, Heasman J. Wnt5a and Wnt11 interact in a maternal Dkk1-regulated fashion to activate both canonical and non-canonical signaling in Xenopus axis formation. Development. 2008;135(22):3719-29.
316. Jayaraman S, Doucet M, Kominsky SL. CITED2 attenuates macrophage recruitment concordant with the downregulation of CCL20 in breast cancer cells. Oncol Lett. 2018;15(1):871-8.
317. Canesin G, Evans-Axelsson S, Hellsten R, Krzyzanowska A, Prasad CP, Bjartell A, et al. Treatment with the WNT5A-mimicking peptide Foxy-5 effectively reduces the metastatic spread of WNT5A-low prostate cancer cells in an orthotopic mouse model. PLoS One. 2017;12(9):e0184418.
318. Safholm A, Tuomela J, Rosenkvist J, Dejmek J, Harkonen P, Andersson T. The Wnt-5a-derived hexapeptide Foxy-5 inhibits breast cancer metastasis in vivo by targeting cell motility. Clin Cancer Res. 2008;14(20):6556-63.
319. Greenberg JA, Bell SJ, Guan Y, Yu YH. Folic Acid supplementation and pregnancy: more than just neural tube defect prevention. Rev Obstet Gynecol. 2011;4(2):52-9.

CHAPTER 10

Appendices

Table 10.1. Reference list of genes expressed in the three primary embryonic lineages. P-value is referent to DEGS in Cited2fl/fl [Cre], treated with EtOH, compared to Cited2fl/fl [Cre], treated with 4HT, at D4 of differentiation. List adapted from (271)

Gene	Name	Lineage	P-value
Egr2	Early Growth Response 2	Ectoderm	n/s
Fgf5	Fibroblast growth factor 5	Ectoderm	n/s
Foxj3	Forkhead Box J3	Ectoderm	n/s
Gbx2	Gastrulation Brain Homeobox 2	Ectoderm	n/s
Lhx5	Lim Homeobox protein 5	Ectoderm	n/s
Lmx1a	LIM Homeobox Transcription Factor 1 Alpha	Ectoderm	n/s
Meis1	Meis Homeobox 1	Ectoderm	n/s
Meis2	Meis Homeobox 2	Ectoderm	n/s
Nes	Nestin	Ectoderm	n/s
Pard6b	Par-6 Family Cell Polarity Regulator Beta	Ectoderm	n/s
Pax2	Paired box gene 2	Ectoderm	n/s
Pax6	Paired box gene 6	Ectoderm	n/s
Penk	Proenkephalin	Ectoderm	n/s
Rbm27	RNA Binding Motif Protein 27	Ectoderm	n/s
Sox1	SRY-Box 1	Ectoderm	n/s
Tfcp2l1	transcription factor CP2-like 1	Ectoderm	-1.44
Trim33	Tripartite Motif Containing 33	Ectoderm	n/s
Tubb3	Tubulin Beta 3 Class III	Ectoderm	n/s
Vim	Vimetin	Ectoderm	1.50
Zic1	Zinc finger of the cerebellum 1	Ectoderm	n/s
Afp	Alpha-fetoprotein	Endoderm	n/s
Calcr	Calcitonin receptor	Endoderm	n/s
Cckbr	cholecystokinin B receptor	Endoderm	n/s
Cer1	Cerberus 1	Endoderm	2.76
Cxcr4	chemokine (C-X-C motif) receptor 4	Endoderm	3.40
Cyp26a1	cytochrome P450, family 26, subfamily a, polypeptide 1	Endoderm	4.12
Dab2	Disabled homolog 2	Endoderm	n/s
Dkk4	Dickkopf WNT Signaling Pathway Inhibitor 4	Endoderm	n/s
Dlx3	Distal-Less Homeobox 3	Endoderm	n/s

Dlx5	Distal-Less Homeobox 5	Endoderm	n/s
Elf4	ETS-related transcription factor 4	Endoderm	n/s
Eya2	Eyes absent homolog 2	Endoderm	n/s
Fgf17	Fibroblast growth factor 17	Endoderm	n/s
Foxa2	forkhead box A2	Endoderm	1.83
Foxa3	forkhead box A3	Endoderm	n/s
Foxc1	forkhead box C1	Endoderm	2.69
Foxf1	forkhead box F1	Endoderm	3.03
Foxh1	forkhead box H1	Endoderm	1.84
Foxq1	forkhead box Q1	Endoderm	n/s
Gata6	GATA binding protein 6	Endoderm	1.54
Gpc1	Glypican-1	Endoderm	n/s
Hhex	hematopoietically expressed homeobox	Endoderm	1.39
Id4	DNA-binding protein inhibitor 4	Endoderm	n/s
Krt19	Keratin, type I cytoskeletal 19	Endoderm	n/s
Nts	Neurotensin	Endoderm	n/s
Pax9	Paired box gene 9	Endoderm	n/s
Plxna2	plexin A2	Endoderm	2.02
Prdm1	PR domain containing 1, with ZNF domain	Endoderm	1.49
Pyy	Peptide YY	Endoderm	n/s
Shisa2	Shisa 2	Endoderm	n/s
Sox17	SRY box 17	Endoderm	2.30
Sox7	SRY box 7	Endoderm	n/s
Sp6	Transcription Factor Sp6	Endoderm	n/s
Tle2	Transducin-like enhancer protein 2	Endoderm	n/s
Trim22	Tripartite Motif Containing 22	Endoderm	n/s
Tspan7	Tetraspanin-7	Endoderm	n/s
Cxcl12	C-X-C motif chemokine 12	Mesoderm	n/s
Ednrb	Endothelin Receptor Type B	Mesoderm	n/s
Foxf1	forkhead box F1	Mesoderm	n/s
Lhx1	LIM homeobox 1	Mesoderm	4.23
Lmo2	LIM domain only 2	Mesoderm	n/s

Meox1	Homeobox protein MOX-1	Mesoderm	n/s
Meox2	Homeobox protein MOX-2	Mesoderm	n/s
Mesdc2	Mesoderm candidate gene 2	Mesoderm	n/s
Msx1	msh homeobox 1	Mesoderm	n/s
Msx2	msh homeobox 2	Mesoderm	1.63
Myl4	Myosin light chain4	Mesoderm	n/s
Myocd	Myocardin	Mesoderm	n/s
Pbx1	pre B cell leukemia homeobox 1	Mesoderm	2.09
Ror2	Receptor Tyrosine Kinase Like Orphan Receptor 2	Mesoderm	n/s
Sox6	SRY box 6	Mesoderm	n/s
Tbx6	T-box 6	Mesoderm	2.88
Tcf15	Transcription factor 15	Mesoderm	n/s
Wnt5a	Wnt Family Member 5A	Mesoderm	n/s
Wnt5b	Wnt Family Member 5B	Mesoderm	n/s
Wnt8a	Wnt Family Member 8A	Mesoderm	n/s
Anxa4	Annexin A2	Mesoderm/Endoderm	n/s
Bmp2	bone morphogenetic protein 2	Mesoderm/Endoderm	2.13
Bmp4	bone morphogenetic protein 4	Mesoderm/Endoderm	n/s
Cdx2	caudal type homeobox	Mesoderm/Endoderm	2.28
Dkk1	dickkopf WNT signaling pathway inhibitor 1	Mesoderm/Endoderm	2.52
Dsg2	Desmoglein-2	Mesoderm/Endoderm	n/s
Eomes	Eomesodermin	Mesoderm/Endoderm	n/s
Fgf8	Fibroblast growth factor 8	Mesoderm/Endoderm	n/s
Foxa1	forkhead box A1	Mesoderm/Endoderm	1.77
Gata3	GATA binding protein 3	Mesoderm/Endoderm	n/s
Gata4	GATA binding protein 4	Mesoderm/Endoderm	2.60
Gdf3	growth differentiation factor 3	Mesoderm/Endoderm	-2.50
Gsc	goosecoid homeobox	Mesoderm/Endoderm	1.02
Hand1	Heart and Neural Crest Derivatives Expressed 1	Mesoderm/Endoderm	n/s
Hand2	Heart and Neural Crest Derivatives Expressed 2	Mesoderm/Endoderm	n/s
Hnf4a	Hepatocyte Nuclear Factor 4 Alpha	Mesoderm/Endoderm	n/s
Hox1a	homeobox A1	Mesoderm/Endoderm	n/s

Hoxb1	homeobox B1	Mesoderm/Endoderm	1.22
Isl1	ISL1 transcription factor, LIM/homeodomain	Mesoderm/Endoderm	2.99
Kdr	Kinase Insert Domain Receptor	Mesoderm/Endoderm	5.06
Mesp1	mesoderm posterior 1	Mesoderm/Endoderm	1.46
Mesp2	mesoderm posterior 2	Mesoderm/Endoderm	n/s
Mixl1	Mix1 homeobox-like 1	Mesoderm/Endoderm	2.60
Otx1	Orthodenticle Homeobox 1	Mesoderm/Endoderm	n/s
Otx2	Orthodenticle Homeobox 2	Mesoderm/Endoderm	n/s
Pdgfra	platelet-derived growth factor receptor alpha	Mesoderm/Endoderm	n/s
Pdgfrb	platelet-derived growth factor receptor beta	Mesoderm/Endoderm	n/s
Ripk4	Receptor-interacting serine/threonine-protein kinase 4	Mesoderm/Endoderm	n/s
T	brachyury, T-box transcription factor T	Mesoderm/Endoderm	2.34
Wnt3a	Wnt Family Member 3A	Mesoderm/Endoderm	n/s